

การปรับปรุงสมรรถนะการควบคุมของตัวหนองปรับค่าชนิดของเหลวแบบมีแกนสำหรับอาคาร
ภายใต้การสั่นไหวจากแผ่นดินไหว



นาย ภาสกร ชัยวิริยะวงศ์

สถาบันวิทยบริการ

วิทยานิพนธ์นี้เป็นส่วนหนึ่งของการศึกษาตามหลักสูตรปริญญาวิศวกรรมศาสตรดุษฎีบัณฑิต

สาขาวิชาวิศวกรรมโยธา ภาควิชาวิศวกรรมโยธา

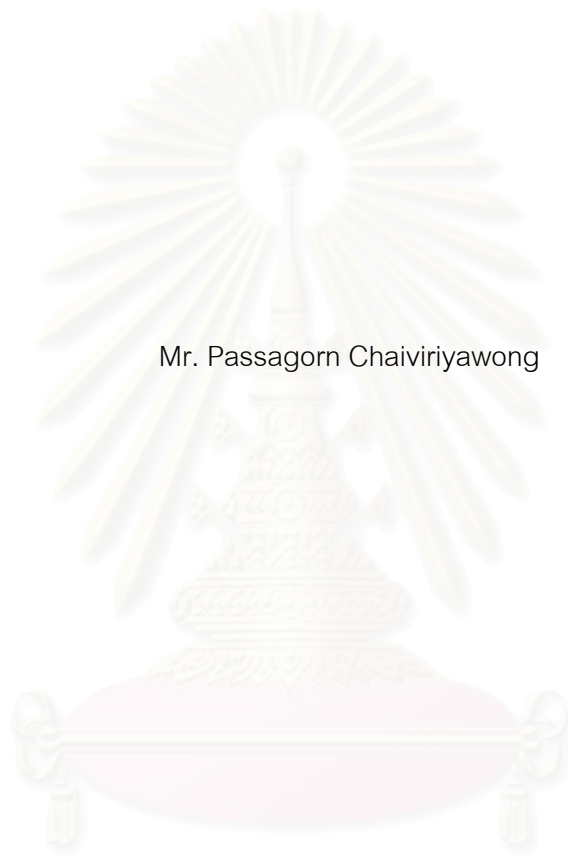
คณะวิศวกรรมศาสตร์ จุฬาลงกรณ์มหาวิทยาลัย

ปีการศึกษา 2548

ISBN 974-17-3684-3

ลิขสิทธิ์ของจุฬาลงกรณ์มหาวิทยาลัย

IMPROVEMENT OF CONTROL PERFORMANCE OF TUNED LIQUID COLUMN
DAMPERS IN BUILDINGS UNDER EARTHQUAKE EXCITATIONS



Mr. Passagorn Chaiviriyawong

A Dissertation Submitted in Partial Fulfillment of the Requirements
for the Degree of Doctor of Philosophy Program in Civil Engineering

Department of Civil Engineering

Faculty of Engineering

Chulalongkorn University

Academic year 2005

ISBN 974-17-3684-3

Copyright of Chulalongkorn University

Thesis Title Improvement of Control Performance of Tuned Liquid Column
Dampers in Buildings Under Earthquake Excitations


By Mr. Passagorn Chaiviriyawong

Field of study Civil Engineering

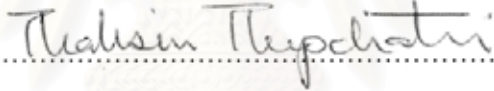
Thesis Advisor Professor Panitan Lukkunaprasit, Ph.D


Thesis Co-advisor Associate Professor Tospol Pinkeaw, Ph.D

Accepted by the Faculty of Engineering, Chulalongkorn University in Partial
Fulfillment of the Requirements for the Doctor's Degree


..... Dean of the Faculty of Engineering
(Professor Direk Lavansiri, Ph.D.)

THESIS COMMITTEE

..... Chairman
(Professor Thaksin Thepchatri, Ph.D.)

..... Thesis Advisor
(Professor Panitan Lukkunaprasit, Ph.D.)

..... Thesis Co-advisor
(Associate Professor Tospol Pinkeaw, Ph.D.)

..... Member
(Professor William C. Webster, Ph.D.)

..... Member
(Assistant Professor Anat Ruangrassamee, Ph.D.)

ภาสกร ชัยวิริยะวงศ์ : การปรับปรุงสมรรถนะการควบคุมของตัวหน่วงปรับค่าชนิดของเหลวแบบมีแกนสำหรับอาคารภายใต้การสั่นไหวจากแผ่นดินไหว. (IMPROVEMENT OF CONTROL PERFORMANCE OF TUNED LIQUID COLUMN DAMPERS IN BUILDINGS UNDER EARTHQUAKE EXCITATIONS) อ. ที่ปรึกษา : ศ.ดร.ปณิธาน ลักคุณะประสิทธิ์, อ.ที่ปรึกษาร่วม : รศ.ดร.ทศพล ปิ่นแก้ว จำนวนหน้า 102 หน้า. ISBN 974-17-3684-3.

ในงานวิจัยในอดีตการทำนายค่าความถี่ธรรมชาติของตัวหน่วงปรับค่าชนิดของเหลวแบบมีแกนและตัวดูดซับการสั่นไหวชนิดของเหลวแบบมีแกนนี้มีพื้นฐานโดยใช้สมมติฐานที่ว่าความเร็วของของเหลวในแต่ละส่วนของตัวหน่วงมีค่าคงที่ตลอดและช่วงเปลี่ยนของการไหลจากแกนแนวตั้งไปยังท่อแนวนอนเกิดขึ้นที่จุดเพียงจุดเดียว ซึ่งสมมติฐานนี้สามารถใช้ได้ในกรณีที่มีความกว้างของท่อในแนวนอนและแกนในแนวตั้งมีขนาดเล็กเมื่อเทียบกับมิติทั้งหมดของตัวหน่วง มีนักวิจัยหลายท่านได้เสนอสูตรอย่างง่ายสำหรับการคำนวณความถี่ธรรมชาติที่ต่างกันยังผลให้ค่าความถี่ธรรมชาติที่ได้จากแต่ละสูตรอย่างง่ายมีค่าต่างกันด้วย สำหรับอาคารที่มีพื้นที่จำกัดอาจจะต้องใช้ตัวหน่วงปรับค่าชนิดของเหลวแบบมีแกนที่มีความกว้างของแกนแนวตั้งทั้ง 2 ไม่ได้มีขนาดเล็กเมื่อเทียบกับมิติทั้งหมดของตัวหน่วง ซึ่งเป็นรูปแบบของตัวหน่วงปรับค่าชนิดของเหลวแบบมีแกนที่ยังไม่เคยถูกศึกษาวิจัยมาก่อน โดยรูปแบบใหม่มีการแปรผันของความเร็วของเหลวในบริเวณที่มีการเปลี่ยนทิศการไหลระหว่างแกนแนวตั้งและท่อแนวนอนนั้นมีขนาดใหญ่จึงไม่อาจสมมติให้เกิดที่จุดเพียงจุดเดียวได้ วิธีคำนวณการไหลศึกษาภาพเชิงตัวเลขซึ่งรู้จักกันในชื่อวิธีแผ่นผิวแข็งจำลองเชิงตัวเลขได้ถูกใช้ในการคำนวณหาการแผ่กระจายของความเร็วของของเหลวภายในตัวหน่วงชนิดของเหลวนี้ โดยวิธีนี้ได้ใช้สมการปฏิยานุพันธ์สำหรับศึกษาภาพของการไหลในการแก้สมการเชิงตัวเลขเพื่อหาลักษณะการไหลของของเหลว ผลการจำลองเชิงตัวเลขเหล่านี้ได้ถูกเปรียบเทียบความถูกต้องกับผลการทดสอบที่เคยมีมา และยังได้มีการทดสอบเพิ่มเติมโดยใช้แบบจำลองขนาดเท่าของจริงจำนวน 3 แบบจำลองในการทดสอบศึกษาภายใต้ การสั่นสะเทือนที่ความถี่ธรรมชาติ, การทดสอบแบบสเปกทริล และ การสั่นไหวที่ฐานซึ่งถูกกำหนดขึ้น ผลของวิธีแผ่นผิวแข็งจำลองเชิงตัวเลขนี้ นำไปสู่การปรับปรุงการทำนายลักษณะเฉพาะของตัวหน่วงปรับค่าชนิดของเหลวแบบมีแกนโดยครอบคลุมในทุกรูปแบบซึ่งเป็นประโยชน์อย่างยิ่งในการควบคุมเพื่อให้ได้ประสิทธิผลที่น่าพอใจที่สุดสำหรับอาคาร

จุดด้อยของระบบตัวหน่วงแบบแพลสทิคทุกชนิดคือการขาดความสามารถในการลดการสั่นไหวในสภาวะที่ไม่สั่นไหวได้อย่างมีนัยสำคัญ เช่นแรงที่มากกระทำต่ออาคารมีค่าสูงในตอนเริ่มต้นของเหตุการณ์ ซึ่งในกรณีนี้จะทำให้การทำงานของตัวหน่วงได้ผลที่แย่มากที่สุด เพื่อที่จะปรับปรุงประสิทธิภาพของตัวหน่วงปรับค่าชนิดของเหลวแบบมีแกนเมื่อต้องเผชิญกับแผ่นดินไหวที่มีสภาวะไม่คงตัวสูงนี้ ตัวหน่วงปรับค่าชนิดของเหลวแบบมีแกนติดตั้งด้วยอุปกรณ์กระตุ้นการไหลซึ่งสามารถรักษาระดับของของเหลวภายในให้ต่างกันทำให้ระบบมีพลังงานศักย์สูงและสามารถที่จะปลดปล่อยการไหลได้อย่างทันทีทันใดในเวลาที่เหมาะสม

พบว่าจากผลการทดสอบตัวหน่วงปรับค่าชนิดของเหลวแบบมีแกนติดตั้งด้วยอุปกรณ์กระตุ้นการไหลค่าความหน่วงที่มีค่าสูงเกินกว่าค่าความหน่วงที่เหมาะสมซึ่งจะทำให้ประสิทธิภาพในการควบคุมการสั่นไหวด้อยลง ดังนั้นในการทำการศึกษาเชิงตัวเลขจึงได้ใช้ค่าความหน่วงที่เหมาะสมแทน และได้พบว่าตัวหน่วงปรับค่าชนิดของเหลวแบบมีแกนติดตั้งด้วยอุปกรณ์กระตุ้นการไหลนี้มีประสิทธิภาพที่ดีกว่าตัวหน่วงปรับค่าชนิดของเหลวแบบมีแกนธรรมดาเมื่อสามารถปรับค่าอัตราส่วนความหน่วงเป็นค่าที่เหมาะสมได้

ภาควิชา...วิศวกรรมโยธาลายมือชื่อนิสิต...ภาสกร ชัยวิริยะวงศ์.....
 สาขาวิชา...วิศวกรรมโยธา.....ลายมือชื่ออาจารย์ที่ปรึกษา.....
 ปีการศึกษา 2548ลายมือชื่ออาจารย์ที่ปรึกษาร่วม.....

4271814521 : MAJOR CIVIL ENGINEERING

KEY WORD: TLCD / LCVA / PANEL METHOD / EFFECTIVE LENGTH / NATURAL FREQUENCY

PASSAGORN CHAIVIRIYAWONG: IMPROVEMENT OF CONTROL PERFORMANCE OF TUNED LIQUID COLUMN DAMPERS IN BUILDINGS UNDER EARTHQUAKE EXCITATIONS. THESIS ADVISOR : PROF.PANITAN LUKKUNAPRASIT, Ph.D, THESIS COADVISOR : ASSOC. PROF. TOSPOL PINKAEW, Ph.D, 102 pp. ISBN 974-17-3684-3.

In previous research, prediction of the natural frequency of tuned liquid column dampers (TLCDs) including a liquid column vibration absorbers (LCVA) is based on the assumption that the liquid velocity within each leg of these dampers is constant and the transition between the vertical and horizontal flows occurs at a single point. This assumption is valid for a TLCD and LCVA when the widths of both the horizontal cross-over duct and vertical columns are small compared to the overall dimensions of the damper. For buildings with limited space, it will be necessary to configure a TLCD with the width of the vertical columns that is not small with respect to the overall dimensions of the damper, a configuration which has not yet been investigated in research. In this case, the variation of liquid velocity in the relatively large transition zone between the vertical columns and the cross-over duct cannot be ignored. A numerical potential-flow method, known as the numerical panel method, is utilized to simulate the velocity distribution of the fluid inside liquid dampers. The method allows an integral equation for the velocity potential to be formulated and solved numerically to determine the flow. These numerical solutions are verified with those obtained from existing experimental results. In addition, three full-scale models of LCVAs are investigated experimentally under free-vibration, spectral and prescribed base excitations. The results from the numerical panel method lead to improved prediction of the characteristics of TLCDs over a wide range of configurations, which is essential in control problems for optimum performance of buildings.

The weakness of all passive systems is the inability to provide significant reduction in motion to non-harmonic excitations, such as those encountered when the loadings are of impulsive type. In this case the very first excursion of the building's motion may be the worst in terms of its performance. To improve the TLCD's performance for such earthquake loadings, a TLCD equipped with a flow-triggering device is proposed and investigated experimentally and numerically. The TLCD equipped with a flow-triggering device can keep the fluid in an unbalanced state with a high potential energy. The fluid can be abruptly released at an appropriate time, counteracting the response of the structure induced by the earthquake excitation.

It is found that the damping ratio of TLCD equipped with the flow-triggering device tested in this study is higher than typical TLCD. This excessive damping ratio can deteriorate the control performance of the damper. Then, the designed optimum damping ratio is used to simulate in the numerical investigations under various types of excitations, and it is found from the numerical investigations that the performance of TLCD equipped with a flow-triggering device when the damping ratio of the system can be adjusted to the designed optimum value is better than the performance of typical TLCD.

Department..Civil Engineering.....Student's signature.. *Passagorn Chaiviriyawong*
 Field of study..Civil Engineering.....Advisor's signature.. *Panitana Lukkunaprasit*
 Academic year 2005..... Co-advisor's signature.. *Tospol Pinkaew*

ACKNOWLEDGEMENTS

I would like to express my sincere appreciation to the many individuals who helped me through this monumental endeavor. I would like to first thank my advisor, Prof. Panitan Lukkunaprasit, who provided encouragement, kindness, continuous support and friendship throughout the length of my research. I wish to express to him all my gratitude. I would also like to thank Assoc. Prof. Tospol Pinkaew and Prof. William C. Webster for their valuable guidance and constructive comments.

Next, I would like to thank my families who have constantly supported me during my years in graduate school.

I would like to acknowledge the financial support from the Royal Golden Jubilee Ph.D. Program under Thailand Research Fund and the partial financial support provided by University of California, Berkeley through Prof. William C. Webster. With both funds, I had an opportunity to study at the University of California at Berkeley for 11 months. This was very useful in broadening my experience and exchanging knowledge with Prof. William C. Webster who is an expert in this research topic.

I don't know what I would have done without my friends and colleagues: Jaruek Teerawong, Assawin Wanitkorkul, Somboon Siangchin, and Tayakorn Jaruchaimontri. Many thanks for their help in conducting experiments.

สถาบันวิทยบริการ
จุฬาลงกรณ์มหาวิทยาลัย

TABLE OF CONTENTS

	Page
Abstract (Thai)	iv
Abstract (English)	v
Acknowledgements	vi
Table of contents	vii
List of tables	ix
List of figures	x
Chapter I Introduction	1
1.1 Introduction	1
1.2 Problem Statement	7
1.3 Research Objectives	8
1.4 Scope of Research	9
1.5 Literature Review	9
1.6 Organization of Dissertation	12
Chapter II Tuned Liquid Column Dampers	13
2.1 Formulation of TLCDs	13
2.2 Modeling TLCD-Primary Structure System	15
2.3 Optimum Absorber Parameters	18
Chapter III The Shake Table Experiment of The Tuned Liquid Column Damper Models	22
3.1 Introduction	22
3.2 Design and Construction of TLCD Models	23
3.3 Measurement Devices	26
3.4 Experiment Investigations	27
3.5 Experimental Data	30
3.5.1 Free-vibration test data	30
3.5.2 Spectral test data	34
3.5.3 Prescribed base excitation test data	36
3.6 Verification of Results from Analytical Method Based on Simplified Effective Length	38
3.6.1 Spectral tests	38

3.6.2 Prescribed base excitation tests	40
3.7 Conclusions	44
Chapter IV Numerical Panel Method	45
4.1 Panel Method Formulation	45
4.2 Verification of Results from Numerical Panel Method	50
4.2.1 Effective lengths and natural frequencies	50
4.2.2 Frequency response curves	55
4.2.3 Improvement of panel method modeling	56
4.3 Conclusions	57
Chapter V Experiments and Simulations of TLCs equipped with a Flow- triggering Device	59
5.1 Introduction	59
5.2 Experimental Set-up	60
5.3 Experiment Investigations	62
5.3.1 Damping ratio for LCVAs equipped with a flow-triggering device	63
5.3.2 Verification of initial condition test results from numerical panel method	67
5.4 Numerical Examples of LCVA with the Initial Liquid Displacement	74
5.4.1 Impulse load and harmonic load	75
5.4.2 Earthquake ground motions	78
5.4.3 Guideline criteria for releasing the initial condition	85
5.5 Conclusions	89
Chapter VI Summary and Conclusion	90
References	93
Appendices	99
Appendix A Integral of Velocity Potential	100
Vita	102

LIST OF TABLES

Tables	Page
2.1 Comparison of optimal parameters for TMD and TLCD	21
2.2 Optimum parameters for white noise excitation for different mass ratios ...	21
4.1 The damper effective lengths and natural frequencies from various procedures	53
5.1 Summary of simulation results in case of impulse load and harmonic load .	77
5.2 Summary of simulation results in case of earthquake ground motion records	84



สถาบันวิทยบริการ
จุฬาลงกรณ์มหาวิทยาลัย

LIST OF FIGURES

Figures	Page
1.1 Classification of approaches for structural response control	2
1.2 Types of passive/ controllable-passive tanks for ships	5
1.3 (a) Liquid damper with pressure adjustment concept (b) Installed in Cosima Hotel, Tokyo	6
1.4 Millennium towers: passive and active TLCD concept (Sudjic, 1993)	7
1.5 Geometry of a LCVA	12
2.1 Geometry of TLCD	14
2.2 Schematic of the TLCD-Primary Structure system	16
2.3 Variation of dynamic magnification factor with the head-loss coefficient and frequency ratio for a TLCD	16
3.1 Water tank, which is made of acrylic plate for flow visualization	24
3.2 Tuned Liquid Column Damper Model with Insert Type I	24
3.3 Liquid Column Vibration Absorber Model with Insert Type II	25
3.4 Liquid Column Vibration Absorber Model with Insert Type III	25
3.5 KEYENCE laser displacement system	26
3.6 Force Measurement System	27
3.7 Time History Excitation no.1-3	28
3.8 Time History Excitation no.4-6	29
3.9 Free-vibration test data for LCVAs with inserts types II and III - liquid amplitude = 7 cm	30
3.10 The relationship between the damping ratio and liquid velocity: (a) TLCD with insert type I; (b) LCVA with insert type II; (c) LCVA with insert type III	32
3.11 Spectral test data at the natural frequency of each damper model	34
3.12 Responses due to prescribed base excitation no. 5	36
3.13 Experimental and analytical results of spectral tests of TLCD with Insert Type I	38
3.14 Experimental and analytical results of spectral tests of LCVAs with Inserts Types II&III	39
3.15 Experimental and analytical results of prescribed excitation test no.1 for TLCD with Insert Type I	41

Figure	Page
3.16 Experimental and analytical results of prescribed excitation test no.1 for LCVA with Insert Type II	42
3.17 Experimental and analytical results of prescribed excitation test no.1 for LCVA with Insert Type III	43
4.1 A linear combination of singularities	46
4.2 Source panel in global and local coordinates	48
4.3 Panel method modeling for TLCs and LCVAs	50
4.4 Induced velocity distribution in liquid column vibration absorber model .	51
4.5 Induced velocity distribution of 5 LCVA configurations investigated by Hitchcock (1997)	52
4.6 Variation of LCVA natural frequency with area ratio and vertical column height	54
4.7 Frequency response curves from experiment, existing analytical method and panel method	55
4.8 Induced velocity distribution in liquid column vibration absorber models with estimate of the effect of vortices	56
5.1 Photograph of the experimental set-up	60
5.2 Schematic diagram of the experimental set-up	61
5.3 Solenoid valve specification	62
5.4 The relationship between the decay rate of liquid displacement of LCVA without cover plate and LCVA with cover plate for insert type II	63
5.5 The relationship between the decay rate of liquid displacement of LCVA without cover plate and LCVA with cover plate for insert type III	64
5.6 The Relationship between the liquid amplitude and damping ratio for LCVA with insert type II	66
5.7 The Relationship between the liquid amplitude and damping ratio for LCVA with insert type III	66
5.8 Initial displacement 10 cm for LCVA with insert type II	67
5.9 Initial displacement 15 cm for LCVA with insert type II	68
5.10 Initial displacement 7.5 cm for LCVA with insert type III	69
5.11 Initial displacement 12.5 cm for LCVA with insert type III	70
5.12 The Relationship between the peak interaction force and initial	

displacement of 5-15 cm for LCVAs with inserts types II and III	71
5.13 Initial displacement 15 cm for LCVA with insert type II (extended in axis of time)	73
5.14 SDOF system with LCVA	75
5.15 Displacement response under impulse load type (initial velocity = 0.2 m/s)	77
5.16 Scale ground motion records	78
5.17 SDOF system response under 1952 Taft	79
5.18 Find minimum peak displacement by releasing the flow in every time step from start of event of 1952 Taft ground motion (Initial Condition = -0.5 m)	82
5.19 SDOF system response; (a) 1989 Loma Prieta; (b) 1985 Mexico city	83
5.20 SDOF system with LCVA mass response (but not released) subjected to 1989 Loma Prieta	87
5.21 SDOF system with LCVA applying with initial condition response (releasing time = 4.8 sec since the earthquake began) subjected to 1989 Loma Prieta	88

CHAPTER I

INTRODUCTION

1.1 Introduction

Vibration control of environmentally induced motions in civil engineering structures has been a topic of intensive research over the last 30 years. A need for new and better means of designing new structures and retrofitting existing ones from the damaging effects of severe environmental loadings has motivated civil engineers to embark on rather unfamiliar but innovative concepts of structural control. With the current trend of taller and more flexible building structures, which are prone to cause human discomfort, structural damage or even failure in extreme environmental loadings, means to suppress undesirable levels of vibration have become essential and integral aspect structural system in tall buildings.

One general way of classifying different approaches to suppressing the dynamic response of structural systems may be as follows:

- a) Input Reduction – to reduce the level of excitation or external energy transmitted to the structure, e.g. by means of base/seismic isolation.
- b) Damping Augmentation – to increase the damping capacity of the structure. Tuned mass dampers and tuned liquid column dampers are examples in this category.
- c) Structural Modification – to change the structural properties or configuration. Stiffening of structural components is one commonly used method.

The control approaches shown in Fig. 1.1 may be further classified into passive and active, depending on the requirements for both information and energy. The distinction between the two is obvious as the term active implies a control or modification by means of the action of a control system through some external energy supply, that is not required for passive control.

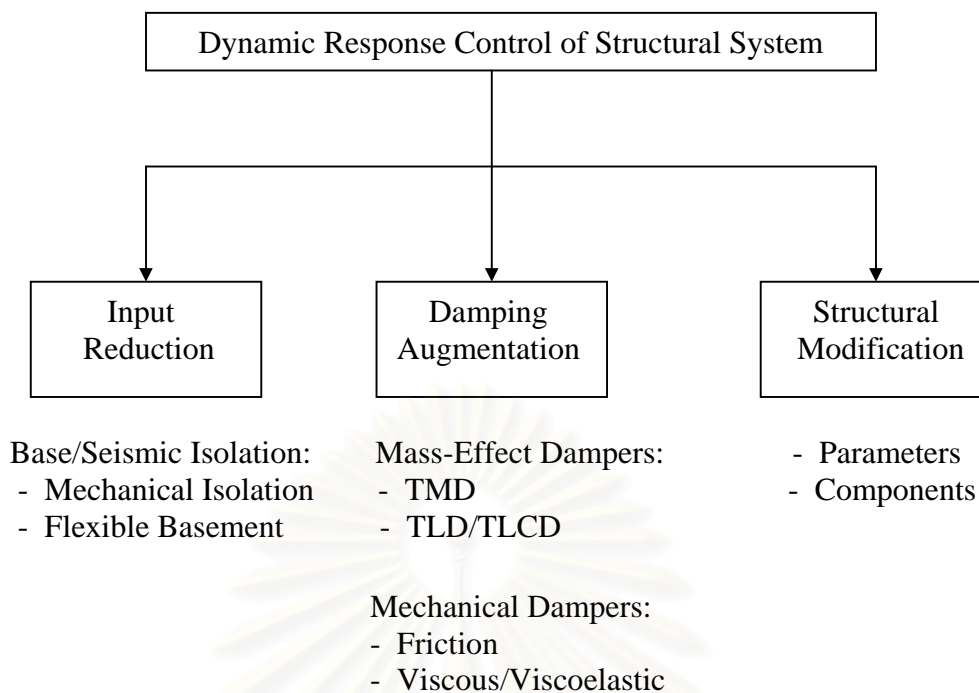


Fig. 1.1 Classification of approaches for structural response control (Izumi *et al.* 1992)

According to Soong (1997), the goal of structural control is to provide safety of the structures with acceptable human comfort and serviceability. Various passive control systems, e.g., tuned mass dampers and tuned liquid column dampers have been implemented with some degree of success. The active control systems, however, are yet to prove their reliability in performance in actual applications.

Much of the built environments around the seismic regions in the world were constructed during times when design codes either did not address seismic safety or were not adequate. Seismic safety codes are a developing process. With each new earthquake we find out conditions that were not well taken care of in previous design codes. Since the last decade or so, the Hanjin, Northridge, Loma Prieta and Kobe earthquakes have had much impact on design codes. The bottom line is that there are a large number of today's existing buildings that are unsafe by current standards.

To improve those building to meet current earthquake standards, there exist a number of different improvement methods. Strengthening of the buildings or installation of base isolation system may involve a lot of details, times, and cost while incorporating the passive dampers into the buildings is relatively simple and inexpensive. Therefore the research on the topics related to passive dampers has attracted increasing interest in recent years. Although there are many kinds of passive

dampers, the liquid type dampers are found to be attractive due to their unique advantages such as lower cost, easy handling, fewer maintenance requirements and no weight penalty to the structure when the water in the tanks is also used for fire fighting.

A proposed passive device for control of wind-induced motions in flexible structure is the tuned liquid column damper (TLCD). This simple device, liquid in a U-shaped container with an orifice, achieves the effect of vibration absorber or tuned mass damper (TMD). It has been implemented in the Higashi-Kobe cable-stayed bridge to reduce wind-induced vibration of the bridge towers. It has been shown that the system is simple, even simpler than TMDs as it requires no mechanical components, and extremely versatile in its application for temporary use and easy adaptation for retrofit schemes for existing structures. This device is particularly well suited for tall buildings since they usually contain water storage for potable or emergency use. Utilizing the already available water and proper modifications to the existing storage tanks, a TLCD can be formed without introducing an unnecessarily large additional mass. Furthermore, its natural frequency and damping characteristics can be easily modified.

1.1.1 Applications

1.1.1.1 Ship industry

The operation of a ship is influenced by the motions and forces induced by rolling, which can cause discomfort to passengers, reduction in crew efficiency or even damage to cargo. The first application of devices for ship stabilizing was made by Froude in 1862 followed by a practical application by Watts in 1880. After that, in 1911, A U-shaped tank is proposed as a roll stabilizer by Frahm. Widespread applications on commercial ships started in the 1950s. Advanced stabilizers with a microprocessor-based roll indicator were introduced in 1990.

Three basic categories of passive/ controlled passive dampers for roll stabilization in ships (Honkanen 1990), are shown in Fig. 1.2, namely,

- a) Free surface open tanks. These may be equipped with baffles/nozzle plates to generate internal damping. The required rolling frequencies can be obtained by providing an appropriate liquid level in the tank.

- b) U-tube tanks. In this category, two tanks are connected by a cross-over duct at the bottom with the air spaces above the fluid connected by a duct. Restricting the flow of air between the tanks creates the damping required.
- c) Free flooding tanks. This is similar to the U-tube tanks but the free flooding tanks are not connected through a cross-over duct. The top of the tanks is connected by an airduct to adjust the tank natural frequency by setting the size of the inlet ducts relative to the tank's internal free surface.

It should be noted that all these roll stabilizers affect only the roll amplitude and not the roll period (Sellars and Martin 1992).

1.1.1.2 Structural Applications

A TLCD has been installed in the Cosima Hotel in Tokyo (Fig. 1.3). The hotel is a 26 storey steel building with a height of 106.2 meters. This building has a height-to-width ratio of 4 and is therefore wind sensitive. The foundation of the building is firmly anchored to the ground using high-strength steel grout anchors. The 58 ton TLCD with pressure adjustment, called MOVICS, is installed on the top floor and has been observed to reduce the maximum wind-induced acceleration by 50-70% and the RMS acceleration by 50%. Other MOVICS systems have been installed in the Hyatt Hotel in Osaka and the Ichida Building in Osaka (Shimizu and Teramura 1994).

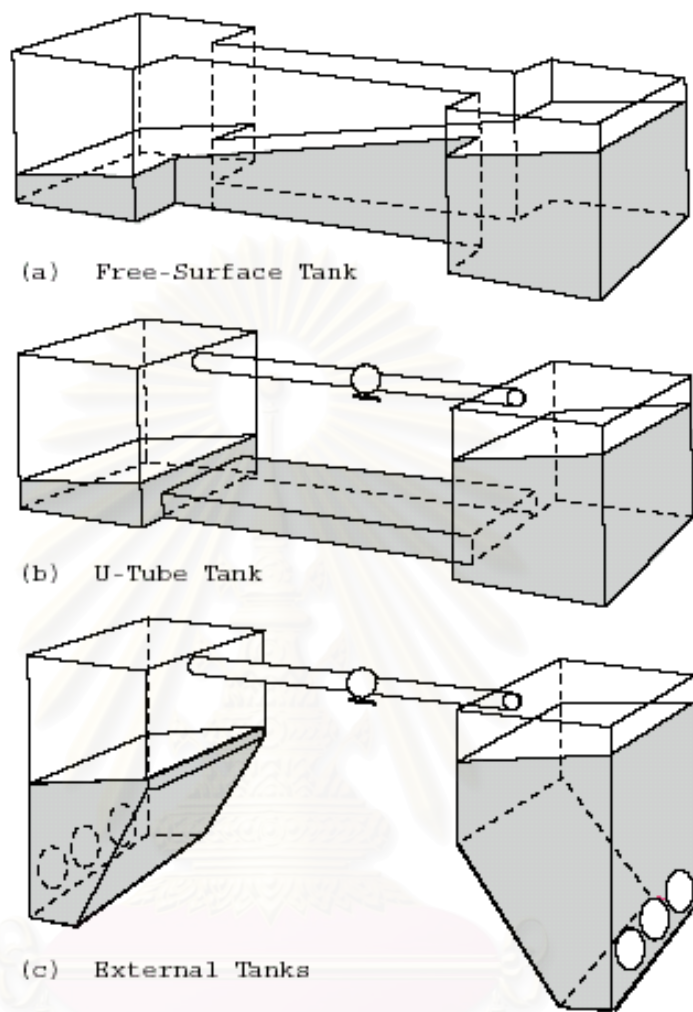


Fig. 1.2 Types of passive/ controllable-passive tanks for ships (Honkanen 1990)

สถาบันวิทยบริการ
จุฬาลงกรณ์มหาวิทยาลัย

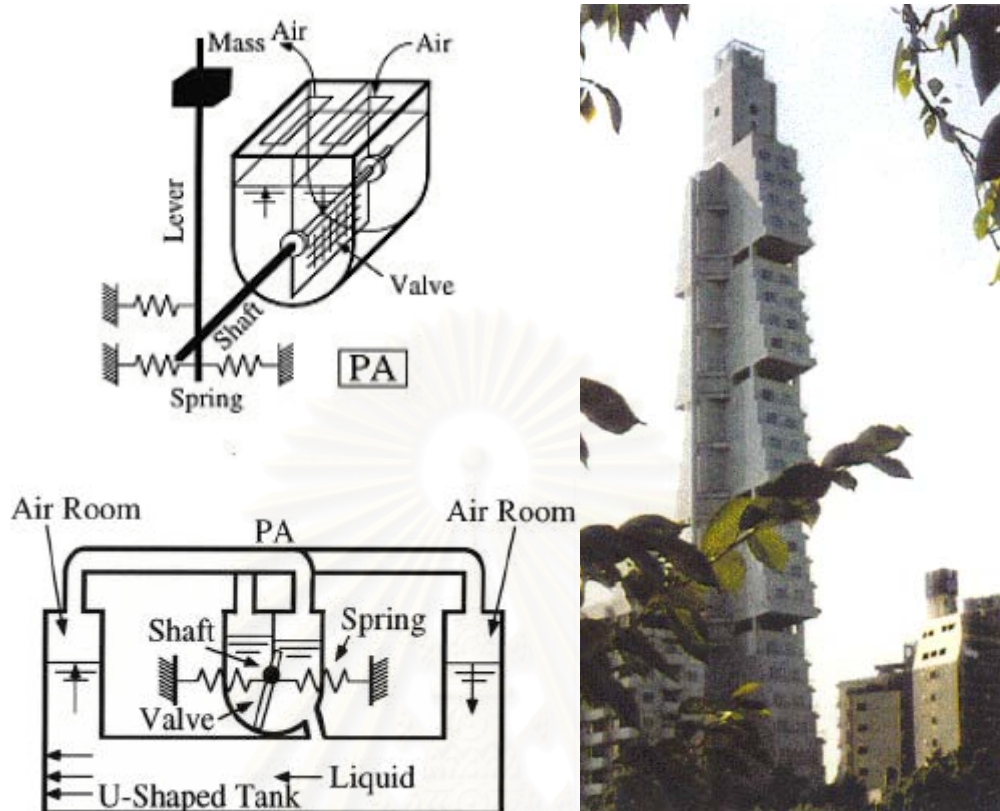


Fig. 1.3 (a) Liquid damper with pressure adjustment concept (b) Cosima Hotel, Tokyo equipped with tuned liquid column damper (Shimizu and Teramura 1994)

Recently, liquid dampers have been planned for the proposed Millennium Tower, Tokyo Bay, Japan. Due to this super-tall building's exposure to typhoons, external damping sources are supplemented to control the wind-induced vibrations. In addition to the massive steel blocks at the top, there are water tanks with ducts between them. The water would oscillate in the passive control mode under normal conditions, but under high winds, the sensors would trigger a pumping mechanism, changing the control mode from passive to active (Sudjic 1993). Fig. 1.4 shows the schematic of the circular TLCD concept in this tower.

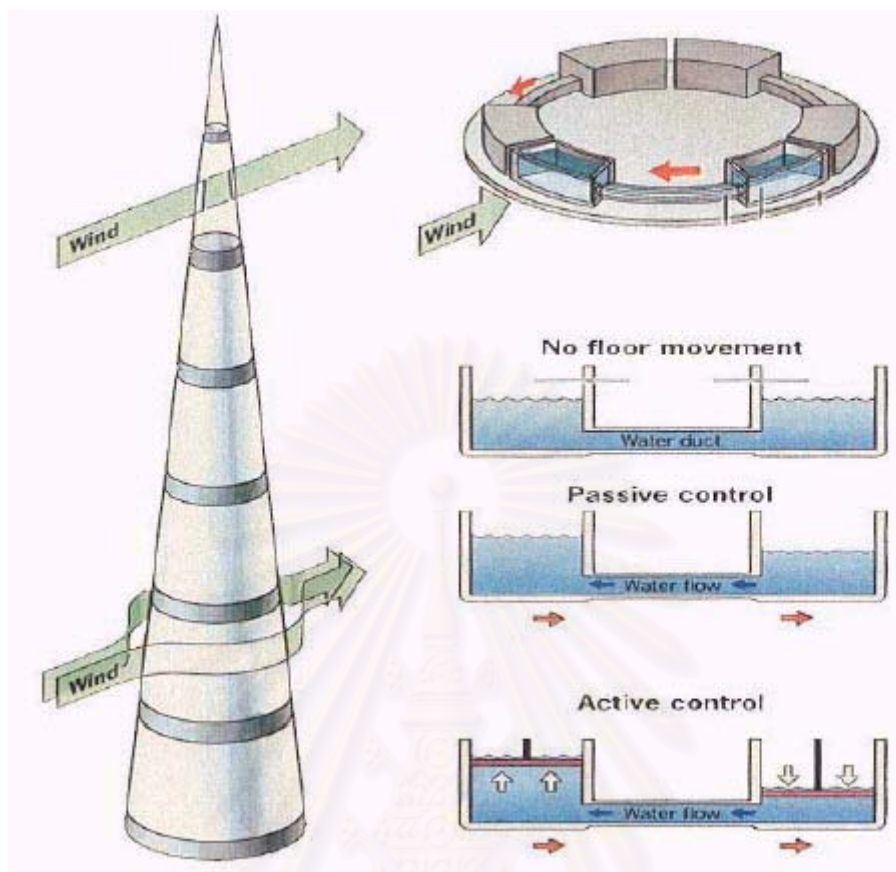


Fig. 1.4 Millennium towers: passive and active TLCD concept (Sudjic 1993)

1.2 Problem Statement

The control performance of liquid type dampers under wind excitations has been well established and consequently has been successfully applied to some practical structures including the Sakitama Bridge and the Shin Yokohama Prince Hotel, in Japan. Unlike the case of wind excitations, the studies of the dampers under seismic excitations are quite limited. This is mainly because some earlier works indicated rather poor performance of these dampers under seismic excitations.

Existing buildings that have been designed and built without consideration of seismic effects may need to be retrofitted. Utilization of passive dampers, e.g. tuned mass dampers (TMDs) for vibration reduction is one possible method. However, if the TMD is either large in physical size or heavy, then bringing the damper to the appropriate location in the existing building (normally high in the building) can

become a significant problem. On the other hand, small light-weight containers without water (which needs not be filled in until they are in place) may be easily transported to the desired locations in the building. Thus, liquid dampers appear to be attractive for use as seismic dampers in existing buildings.

The weakness of all passive systems is their lack of ability to provide significant reduction in motion to non-harmonic situations, such as those encountered when the loadings are of impulsive nature at the very beginning of the event. In this case the very first excursion of the building's motion may be the worst in terms of its performance. To improve the TLCD's performance for highly transient earthquake loadings, TLCD equipped with a flow-triggering device is proposed. The TLCD equipped with a flow-triggering device could keep the fluid in an unbalanced state with a high potential energy and could abruptly release the fluid at an appropriate time to counteract the motion of the primary structure.

1.3 Research Objectives

The goal of this study is to evaluate the performance of TLCD with various configurations. The main emphasis in this study is limited to a conceptual development of TLCD system equipped with a flow-triggering device for reduction of seismic-induced motion. An approximate numerical modeling for the system is developed, method to control the flow-triggering device is determined, and its potential as a control device for seismically induced motions in flexible structures is assessed by numerical simulations. The general objectives of this study are:

- a) To numerically and experimentally study the control characteristics of TLCDs with various configurations.
- b) To numerically and experimentally study the control characteristics of the TLCD equipped with a flow-triggering device.
- c) To numerically investigate the control performances of a SDOF system installed with TLCD and TLCD equipped with a flow-triggering device subjected to various cases of external loadings (such as impulse load, harmonic load and earthquake ground motions).

1.4 Scope of Research

The general scope of this study is limited to the following:

- a) The motion of the system is considered to be in one direction only.
- b) A long period primary system with a natural period in the 2 seconds range is investigated for damper performance.
- c) The performance of the TLCD-equipped system is evaluated within the elastic range of the primary structure using a numerical simulation. Furthermore the investigations are conducted based on a set of selective earthquake ground motion records.

1.5 Literature Review

A TLCD, the parent system of subject study, was first introduced by Saoka *et al.* (1988). The oscillation of the liquid mass in TLCD can be approximated by a single coordinate system. Therefore, the liquid oscillation may be idealized by one-dimensional rigid-body motion in contrast to the two-dimensional sloshing in tuned liquid damper (TLD). Saoka *et al.* (1988) showed that TLCD exhibits characteristics often found in TMD systems, and different levels of damping can be obtained with an orifice at various opening ratios. The relationship between the orifice opening ratio and the headloss coefficient for standard orifices can be found in earlier work (Blevins 1984). Sakai *et al.* (1989) further proposed the concept of a tuned liquid column damper and described an application for cable-stayed bridge towers. A similitude study of the tower of the Higashi-Kobe cable-stayed bridge was conducted, and TLCD was designed and later installed for the structure.

To obtain an effective liquid damper, it is essential that the fundamental modal frequency of liquid motion be tuned to the natural frequency of structure and the damping ratio of its motion be set to an optimal value. TLCDs were investigated for wind excited structures by Xu *et al.* (1992) and Balendra *et al.* (1995). Studies were also made for determining certain optimal characteristics of these passive devices by Gao *et al.* (1997); Chang and Hsu (1999); and Gao *et al.* (1999). Chang *et al.* (1998) investigated the control performance of TLCD under Gaussian white noise excitation.

The structure was modeled as a linear SDOF system while TLCD's properties such as the effective length and head-loss were varied in order to determine the optimal condition of TLCD. Based on numerical simulation, it was found that the performance of TLCD would vary as the excitation amplitude changes due to the nonlinearity in the damping term. In addition its performance is in general slightly inferior to that of TMD with the same mass since only a portion of its mass is effective.

The effectiveness of liquid type dampers has also been investigated under typical seismic excitations. The performance of TLCDs for seismic applications has been studied by Won *et al.* (1996) and Sadek *et al.* (1998). Sadek *et al.* numerically investigated the control performance of TLCD for a SDOF and a 10-storey building under 72 earthquake ground motion records. The results indicated that a proper selection of TLCD's parameters led to the reductions of the displacement and acceleration responses up to 47 percent. The study also concluded that although multiple-TLCDs are not necessarily superior to single TLCD, they are robust with regard to errors in estimating the structural parameters.

It should be noted that in most of the related investigations, the structures are assumed to vibrate within the elastic range, and the displacement reduction of the structures is taken as the control performance index. It has been recently shown that this index is inadequate for seismic application (Lukkunaprasit and Wanitkorkul 2001 and Pinkaew *et al.* 2001), since under high intensity earthquakes, the structure inevitably will experience inelastic deformation. Therefore, the performance of the control system will be better described by the reduction of damage or the reduction in the hysteretic energy absorption in the system rather than the displacement reduction.

Most of the studies described normally concern passive TLCDs without any active adjustment of the damping characteristics during operation. The passive damper is designed to be optimal at design amplitudes of excitation. Therefore, its performance generally deteriorates at other amplitudes of excitation. In order to solve this difficulty, semi-active and active systems have been proposed by Kareem (1994), Haroun *et al.* (1994), and Abe *et al.* (1996).

The semi-active control systems with variable damping have been widely studied in the area of structural control. Haroun *et al.* (1994) numerically investigated a hybrid liquid column damper (HLCD), which actively controls the orifice-induced damping forces by opening and closing the orifice under wind load and earthquake ground motions. The numerical results show that HLCD can be significantly more

effective over its parent TLCD system for long duration, periodic disturbances, while only a small amount of control effort is required to control the orifice. In seismic condition, HLCD with the orifice control can also be effective in quickly damping out the secondary response of the structure. Yalla *et al.* (2001) investigated a variable-damping semi-active TLCDS for vibration control of structures using numerical simulation. Both harmonic and random wind excitations were considered. In the case of harmonic loading the improvement of the semi-active system over the passive one was about 25-30% while for random excitation the improvement was about 10-15%.

Multiple Tuned Liquid Column Dampers (MTLCDs) with natural frequencies distributed around the natural frequency of the primary structure have been studied extensively by Chang *et al.* (1998); Gao *et al.* (1999) and Yalla and Kareem (2000). Such systems with smaller sizes of TLCDS facilitate construction, installation and maintenance. The dampers, when strategically located, can also be more effective than a single damper in reducing the motions of buildings undergoing complex motions (Bergman *et al.* 1990).

The TLCDS in the aforementioned works have the same widths in the two vertical columns and the cross-over duct. Another variation of TLCD, denoted as Liquid Column Vibration Absorbers (LCVAs), has been proposed by Watkins (1991) in which the fluid column cross-section is not uniform (as shown in Fig. 1.5). The performance of LCVA has been found to be as effective as or even more effective than TLCD (Chang and Hsu 1998). As will be described in a subsequent chapter, the natural frequency of the damper is determined by its “effective length” and this is related to the geometry of the tank and particularly to the ratio of the cross-section areas of the vertical columns and the cross-over duct (Hitchcock 1997).

Most previous research focuses on LCVAs with a small ratio of the transition zone between the vertical and horizontal portion (corner-to-corner width) to the horizontal length (in the range of 0.04 – 0.20). For buildings with limited space, it will be necessary to configure a LCVA with a significantly larger ratio of the corner-to-corner width to the horizontal length, for which research work is still lacking. It is thus significant to investigate the characteristics of TLCDS and LCVAs with a significantly larger ratio of the corner-to-corner width to the horizontal length.

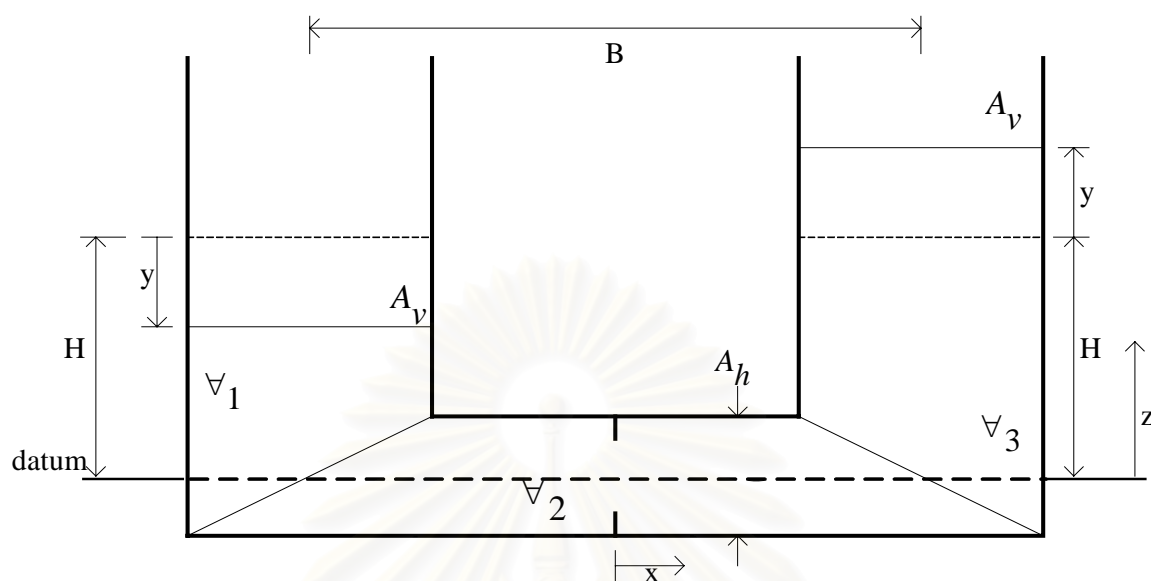


Fig. 1.5 Geometry of LCVA

1.6 Organization of Dissertation

The state-of-the-art of liquid dampers is introduced in Chapter 1. The problem statement and objectives are also given.

In Chapter 2, the fundamental concepts and principles of TLCD system in its passive mode are presented. The optimum absorber parameters for TLCDs are given for various load cases.

The experiments of a TLCD and LCVAs appropriate for application in long period buildings are described in Chapter 3. The test results are compared with existing analytical predictions, and the need for improvement is spelled out.

Chapter 4 discusses the development of the numerical panel method for accurately predicting the characteristics of LCVAs with various configurations

Those models tested in chapter 3 are equipped with a flow-triggering device and tested by varying the values of initial conditions. The test results are presented and compared to the numerical results in Chapter 5.

Finally, Chapter 6 presents important conclusions as well as recommendations for future research.

CHAPTER II

TUNED LIQUID COLUMN DAMPERS

In this chapter, the mathematical models of the TLCD and coupled SDOF-TLCD system are presented. Next, existing numerical optimization studies are given to determine the important parameters for optimum TLCD performance, namely, the tuning ratio and the damping ratio.

2.1 Formulation of TLCDs

Consider a TLCD with configuration shown in Fig. 2.1 excited by a base displacement, X_s . The vertical and the horizontal column cross-sectional areas are denoted as A_v and A_h , respectively. As shown in Fig. 2.1, during the motion, the liquid volume inside the TLCD can be divided into two vertical portions (\forall_1 and \forall_3), and one horizontal portion (\forall_2). From the continuity of liquid motion, the liquid moves horizontally relative to the tube with a homogenous velocity of $r\dot{x}_f$ in portion \forall_2 , where r is the area ratio of the TLCD defined as $r = \frac{A_v}{A_h}$, while in portions \forall_1 and \forall_3 , the liquid moves vertically relative to the tube with a homogenous velocity of \dot{x}_f .

By using the energy principles, assuming the internal energy of the liquid remains unchanged during the motion, the unsteady, non-uniform and incompressible flow equation along the streamline for the TLCD can be derived using the Lagrange equation:

$$\frac{d}{dt} \left(\frac{\partial T}{\partial \dot{x}_f} \right) - \frac{\partial T}{\partial x_f} + \frac{\partial V}{\partial x_f} = Q \quad (2.1)$$

where T and V are the total kinetic energy and the total potential energy of the system, respectively. Q is the total non-conservative force in the direction of x_f , which can be related to the head loss.

The kinetic energy of the oscillating liquid body can be obtained as follows:

$$\begin{aligned} T &= \int_{v_1} \frac{\dot{x}_f^2}{2} \rho dv + \int_{v_2} \frac{(r\dot{x}_f + \dot{X}_s)^2}{2} \rho dv + \int_{v_3} \frac{\dot{x}_f^2}{2} \rho dv \\ &= \rho A_v h \dot{x}_f^2 + \rho A_h b \frac{(r\dot{x}_f + \dot{X}_s)^2}{2} \end{aligned} \quad (2.2)$$

where ρ = The density of liquid inside the TLCD

b = The horizontal width of liquid inside the TLCD

h = The vertical height of liquid inside the TLCD.

The potential energy of the liquid can be expressed as

$$\begin{aligned} V &= \rho g A_v \int_0^{h-x_f} z dz + \rho g A_v \int_0^{h+x_f} z dz \\ &= \rho g A_v (h^2 + x_f^2) \end{aligned} \quad (2.3)$$

in which g = The acceleration due to gravity

z = The vertical coordinate measuring from a reference datum.

The non-conservative force in this case is the damping force of liquid motion, and it can be expressed as (Saoka *et al.* (1988))

$$Q = -(\rho g A_h) \left(\frac{\xi}{2g} \frac{r|\dot{x}_f|}{|\dot{x}_f|} \right) = -\frac{1}{2} \rho A_v r \xi |\dot{x}_f| \dot{x}_f \quad (2.4)$$

It should be noted that the damping force is a nonlinear function of velocity. Therefore, TLCD exhibits nonlinear damping characteristic. The absolute value sign

on \dot{x}_f is to ensure that the damping force, Q , is always opposite to the flow velocity.

By substituting Eqs. (2.2)-(2.4) into (2.1), the resulting governing equation for the motion of the fluid in the tube is

$$\rho A_v L_e \ddot{x}_f + \frac{1}{2} \rho A_v r \xi \left| \dot{x}_f \right| \dot{x}_f + 2 \rho A_v g x_f = -\rho A_v b \ddot{X}_s \quad (2.5)$$

where ξ = The coefficient of head loss

$L_e = rb + 2h$ = The effective length of TLCD

$\omega_f = \sqrt{\frac{2g}{L_e}}$ = The natural frequency of oscillations in the tube.

Eq. (2.5) has the same form as the original formula given by Sakai (1989) when r is equal to one.

Two different definitions for the effective moving fluid in the liquid dampers have been suggested. Gao et al. (1997), and Chang et al. (1998) use the center line dimensions to define the effective width and height, while Hitchcock (1997) uses the outer dimension to define the effective height and the inner length between the two columns as the effective width. These give rise to different effective lengths, which may differ substantially in some cases as will be demonstrated in Chapter 4.

2.2 Modeling of TLCD-Primary Structure System

Fig. 2.2 shows the schematic of a TLCD mounted on a structure represented as an equivalent single-degree-of-freedom (SDOF) system. The base is subjected to a ground motion $\ddot{u}_g(t)$.

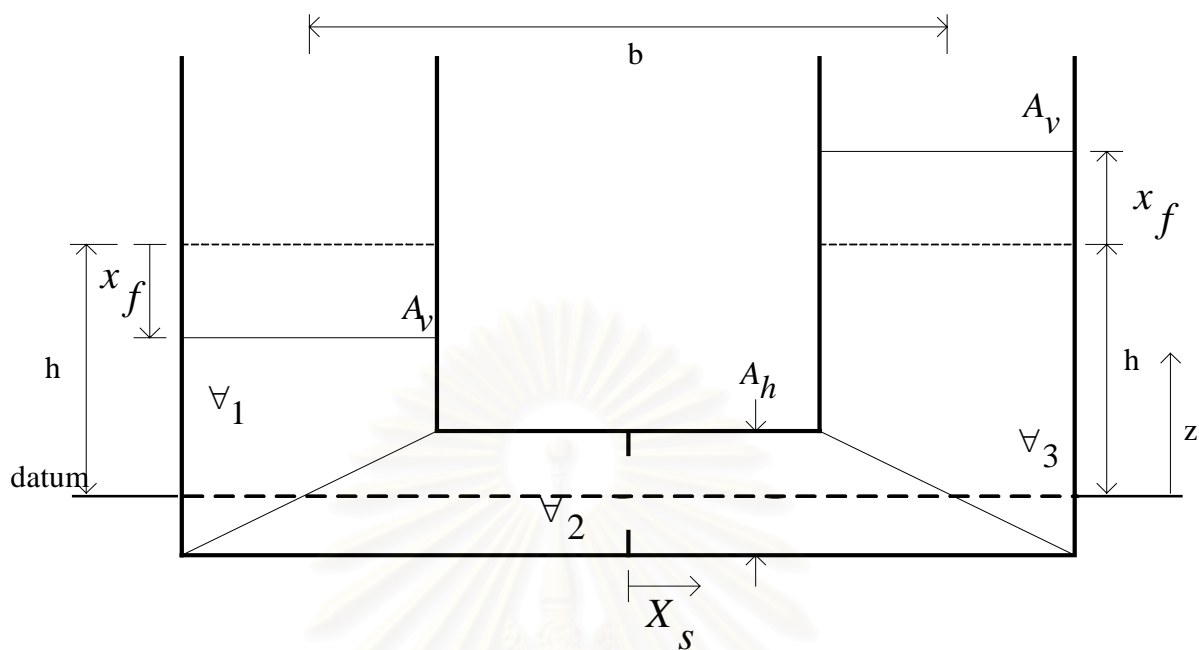


Fig. 2.1 Geometry of TLCD

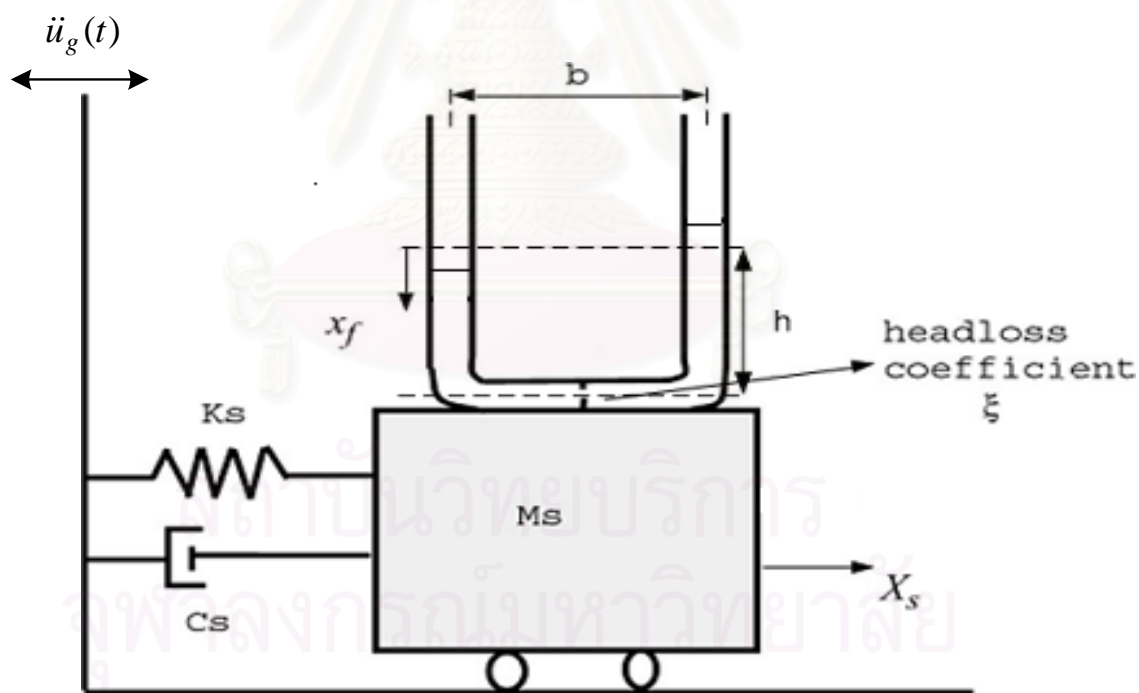


Fig. 2.2 Schematic of the TLCD-Primary Structure system

Applying the Lagrange equations of motion, one obtains the governing equations as follows:

$$\rho A_v L_e \ddot{x}_f(t) + \frac{1}{2} \rho A_v \xi \left| \dot{x}_f(t) \right| \dot{x}_f(t) + 2\rho A_v g x_f(t) = -\rho A_v b (\ddot{X}_s(t) + \ddot{u}_g(t)) \quad (2.6a)$$

$$\begin{aligned} & (M_s + \rho A_v \left(\frac{b}{r} + 2h\right)) \ddot{X}_s(t) + \rho A_v b \ddot{x}_f(t) + C_s \dot{X}_s + K_s X_s(t) \\ & = -(M_s + \rho A_v \left(\frac{b}{r} + 2h\right)) \ddot{u}_g(t) \end{aligned} \quad (2.6b)$$

where M_s = mass of the primary system; X_s = the primary system (structure) response which is the base displacement of the TLCD relative to the ground; K_s = stiffness of the primary system; C_s = damping in the primary system = $2M_s \zeta_s \omega_s$; ζ_s = damping ratio of the primary system and ω_s = natural frequency of the primary system. The two equations can be combined into the following matrix equation:

$$\begin{aligned} & \begin{bmatrix} M_s + \rho A_v \left(\frac{b}{r} + 2h\right) & \alpha m_f \\ \alpha m_f & m_f \end{bmatrix} \begin{bmatrix} \ddot{X}_s \\ \ddot{x}_f \end{bmatrix} + \begin{bmatrix} C_s & 0 \\ 0 & c_f \end{bmatrix} \begin{bmatrix} \dot{X}_s \\ \dot{x}_f \end{bmatrix} + \begin{bmatrix} K_s & 0 \\ 0 & k_f \end{bmatrix} \begin{bmatrix} X_s \\ x_f \end{bmatrix} \\ & = - \begin{bmatrix} M_s + \rho A_v \left(\frac{b}{r} + 2h\right) \\ \alpha m_f \end{bmatrix} \ddot{u}_g(t) \end{aligned} \quad (2.7)$$

subject to $|x_f| \leq h \quad (2.8)$

where α = length ratio = b/L_e ; $m_f = \rho A_v L_e$; c_f = equivalent damping of the liquid damper = $2m_f \omega_f \zeta_f$; ζ_f = damping ratio of TLCD and k_f is the stiffness of the liquid column = $2\rho A_v g$. The constraint condition in Eq. (2.8) is placed so as to

ensure that the liquid in the tube maintains the U-shape and the water does not spill out of the tube, thereby decreasing the dampers effectiveness.

An iterative procedure is needed to solve the nonlinear equations. The coupled nonlinear equations of motion governing the vibration of the SDOF-TLCD system, Eq. (2.7a), are solved by using the sub-system concept (Lukkunaprasit and Wanitkorkul (2001)). Basically, if \ddot{x}_f is assumed, then the first equation of Eq. (2.7) will contain only one unknown variable, X_s , and it can be easily solved by the direct integration method (Newmark (1959) or Chopra (1995)). Then, the obtained value of the primary system displacement, X_s , is substituted into the second equation of Eq. (2.7), from which the liquid displacement, x_f , can be solved. By substituting, x_f , back to the first equation of Eq. (2.7), a new value of X_s is determined. The iterative procedure is repeated by alternatively solving the first and second equation of Eq. (2.7) as described until convergence in X_s , x_f and TLCD damping ratio is achieved within the specified tolerance.

To facilitate estimation of the nonlinear damping, the liquid velocity, \dot{x}_f , at each time increment is estimated by using the first three terms in a Taylor series expansion of \dot{x}_f as (Sadek *et al.* 1998)

$$\dot{x}_f(t) = \frac{5}{2}\dot{x}_f(t-\Delta t) - 2\dot{x}_f(t-2\Delta t) + \frac{1}{2}\dot{x}_f(t-3\Delta t) \quad (2.9)$$

2.3 Optimum Absorber Parameters

It has been observed from numerical studies that the head loss coefficient affects the structure's frequency response curve. As the head loss coefficient (ξ) increases, the response curve changes from a double hump curve to a single hump curve (Fig. 2.3). Numerical studies conducted by Yalla (2000) indicate that the optimal damping ratio is independent of the excitation level.

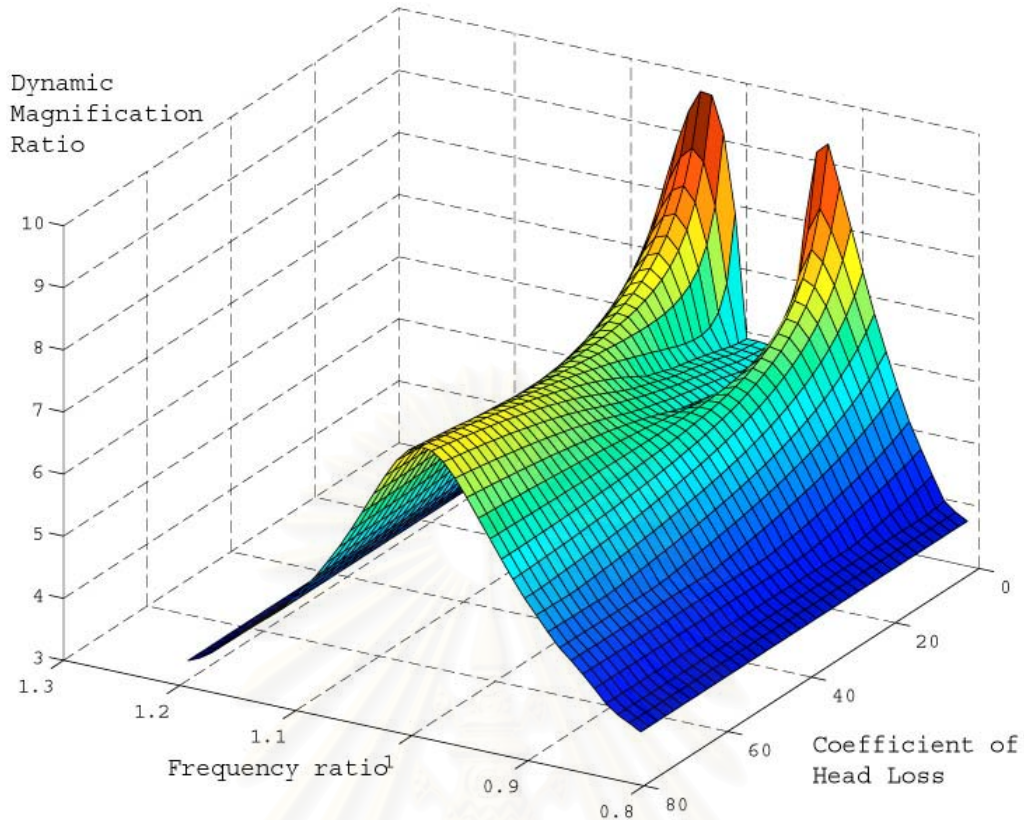


Fig. 2.3 Variation of dynamic magnification factor with the head-loss coefficient and frequency ratio for a TLCD (Yalla 2000)

The optimal absorber parameters are derived for the case of white noise. The optimal absorber parameters (i.e., optimum damping ratio and optimum tuning frequency (ζ_f and $\gamma = \omega_f / \omega_s$)) are obtained numerically for these cases. Based on the white noise excitation models, optimal parameters have been obtained for TLCD attached to a damped and undamped primary systems. For the case of an undamped structure-TLCD system subjected to white noise, an explicit expression can be derived. However, for damped systems and/or other excitations, the development of closed-form solutions is not possible, in general. Therefore, the optimal absorber parameters are obtained numerically for these cases.

The optimal conditions are obtained by setting (Yalla 2000):

$$\frac{\partial \sigma_{x_s}^2}{\partial \zeta_f} = 0; \frac{\partial \sigma_{x_s}^2}{\partial \gamma} = 0 \quad (2.10)$$

where $\sigma_{x_s}^2$ = the variance of the primary system displacement. One can obtain ζ_{opt} and γ_{opt} by solving the two conditions given by Eq. (2.10)

For an undamped primary system, solving the two optimization conditions in Eq. (2.10) and setting $\zeta_s = 0$ yields:

$$\zeta_{opt} = \frac{\alpha}{2} \sqrt{\frac{\mu(1+\mu-\alpha^2\frac{\mu}{4})}{(1+\mu)(1+\mu-\alpha^2\frac{\mu}{2})}}; \gamma_{opt} = \frac{\sqrt{1+\mu(1-\frac{\alpha^2}{2})}}{1+\mu} \quad (2.11)$$

where μ is the mass ratio = m_f / M_s .

In case one can assume the tuning ratio to be equal to one, i.e. $\gamma_{opt} = 1$, one can obtain a simpler expression for the optimal damping given by

$$\zeta_{opt} = \frac{1}{2} \sqrt{\frac{\mu(\mu+\alpha^2)}{1+\mu}} \quad (2.12)$$

This is justifiable because for the low mass ratios of the order 1-3% practical for tall buildings, the tuning ratio is close to one, and in this case the optimal damping coefficient given by Eq. (2.12) approximates Eq. (2.11) quite well. It is interesting to note that similar expressions exist for an optimal damping coefficient and tuning ratio of a TMD given by Warburton and Ayorinde (1980),

$$\zeta_{opt} = \frac{1}{2} \sqrt{\frac{\mu(1+\frac{3\mu}{4})}{(1+\mu)(1+\frac{\mu}{2})}}; \gamma_{opt} = \frac{\sqrt{1+\frac{\mu}{2}}}{1+\mu} \quad (2.13)$$

Note that in all cases considered, the optimum damping coefficient is independent of the value of the intensity of white noise excitation. It is worth noting that Eq. (2.11) reduces to Eq. (2.13) as α approaches 1. A list of optimal parameters under different optimization criteria is given in Table 2.1 for TMDs and TLCs.

TABLE 2.1 Comparison of optimal parameters for TMD and TLCD (Warburton (1982) and Yalla (2000))

Case number and parameter optimized			TMD		TLCD	
			γ_{opt}	ζ_{opt}	γ_{opt}	ζ_{opt}
1	Random Force acting on Structure	$\langle X_s^2 \rangle$	$\frac{\sqrt{1+\frac{\mu}{2}}}{1+\mu}$	$\frac{1}{2} \frac{\sqrt{\mu(1+\frac{3\mu}{4})}}{\sqrt{(1+\mu)(1+\frac{\mu}{2})}}$	$\frac{\sqrt{1+\mu(1-\frac{\alpha^2}{2})}}{1+\mu}$	$\frac{\alpha}{2} \frac{\sqrt{\mu(1+\mu-\frac{\alpha^2\mu}{4})}}{\sqrt{(1+\mu)(1+\mu-\frac{\alpha^2\mu}{2})}}$
2	Random acceleration at the base	$\langle X_s^2 \rangle$	$\frac{\sqrt{1-\frac{\mu}{2}}}{1+\mu}$	$\frac{1}{2} \frac{\sqrt{\mu(1-\frac{\mu}{4})}}{\sqrt{(1+\mu)(1-\frac{\mu}{2})}}$	$\frac{\sqrt{1+\mu(1-\frac{3\alpha^2}{2})}}{1+\mu}$	$\frac{\alpha}{2} \frac{\sqrt{\mu(1-\mu+3\frac{\alpha^2\mu}{4})}}{\sqrt{(1+\mu)(1+\mu-\frac{3\alpha^2\mu}{2})}}$
3	Random Force acting on Structure	$\langle \dot{X}_s^2 \rangle$	same as case 2	same as case 2	same as case 2	same as case 2
4	Random acceleration at the base	$\langle \dot{X}_s^2 \rangle$	same as case 1	same as case 1	same as case 1	same as case 1

As discussed earlier, it is not possible to obtain closed-form solutions for optimum damper parameters for a damped primary system; therefore, they must be estimated numerically (Warburton 1982). Optimum absorber parameters are presented in Table 2.2 for $\zeta_s = 1, 2$ and 5% and $\mu = 0.5, 1, 1.5, 2$ and 5% along with the undamped case.

TABLE 2.2 Optimum parameters for white noise excitation for different mass ratios (Yalla 2000)

	Undamped primary system		1% Damping		2% Damping		5% Damping	
	γ_{opt}	ζ_{opt}	γ_{opt}	ζ_{opt}	γ_{opt}	ζ_{opt}	γ_{opt}	ζ_{opt}
$\mu=0.5\%$	0.9965	0.0317	0.9962	0.0317	0.9958	0.0317	0.995	0.0317
$\mu=1\%$	0.993	0.0448	0.9925	0.0448	0.9921	0.0448	0.9908	0.0448
$\mu=1.5\%$	0.9896	0.0547	0.989	0.0547	0.9885	0.0547	0.9869	0.0547
$\mu=2\%$	0.986	0.0631	0.9855	0.0631	0.985	0.0631	0.983	0.0631
$\mu=5\%$	0.966	0.0986	0.965	0.0986	0.964	0.0986	0.962	0.0986

CHAPTER III

THE SHAKE TABLE EXPERIMENT OF THE TUNED LIQUID COLUMN DAMPER MODELS

3.1 Introduction

As mentioned in the previous chapter, most previous research focuses on LCVAs with a small ratio of the transition zone between the vertical and horizontal portion (corner-to-corner width) to the horizontal length. Prediction of the natural frequency of a LCVA in those studies is based on the assumption that the liquid velocity can be expressed as one value of an effective average velocity in each considered portion. Different researchers have also suggested different definitions for the effective length of LCVA based on different idealization of the moving fluid, resulting in different values of the natural frequencies (Gao and Kwok (1997), Chang and Hsu (1998) and Hitchcock (1997)). For buildings with limited space, it will be necessary to configure a LCVA with a significantly larger ratio of the corner-to-corner width to the horizontal length, for which research work is still lacking.

This chapter reports the test results of the tuned liquid column dampers (TLCDs) on the shake table. Three models of TLCDD having the same natural period (based on the existing analytical model) are investigated under free-vibration tests, spectral tests and time history tests. One of them has the same cross-sectional area in the horizontal and vertical columns. The others have different cross-sectional areas in the horizontal and vertical columns. Their sizes of the transition regions between the vertical and horizontal portions (corner-to-corner widths) are large compared to the horizontal width and the vertical height in LCVAs. By using the existing analytical model given by Gao and Kwok (1997) or Chang and Hsu (1998), the characteristics of this type of LCVA will be studied and compared with the test results with an aim to verify the existing analytical model.

3.2 Design and Construction of TLCD Models

In most previous research, the TLCDs and LCVAs investigated have small ratios of the transition boundary between the vertical and horizontal portions (corner-to-corner width) to the horizontal length in the range of 0.04 – 0.20. It is thus significant to investigate the characteristics of TLCDs and LCVAs with a significantly larger ratio of the corner-to-corner width to the horizontal length, which may be appealing for buildings with limited space, a situation usually encountered in practice due to high demand for saleable space. This configuration has been used as a roll stabilizer in ships also (Webster, 1989,1998). The damper configurations are studied here and are labeled Type I, Type II and Type III (shown in Figs. 3.1 - 3.4). The corner-to-corner width to horizontal length ratio ranges from 0.35 to 0.75 in the models tested.

The damper model consists of two parts. The first part is a rectangular tank, which is made of acrylic plates for flow visualization. The second part is an insert, which is used to configure the tank to the desired TLCD. Three different inserts, constructed from polyurethane closed-cell foam, are employed in this test to provide three different models of TLCD. All models of TLCD are supposed to be tuned to the structure of approximately 20 stories height, which has the fundamental natural period of about 2 seconds.

The dimensions of three models of TLCDs investigated in all tests are shown in Figs. 3.2 - 3.4. The models are designed to have the same effective lengths of $L_e = 2.07$ m, based on the simplified effective length by Gao and Kwok (1997) or Chang and Hsu (1998), and are expected to have the natural frequencies, f_n , of 0.49Hz.

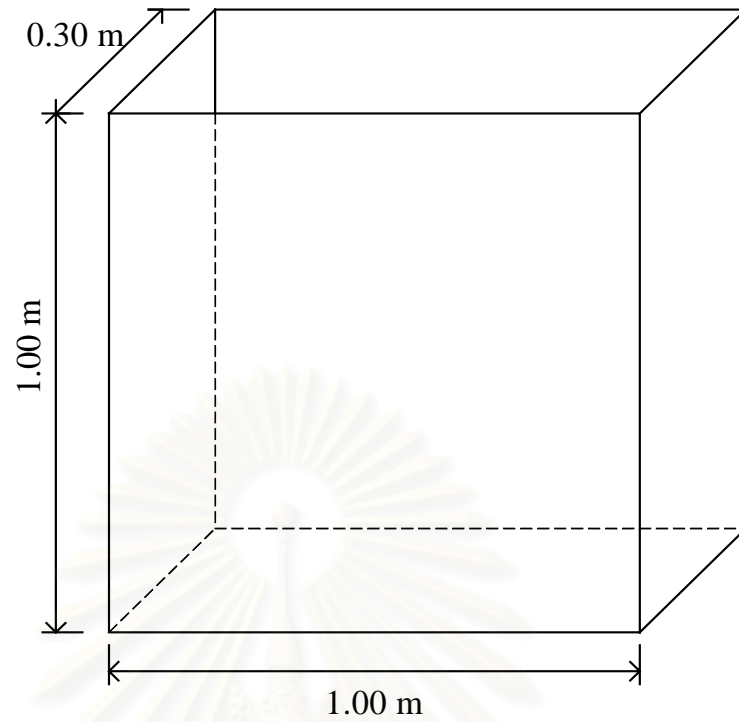


Fig. 3.1 Water tank, which is made of acrylic plate for flow visualization

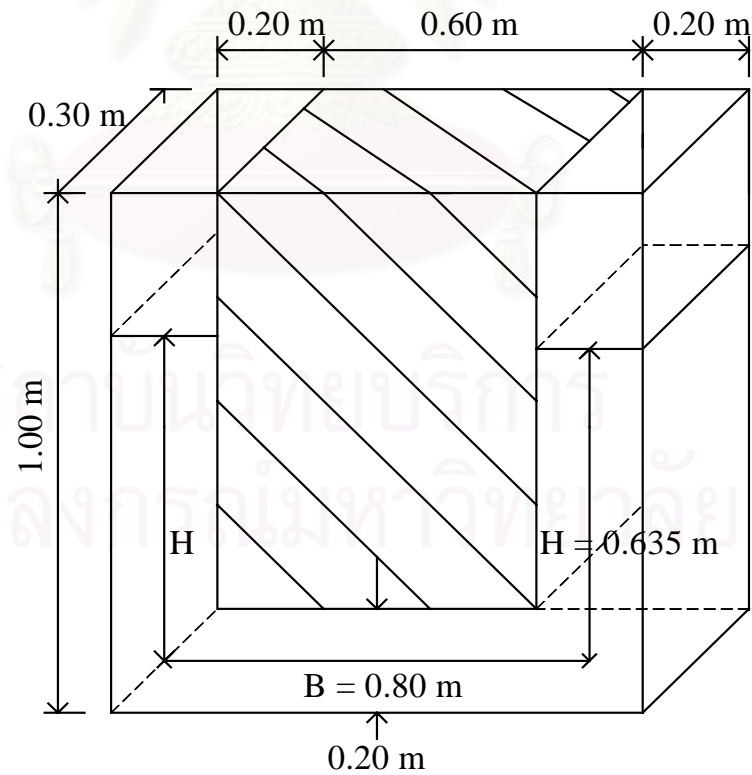


Fig. 3.2 Tuned Liquid Column Damper Model with Insert Type I

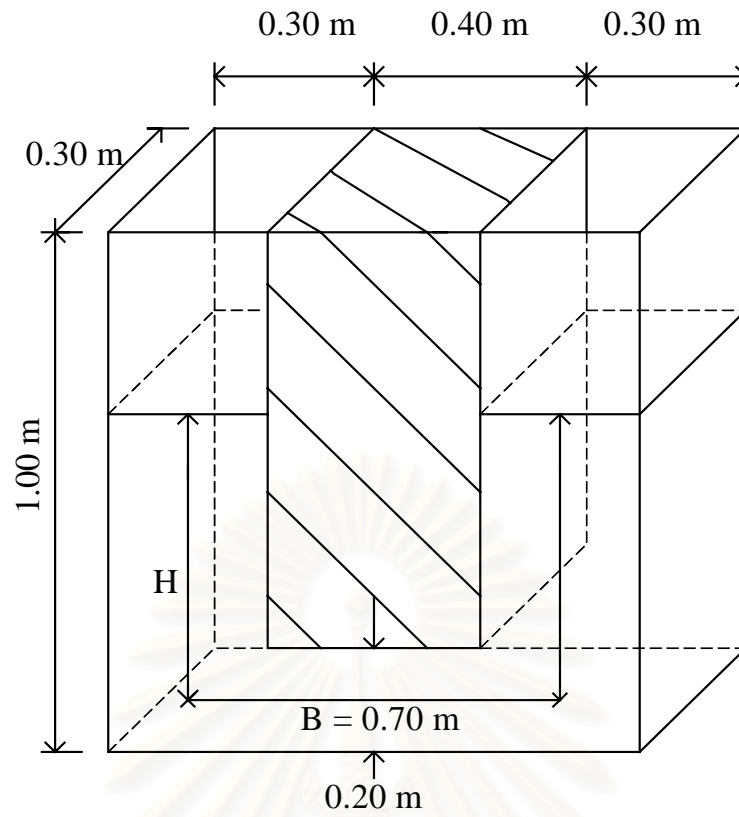


Fig. 3.3 Liquid Column Vibration Absorber Model with Insert Type II

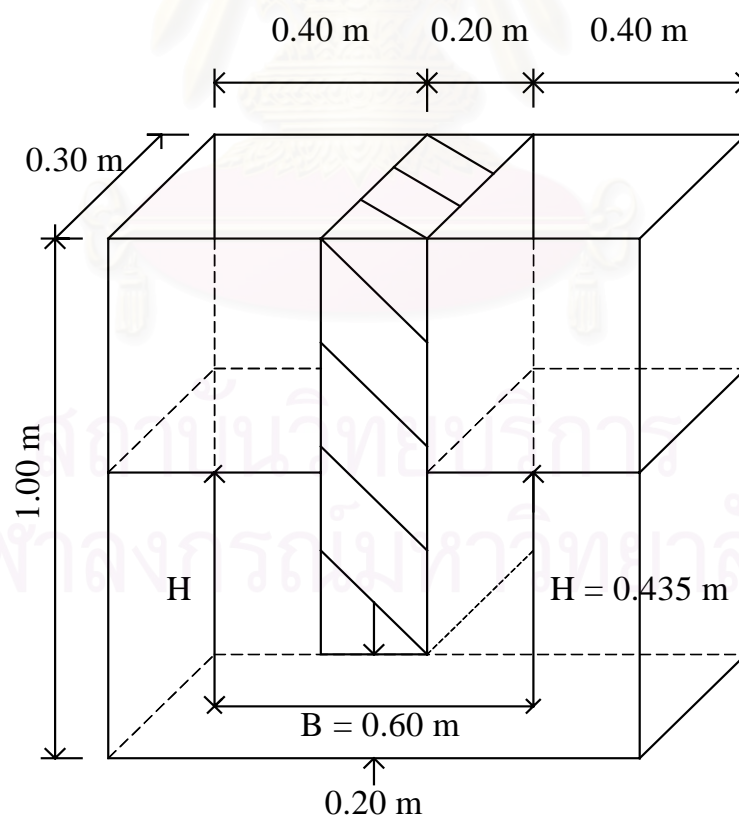


Fig. 3.4 Liquid Column Vibration Absorber Model with Insert Type III

3.3 Measurement Devices

The measurements include water level, lateral force (interaction force) at the base of the damper due to liquid motion, and shake table motion. A Keyence laser displacement sensor (as shown in Fig.3.5) is used to measure the displacement of liquid motion. Its measuring range is ± 100 mm with a resolution of $50\ \mu\text{m}$. The interaction force due to liquid motion in the TLCD is determined by the 2-kN Tokyo Sokki Kenkyujo load cell (as shown in Fig. 3.6). The shake table motion is measured by means of a Kyowa accelerometer and LVDT for its acceleration and displacement, respectively.

All devices were calibrated to ensure accurate measurements. Masses with exact weight are used to calibrate the force measurement system. The plates with exact thickness are used to calibrate the laser displacement system and LVDT. The accelerometer is also calibrated by means of gravity.



Fig. 3.5 KEYENCE laser displacement system



Fig. 3.6 Force Measurement System

3.4 Experimental Investigations

The damper models are firmly fixed on top of the shake table which can be horizontally moved by an actuator. The scope of tests consists of the following:

- (a) **Free-vibration tests** : The purpose of the free vibration tests is to determine the dynamic properties of the liquid motion by using 12 different initial displacements ($\pm 3\text{cm}$ to $\pm 8\text{cm}$). Based on these free vibration responses, the damping ratio and natural frequency of liquid motion for each model of the TLCD can be calculated.
- (b) **Spectral tests** : These tests have been investigated to determine the frequency responses of liquid motion for each model using sinusoidal base excitation with the excitation frequency ranging from $0.7 f_0$ to $1.3 f_0$ where f_0 is the natural frequency of the liquid motion obtained from the free-vibration tests (In spectral tests, the frequency range is between 0.35 Hz – 0.65 Hz).
- (c) **Prescribed base excitation tests** : These tests have been investigated to determine the responses of liquid motion for model under 6 prescribed base excitations as shown in Figs. 3.7 and 3.8. The prescribed base excitations no.1, 3 and 5 will excite the damper model around its resonance frequency. For the prescribed base excitations no.2, 4 and 6, the shapes are similar to the prescribed

base excitations no.1, 3 and 5, respectively, but they will excite the damper model around half of its resonance frequency.

The interaction force of TLCD, its head-loss coefficient, the phase and also the liquid column displacement are measured from all experiments.

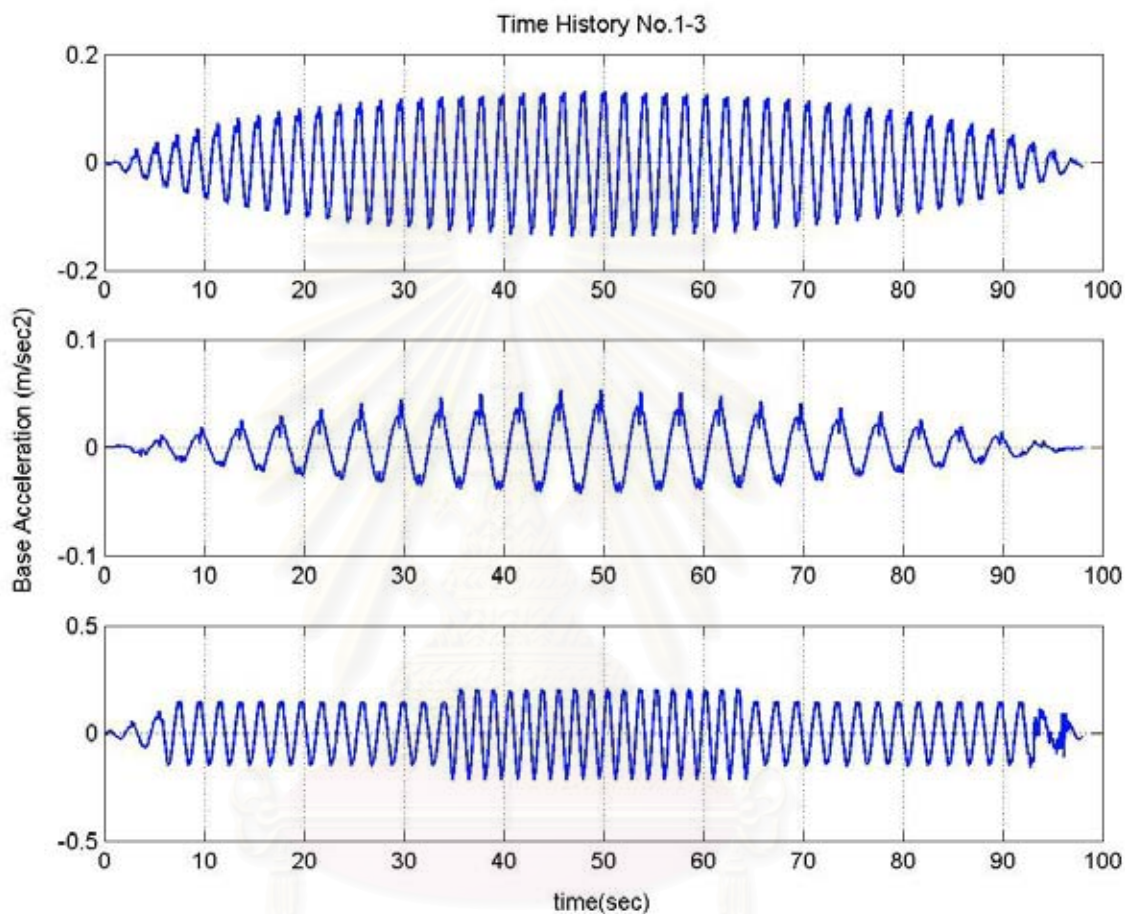


Fig. 3.7 Prescribed Base Excitation no.1-3

สถาบันวิจัยบริการ
จุฬาลงกรณ์มหาวิทยาลัย

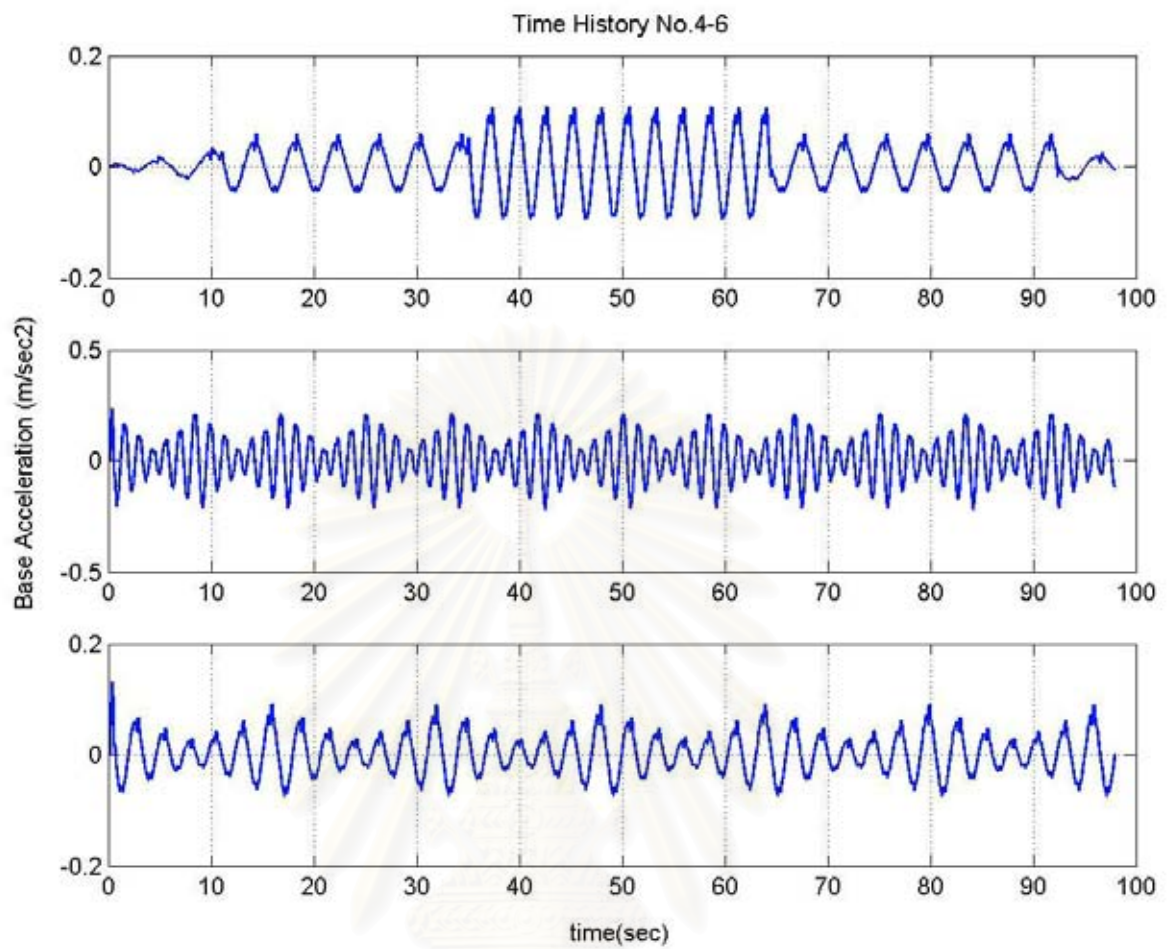


Fig. 3.8 Prescribed Base Excitation no.4-6

สถาบันวิทยบริการ
จุฬาลงกรณ์มหาวิทยาลัย

3.5 Experimental Data

3.5.1 Free-vibration test data

Fig. 3.9 shows the free-vibration test data for LCVAs with inserts types II and III. The liquid amplitude was 7 cm.

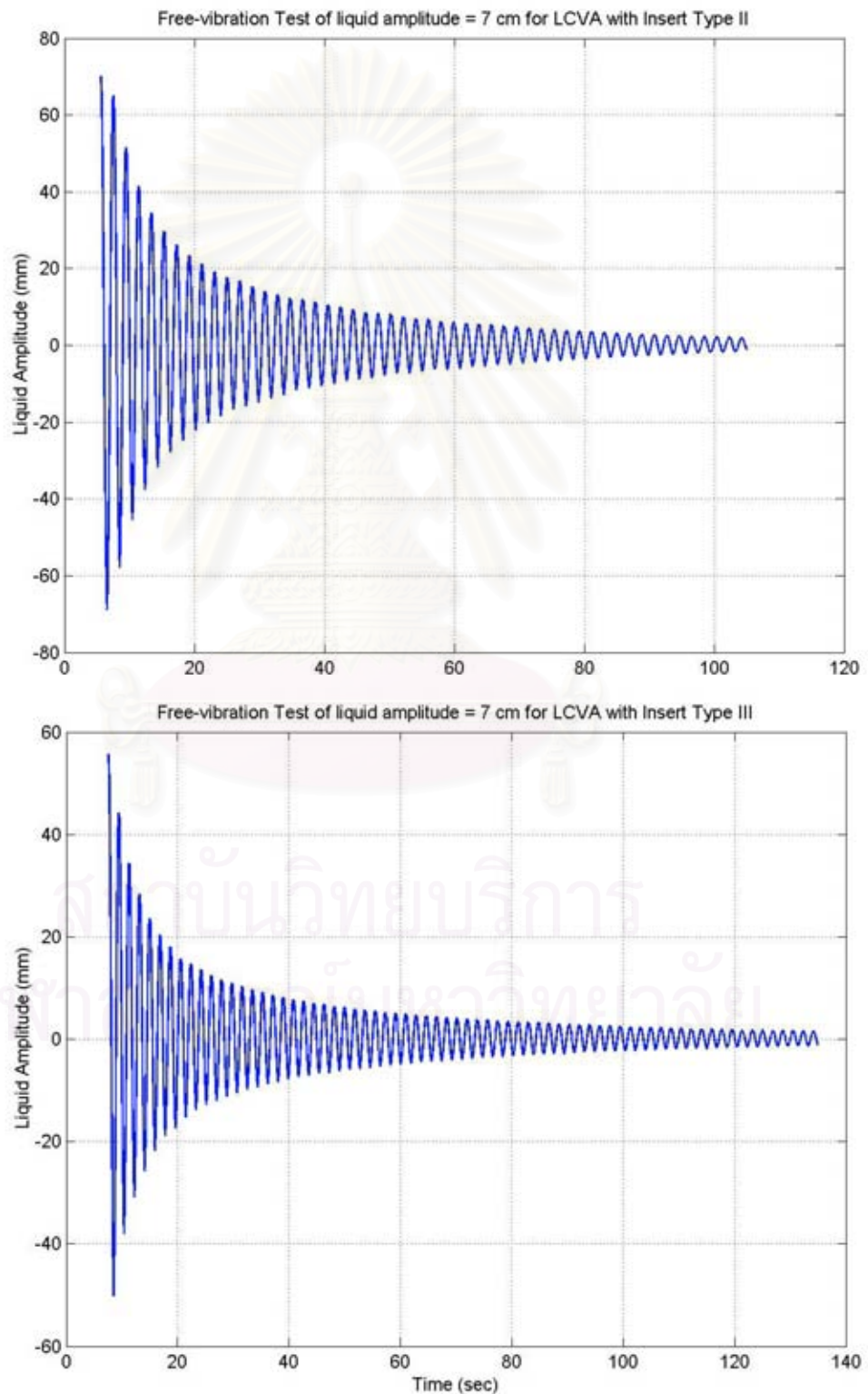


Fig. 3.9 Free-vibration test data for LCVAs with inserts types II and III - liquid amplitude = 7 cm

To determine the damping ratio of each damper model, Eq. (3.1) is used. The damping ratio ζ can be obtained from

$$\zeta = \frac{1}{2\pi} \ln\left(\frac{u_i}{u_{i+1}}\right) = \frac{1}{2\pi} \ln\left(\frac{\dot{u}_i}{\dot{u}_{i+1}}\right) = \frac{1}{2\pi} \ln\left(\frac{\ddot{u}_i}{\ddot{u}_{i+1}}\right) \quad (3.1)$$

where $\left(\frac{u_i}{u_{i+1}}\right)$, $\left(\frac{\dot{u}_i}{\dot{u}_{i+1}}\right)$ or $\left(\frac{\ddot{u}_i}{\ddot{u}_{i+1}}\right)$ is the ratio of successive peaks (maxima).

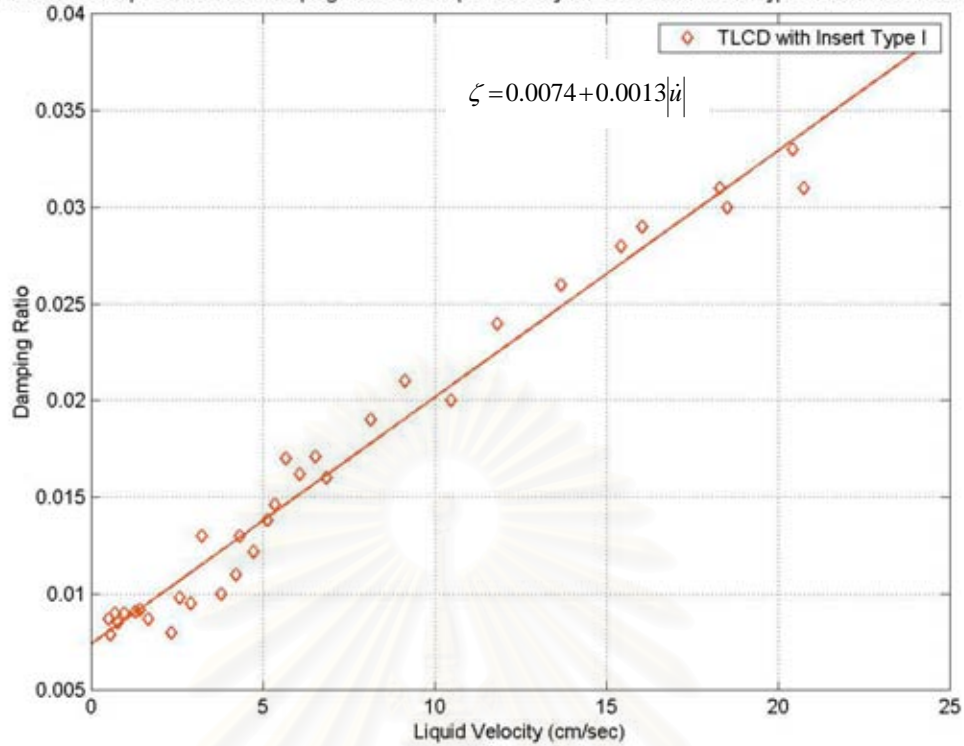
Because TLCD has nonlinear damping characteristic (its damping ratio depends nonlinearly on the liquid velocity), the piecewise linear approximation is used to determine the damping ratio. By plotting this damping ratio ζ against the average amplitude of liquid velocities, $\left(\frac{\dot{u}_i + \dot{u}_{i+1}}{2}\right)$ which are obtained from the first derivative of the liquid displacement, for every successive peak, the linear and quadratic damping ratio can be obtained from linear regression in the form

$$\zeta = c_1 + c_2 |\dot{u}| \quad (3.2)$$

where c_1 and c_2 are the coefficients obtained from regression.

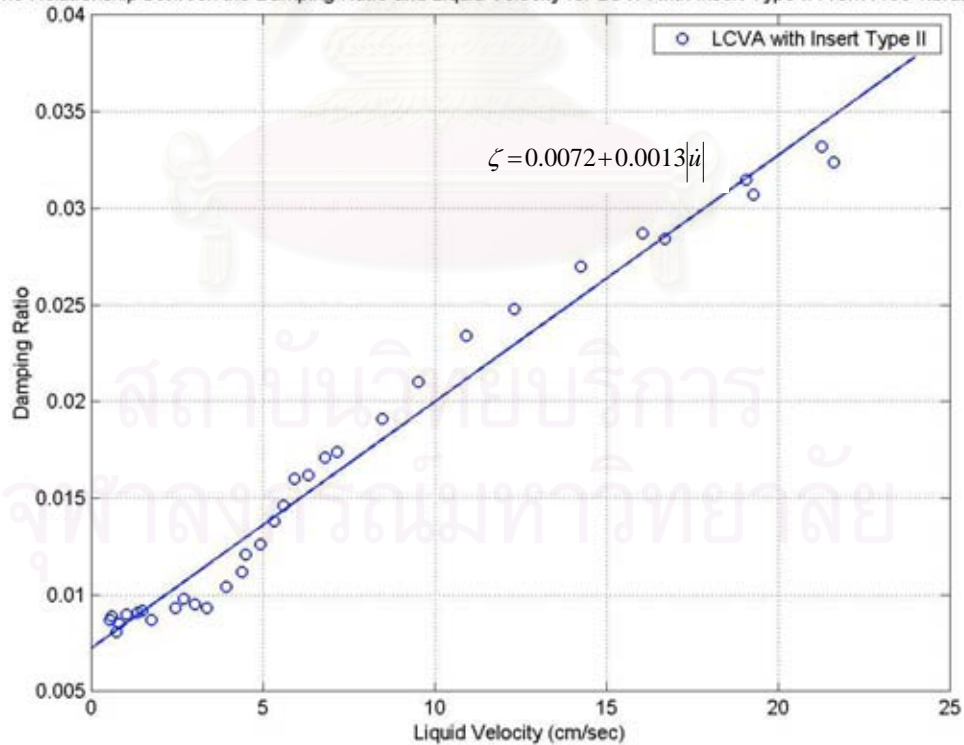
Fig. 3.10 shows the relationship between the damping ratio and liquid velocity for the TLCD with insert type I and LCVAs with inserts types II and III.

The Relationship between the Damping Ratio and Liquid Velocity for TLCD with Insert Type I From Free-vibration Tests



(a) TLCD with insert type I

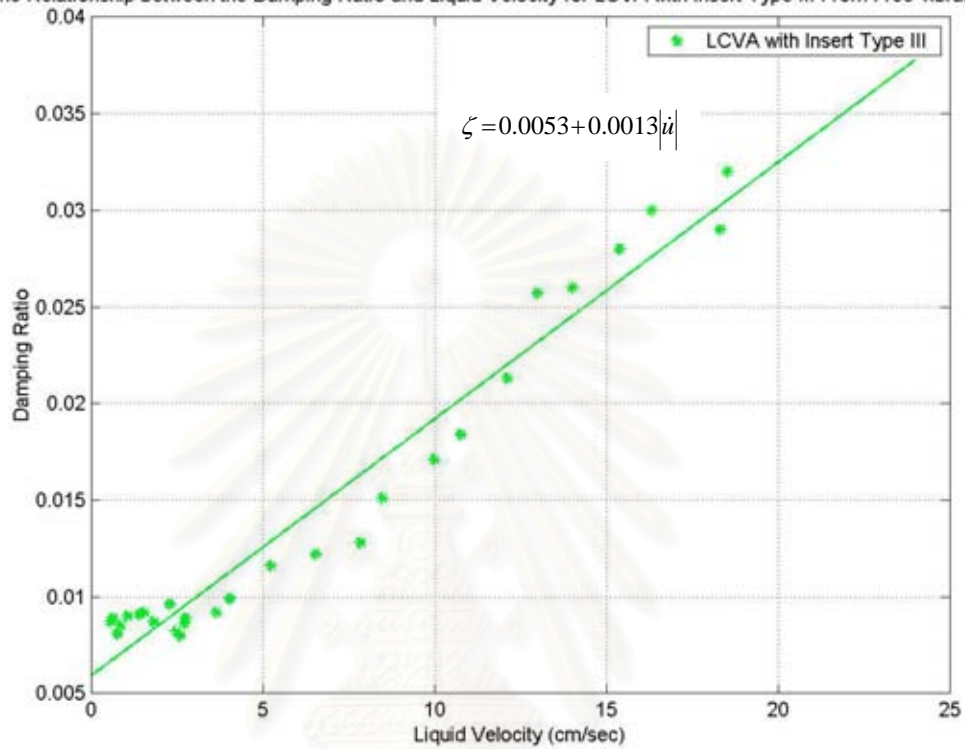
The Relationship between the Damping Ratio and Liquid Velocity for LCVA with Insert Type II From Free-vibration Tests



(b) LCVA with insert type II

Fig. 3.10 The relationship between the damping ratio and liquid velocity: (a) TLCD with insert type I; (b) LCVA with insert type II; (c) LCVA with insert type III

The Relationship between the Damping Ratio and Liquid Velocity for LCVA with Insert Type III From Free-vibration Tests



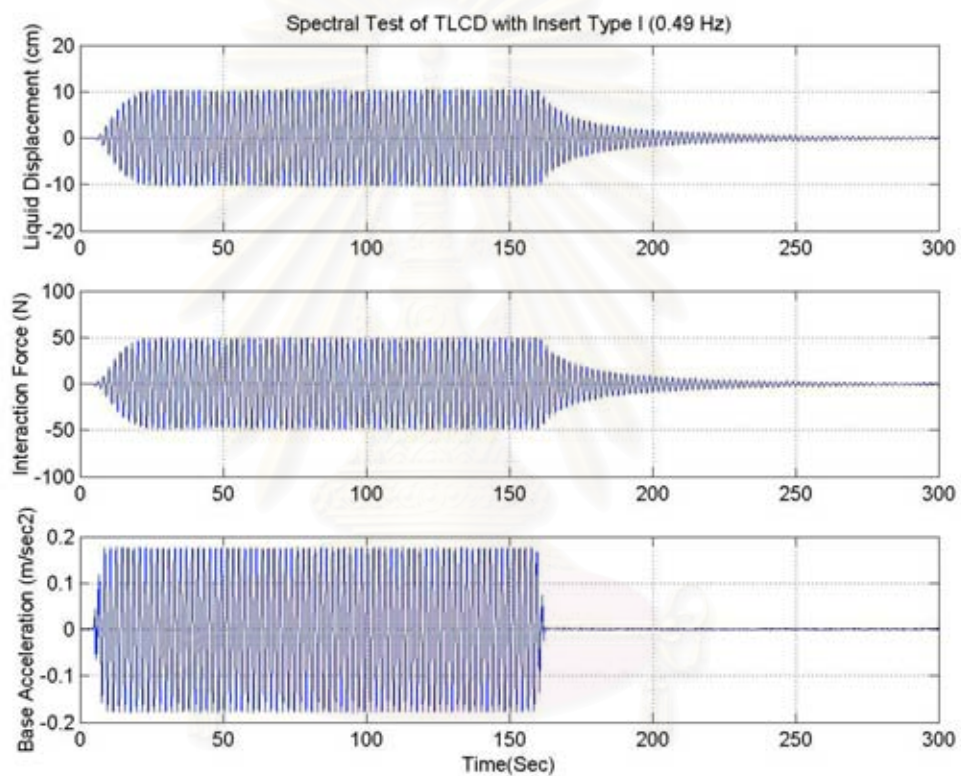
(c) LCVA with insert type III

Fig. 3.10 (continued)

The damping ratios obtained from Fig. 3.10 will be used to simulate the characteristics of three damper models in the next section.

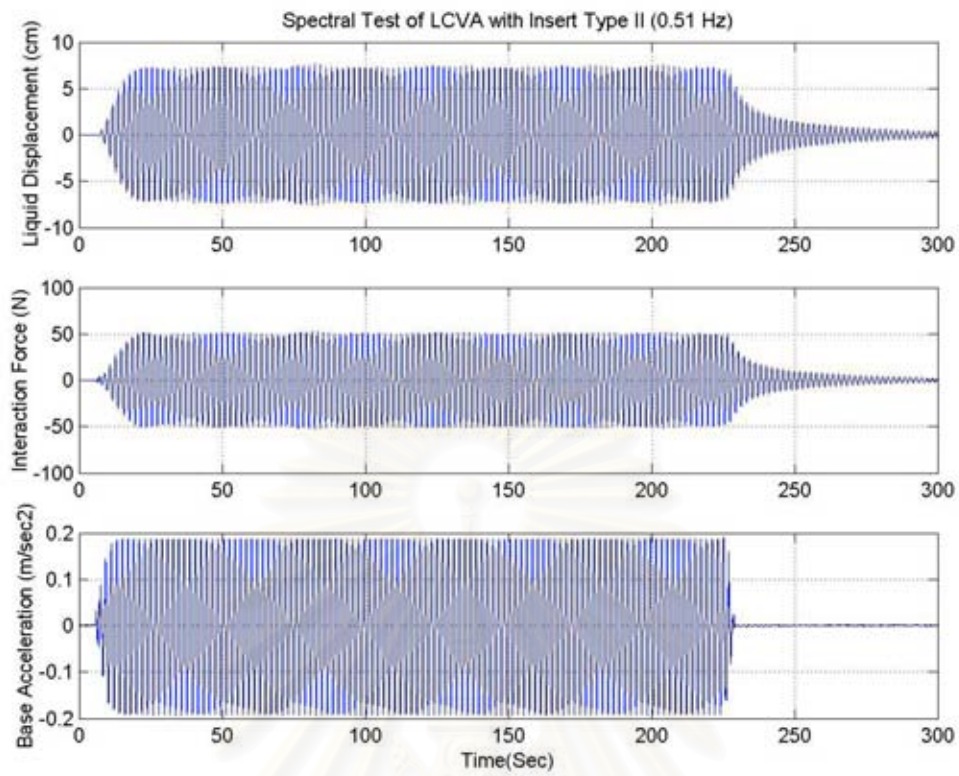
3.5.2 Spectral test data

The liquid displacements, interaction forces due to liquid motion and base accelerations from spectral tests at the natural frequency of each damper model are shown in Fig. 3.11.

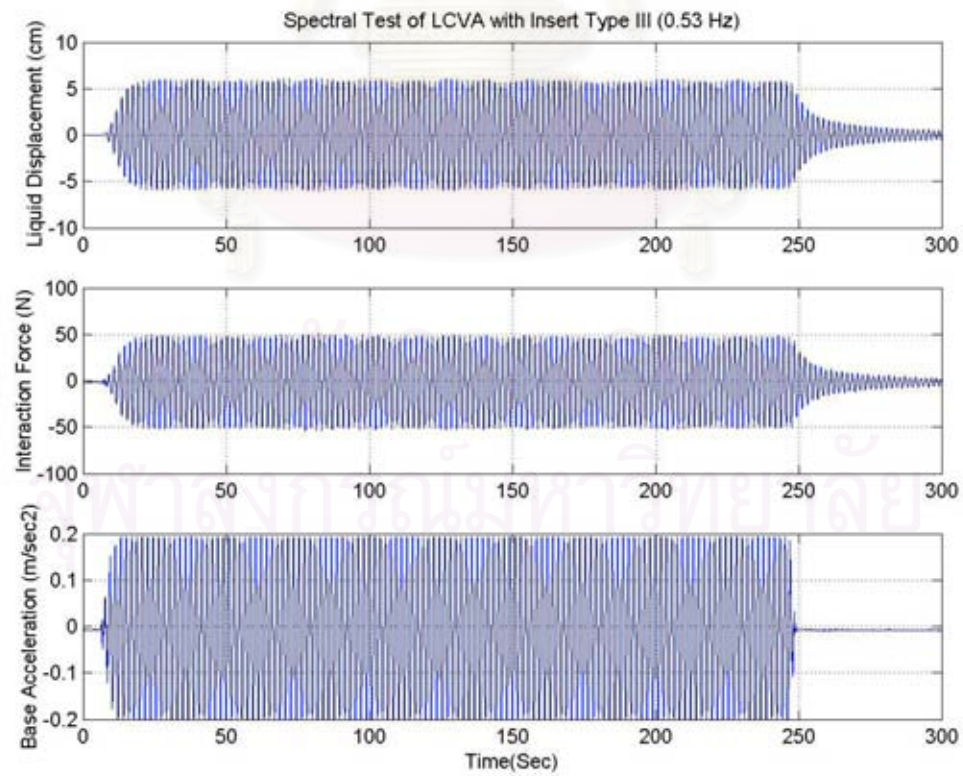


(a) TLCD with insert type I at resonance frequency of 0.49 Hz

Fig. 3.11 Spectral test data at the natural frequency of each damper model



(b) LCVA with insert type II at resonance frequency of 0.51 Hz

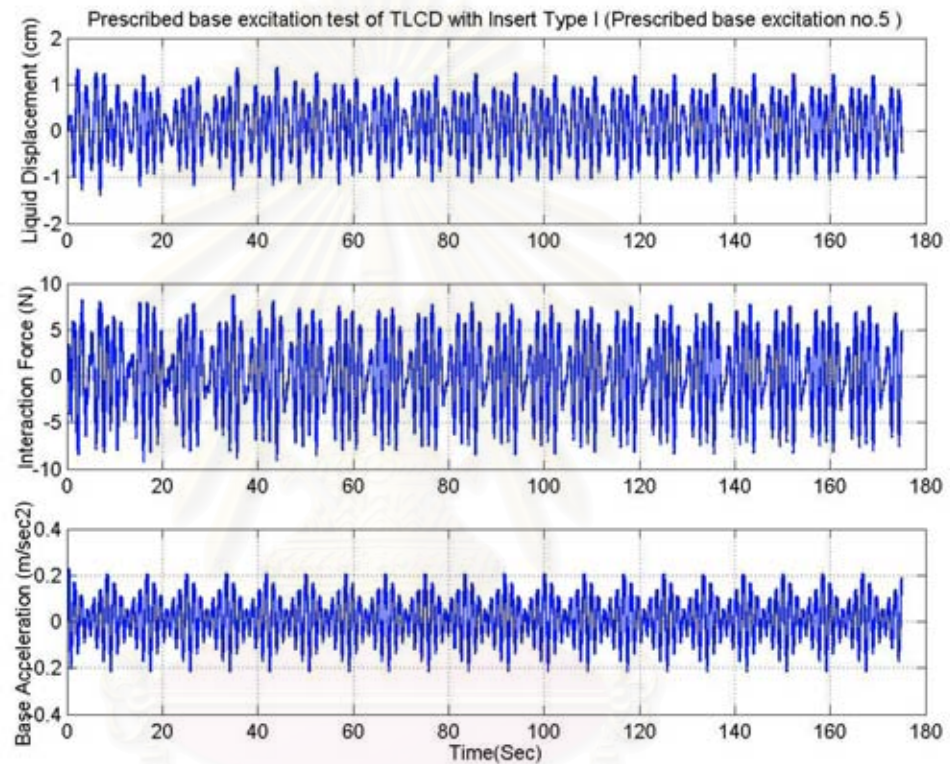


(c) LCVA with insert type III at resonance frequency of 0.53 Hz

Fig. 3.11 (continued)

3.5.3 Prescribed base excitation test data

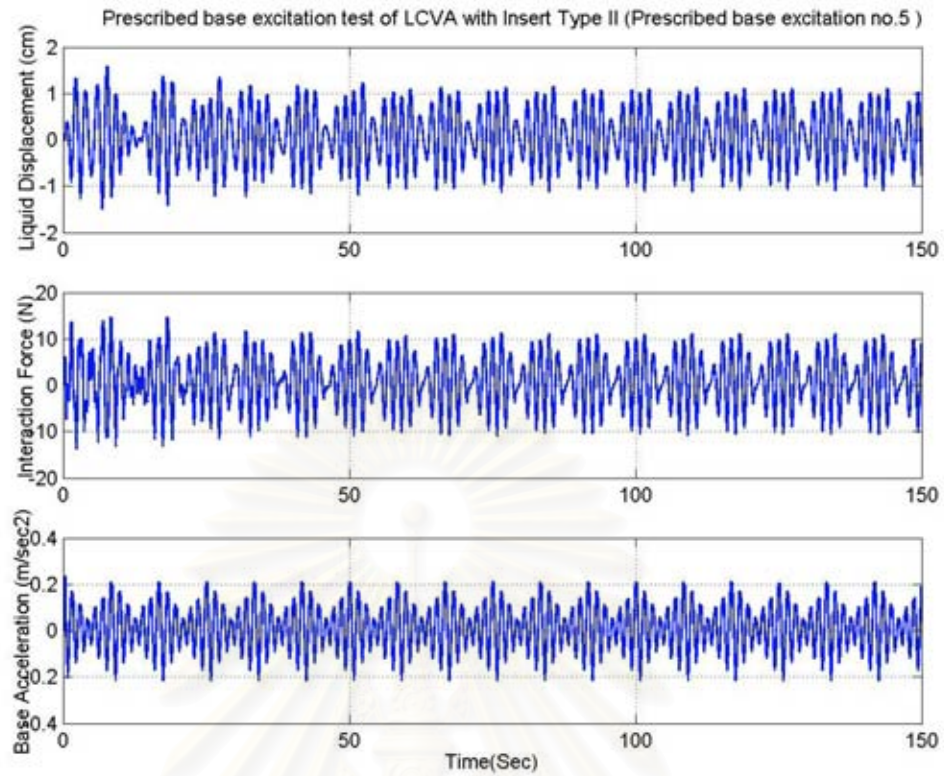
Fig. 3.12 shows the liquid displacements, interaction forces due to liquid motion and base accelerations from prescribed base excitation test of prescribed base excitation no. 5 for TLCD with insert type I and LCVAs with insert type II and III.



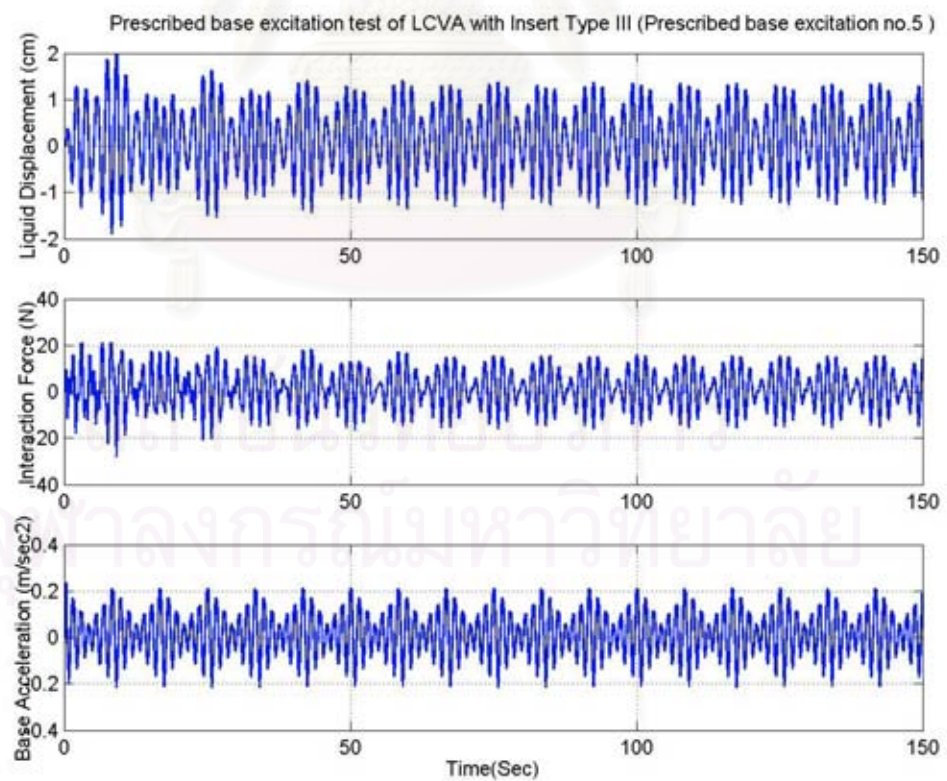
(a) TLCD with insert type I

Fig. 3.12 Responses due to prescribed base excitation no. 5: (a) TLCD with insert type I; (b) LCVA with insert type II; (c) LCVA with insert type III

จุฬาลงกรณ์มหาวิทยาลัย



(b) LCVA with insert type II



(c) LCVA with insert type III

Fig. 3.12 (continued)

3.6 Verification of Results from Analytical Method Based on Simplified Effective Length

3.6.1 Spectral tests

With the damping ratios determined from the free vibration tests, the frequency responses of the TLCDs can be analytically obtained by solving Eq. (2.5) and the results are compared with the spectral test data for three types of inserts as shown in Figs. 3.13 – 3.14. The computation is based on the simplified effective length by Gao and Kwok (1997).

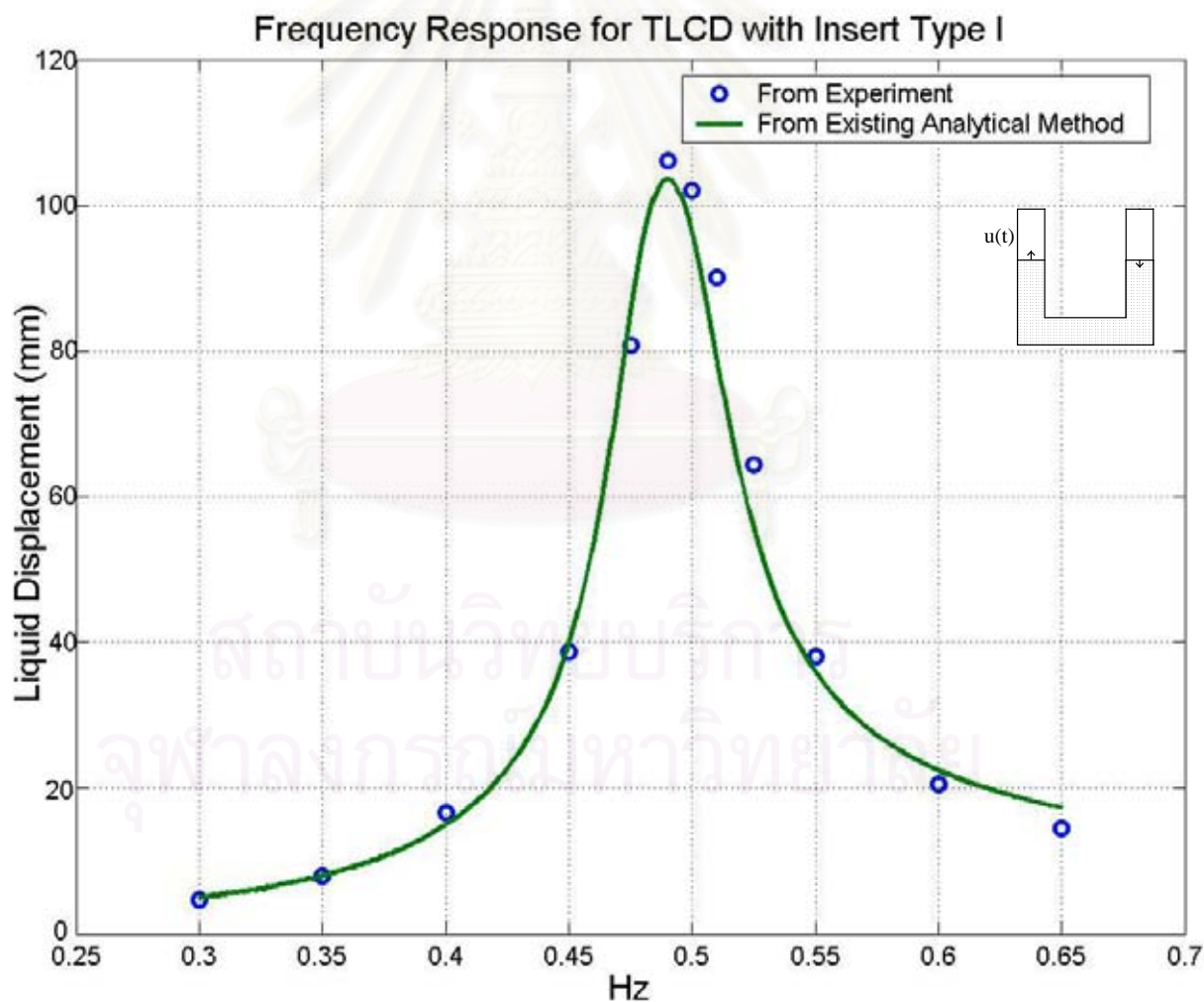


Fig 3.13 Experimental and analytical results of spectral tests for TLCD with insert type I

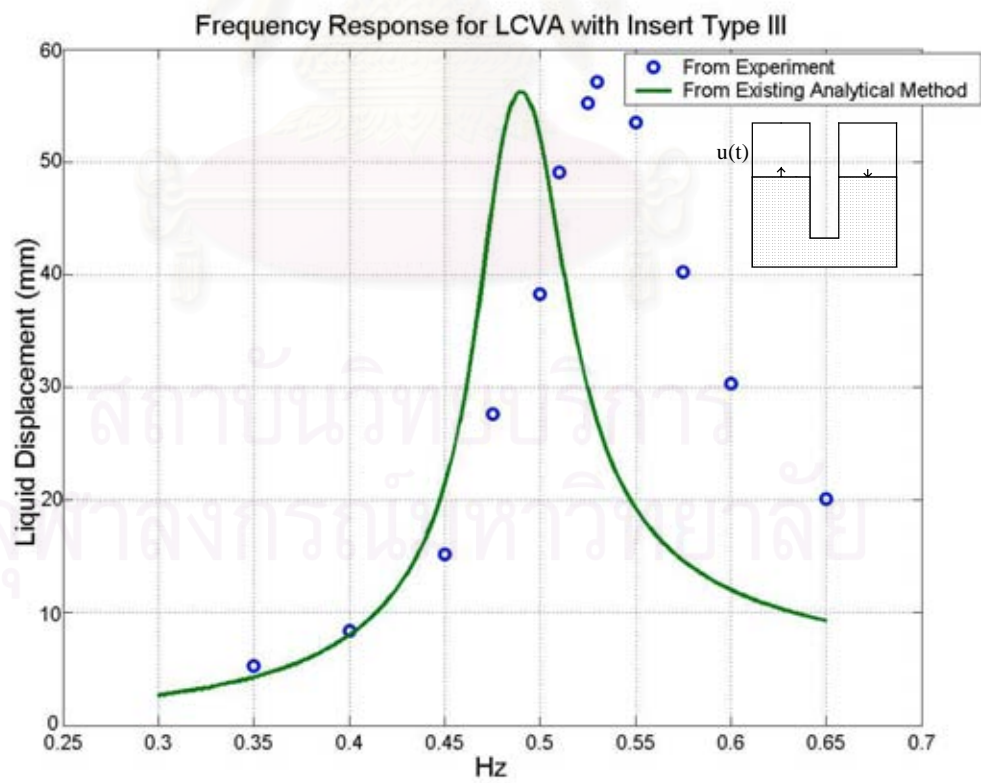
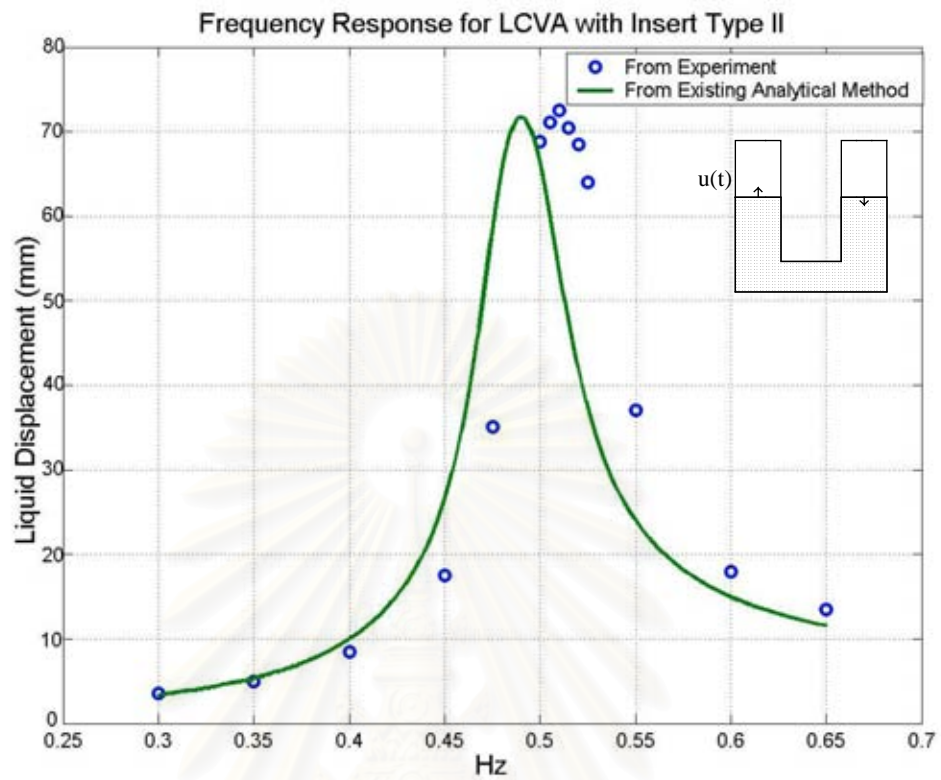


Fig. 3.14 Experimental and analytical results of spectral tests for LCVAs with inserts types II&III

It is found from Fig. 3.13, that the analytical solutions based on the simplified effective length agree very well with the experimental results for the TLCD with insert Type I, but for the LCVAs with inserts types II and III, the simplified effective length method cannot give a satisfactory response. As depicted in Fig. 3.14, both the analytical frequency response curves are significantly shifted to the left-hand side of those obtained from the experimental results. This clearly indicates that the theoretical natural frequency of the damper has not been estimated correctly, leading to mistuning of the system.

3.6.2 Prescribed base excitation tests

For the prescribed base excitation tests, the existing analytical method can predict the behavior quite well in case of the TLCD with insert Type I as shown in Fig. 3.15, but for the LCVAs with inserts types II and III, it cannot predict the real responses (displacements and forces) of the LCVAs for both amplitudes and phases of the motions. Figs. 3.16 and 3.17 show typical results for prescribed base excitation no.1 for LCVAs with inserts types II and III, respectively. Unsatisfactory analytical results are also obtained for other base excitations.

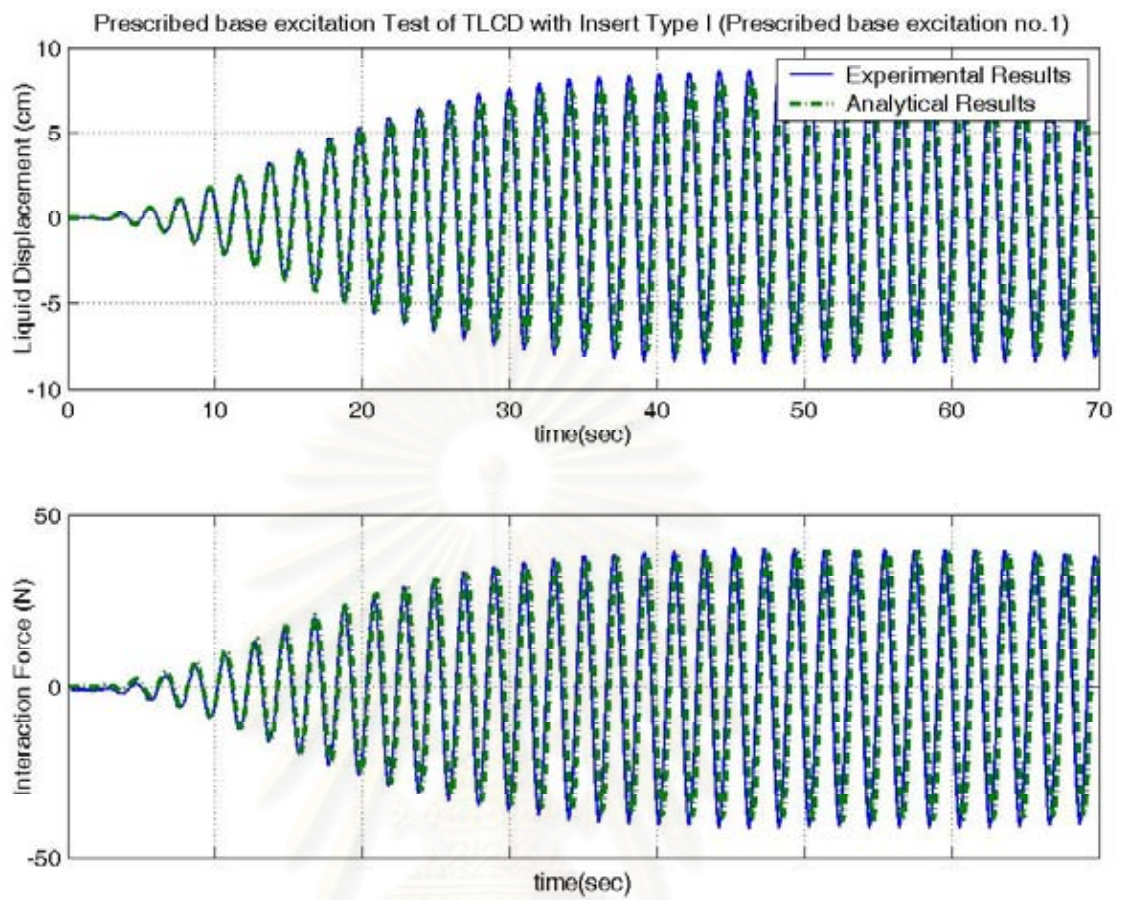


Fig. 3.15 Experimental and analytical results of prescribed excitation test no.1 for TLCD with insert type I

สถาบันวิทยบริการ
จุฬาลงกรณ์มหาวิทยาลัย

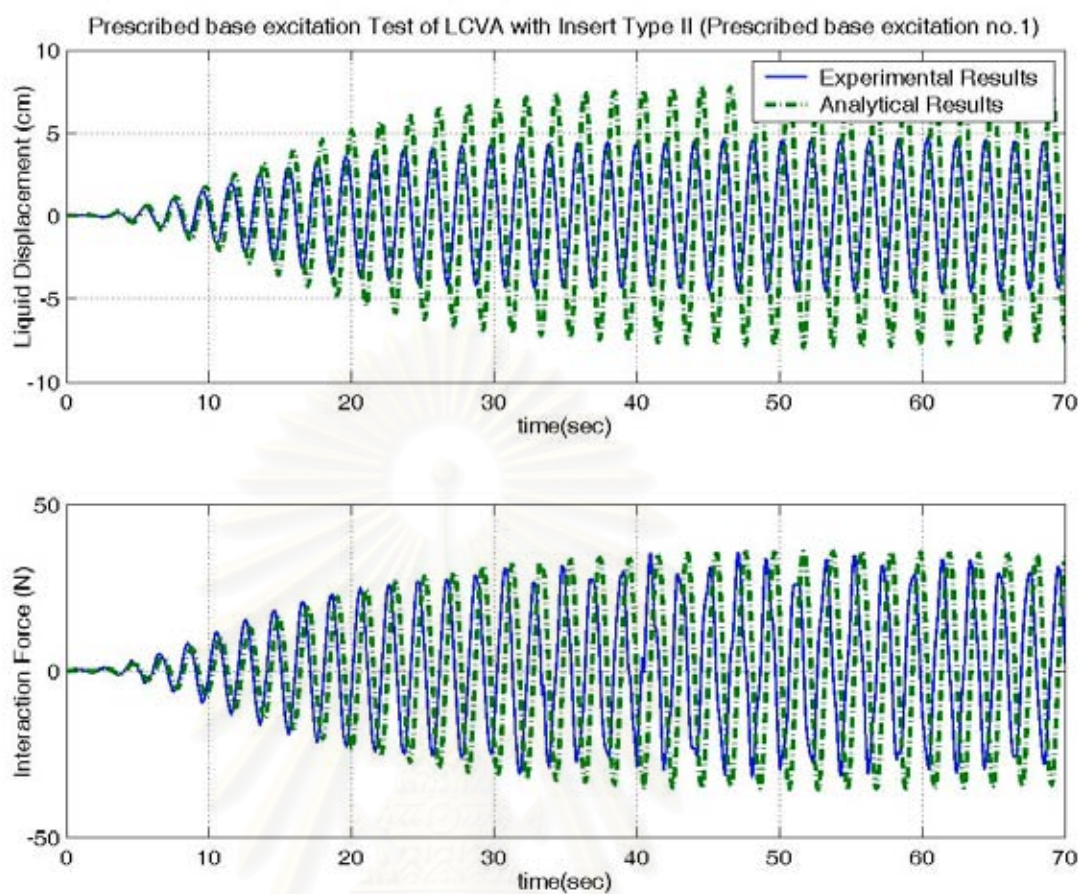


Fig. 3.16 Experimental and analytical results of prescribed excitation test no.1 for LCVA with insert type II

สถาบันวิทยบริการ
จุฬาลงกรณ์มหาวิทยาลัย

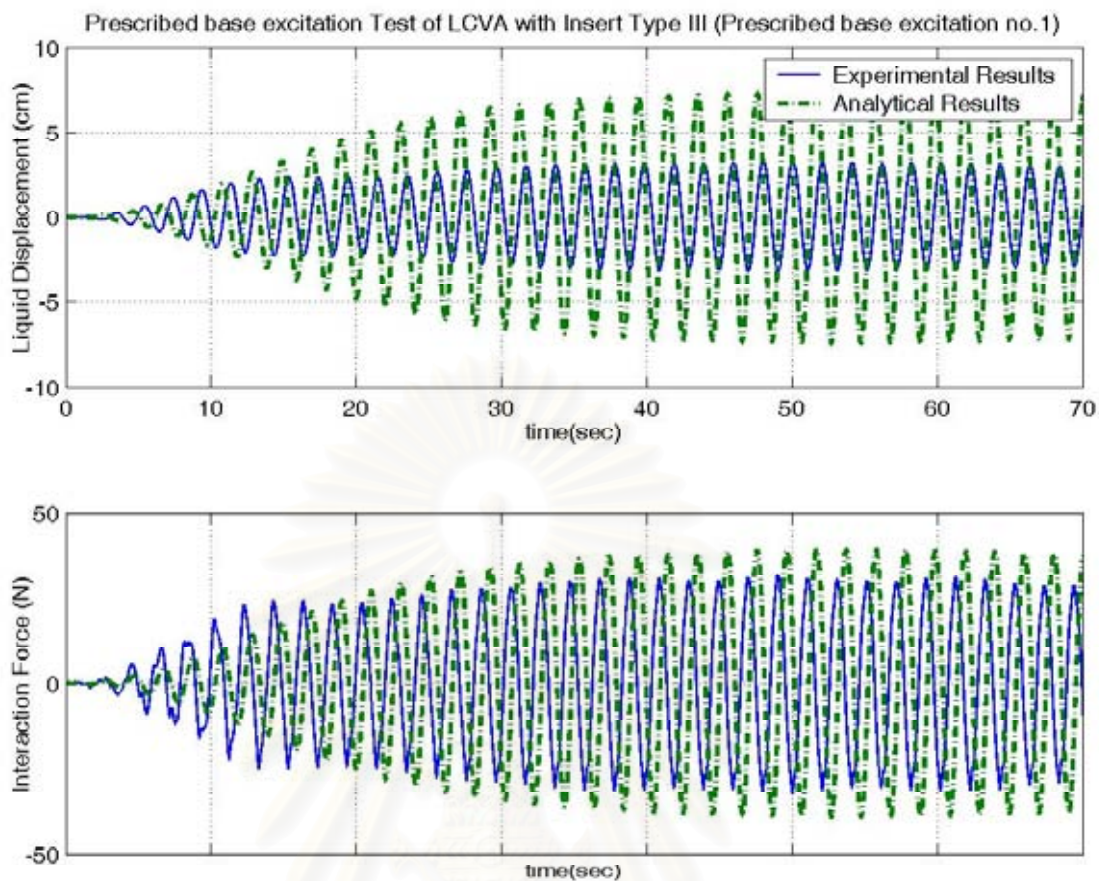
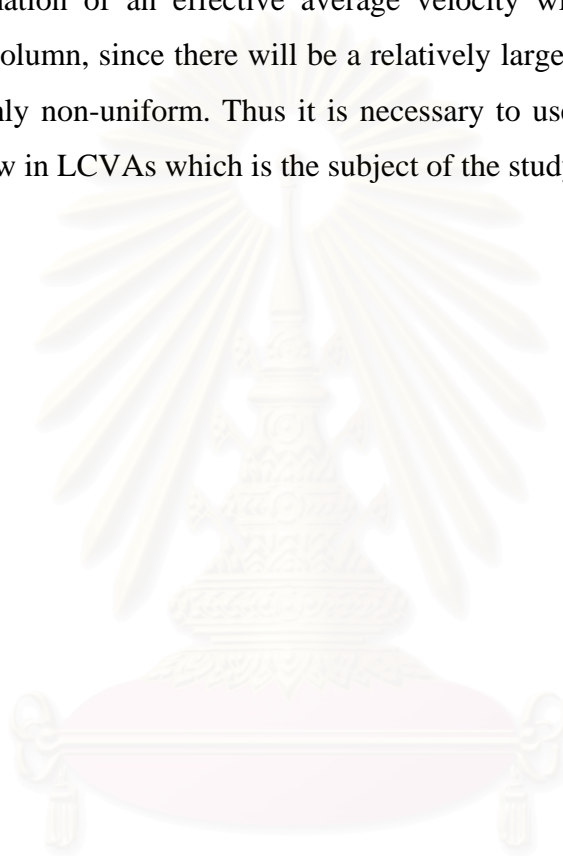


Fig. 3.17 Experimental and analytical results of prescribed excitation test no.1 for LCVA with insert type III

สถาบันวิทยบริการ
จุฬาลงกรณ์มหาวิทยาลัย

3.7 Conclusions

From these tests, it is evident that the simplified effective length approach in existing literature gives good results for TLCD, but fails to give satisfactory prediction of the natural frequencies and responses in the case of LCVAs with relatively large transition boundaries. Such a configuration of the LCVA does not allow approximation of an effective average velocity within each portion of the moving liquid column, since there will be a relatively larger transition zone in which the flow is highly non-uniform. Thus it is necessary to use more refined method to simulate the flow in LCVAs which is the subject of the study in the next chapter.



สถาบันวิทยบริการ
จุฬาลงกรณ์มหาวิทยาลัย

CHAPTER IV

NUMERICAL PANEL METHOD

As accurate prediction of the natural frequency of a damper is crucial in control problems, a more refined analysis is clearly needed. This chapter utilizes a numerical potential-flow method, known as the numerical panel method, to simulate the induced velocity distribution of the fluid inside liquid dampers. The advantage of this approach is twofold. Firstly, a more accurate estimate of the effective length of liquid dampers, and hence the natural frequency can be obtained. Secondly, the method is applicable for any configuration of the LCVA and TLCD. The numerical results are verified with those obtained from existing experimental results. In addition, scaled models with large transition boundary to horizontal length ratios experimentally investigated under various types of excitations consisting of free-vibration, spectral and prescribed base excitations from previous chapter serve to verify the results obtained from the panel method.

4.1 Panel Method Formulation

The panel method developed by Frank (1967) for determining the hydrodynamic forces on rigid ship cross-sections is used to simulate the flow in the TLCD. In this method, the section is approximated by straight-line segments on each of which source singularities of constant strength are distributed. By applying Green's theorem and the Green function method, an integral equation for the velocity potential is obtained using the potential flow theory.

It is possible to develop a numerical solution for the flow past a two-dimensional body of arbitrary shape. In principle this is accomplished by the superposition of uniform flow plus an as yet unknown distributed singularity. By specifying the body shape the problem is reduced to finding the unknown singularity distribution. The distributed singularities may be doublets, vortices, or sources and sinks as shown in Fig.4.1. If the singularities are distributed over a contour fully enclosing the fluid, then a panel method can be applied. This method has had

extensive application in flow modeling (Chow 1979, Hess 1990 and Katz 1991). The foundation reference for the technique is Hess and Smith (1966).

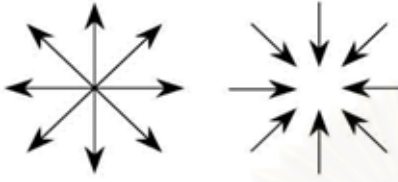


<p>Source and sink</p> 	<p>Origin is singularity point q is volume flow rate per unit depth</p> $V_r = \frac{q}{2\pi r} \quad \psi = \frac{q}{2\pi} \theta$ $V_\theta = 0 \quad \phi = -\frac{q}{2\pi} \ln r$
<p>Vortex</p> 	<p>Origin is singularity point K is strength of the vortex</p> $V_r = 0 \quad \psi = -\frac{K}{2\pi} \ln r$ $V_\theta = \frac{K}{2\pi r} \quad \phi = -\frac{K}{2\pi} \theta$
<p>Doublet</p> 	<p>Origin is singularity point Λ is strength of the doublet</p> $V_r = -\frac{\Lambda}{r^2} \cos \theta \quad \psi = -\frac{\Lambda \sin \theta}{r}$ $V_\theta = -\frac{\Lambda}{r^2} \sin \theta \quad \phi = -\frac{\Lambda \cos \theta}{r}$

Fig. 4.1 A linear combination of singularities (Chow 1979)

Fig. 4.2 shows a source panel in global and local coordinates. A field point in the fluid is assumed to be at (x'_a, y'_a) . The potential, $\varphi(x, y)$, induced at the field point by a distribution of sources with strength, $g(s)$, around the contour enclosing the fluid is given by

$$\varphi(x, y) = \oint \frac{1}{2} \ln \left[\frac{1}{(x - x_a)^2 + y_a^2} \right] g(s) ds \quad (4.1)$$

where the source singularity is given by

$$\hat{\phi}_{source} = \frac{1}{2} \ln \left[\frac{1}{(x-x_a)^2 + y_a^2} \right]$$

It is assumed that the contour is decomposed into a series of straight-line segments and on each of these segments the source strength, $g(s)$, is constant. The situation for line segment n is shown in Fig. 4.2. The field point of interest is given as (x'_a, y'_a) in the $0'x'y'$ system or (x_a, y_a) in the $0xy$ system. The line segment is assumed to lie on the $0x'$ axis and to be centered on the $0y'$ axis. The contribution to the potential from line segment n is given by:

$$\phi_n(x_a, y_a) = g_n \int_{-s}^s \frac{1}{2} \ln \left[\frac{1}{(x-x_a)^2 + y_a^2} \right] dx \quad (4.2)$$

The integral term for the potential can be simplified as the following equation. Eq. (4.3) is fully derived in Appendix A.

$$\begin{aligned} \phi = 2s + y_a \left\{ -Arc \tan \left(\frac{x_a - s}{y_a} \right) + Arc \tan \left(\frac{x_a + s}{y_a} \right) \right\} \\ + (x_a - s) \ln \sqrt{(x_a - s)^2 + y_a^2} - (x_a + s) \ln \sqrt{(x_a + s)^2 + y_a^2} \end{aligned} \quad (4.3)$$

The velocity components are given by the derivatives of the above function with respect to x_a and y_a :

$$\begin{aligned} \frac{\partial \phi}{\partial x_a} = g_n \frac{\partial \phi}{\partial x_a} = g_n \left[\ln \sqrt{(x_a - s)^2 + y_a^2} - \ln \sqrt{(x_a + s)^2 + y_a^2} \right] \\ \frac{\partial \phi}{\partial y_a} = g_n \frac{\partial \phi}{\partial y_a} = g_n \left[-Arc \tan \left(\frac{x_a - s}{y_a} \right) + Arc \tan \left(\frac{x_a + s}{y_a} \right) \right] \end{aligned} \quad (4.4)$$

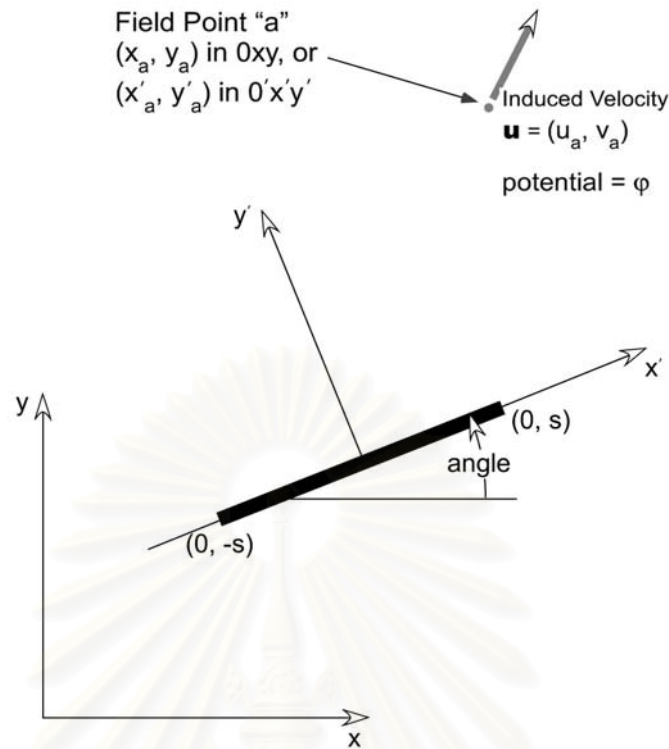


Fig. 4.2 Source panel in global and local coordinates

The LCVA models with inserts types II and III are modeled by using the whole domain of the fluid from the free surface on one side of the tank to the free surface on the other side. It would be complicated to deal with the free surface, so the problem is treated as one where there is a piston pushing down the free surface on the left-hand side and the resulting motion pushes up the piston on the right-hand side as shown in Fig. 4.3. It should be noted that the sloshing frequency of an individual column is approximately three times that of the LCVA. As a result, the dynamics of the sloshing in a single leg of the tank are disjoint from that of the tank as a whole and the free surface effect can be ignored here since it has insignificant influence on the first mode of vibration of LCVA models.

The problem is solved using kinematic conditions defining the normal velocity around the contour. The normal velocity on the bottom of the piston on the left-hand side is given by:

$$\left(-\frac{\partial \phi}{\partial y}\right) = -U_0 \quad (4.5)$$

The normal velocity on the bottom of the piston on the right-hand side is U_0 and the normal velocity is 0 elsewhere. The pressure at any point in the fluid is given by

$$p = -\rho \frac{\partial \varphi}{\partial t} \quad (4.6)$$

where ρ is the mass density of the fluid.

The result is a set of simultaneous equations for the source strengths on each panel, which can be solved to yield the potential distribution on the walls of the tank and the bottom of the pistons. The integral of this potential distribution on the bottom of the pistons yields the force on the piston needed to change the velocity of the fluid. Let us define a new potential:

$$\bar{\varphi} = \frac{\varphi}{a}$$

where a is the assumed velocity of the piston (m/s). The force on the left-hand piston can be expressed as:

$$F_{lh} = \int_{\text{piston area}} \left(-\rho \frac{\partial \varphi}{\partial t} \right) dx dy = -a \rho w \int_{l_{\text{piston}}} \frac{\partial \bar{\varphi}}{\partial t} lh dx \quad (4.7)$$

where w is the constant width of the piston, and lh denotes left-hand piston.

From symmetry, if the total force on the column is equated to the force needed to accelerate the fluid, then the effective length can be obtained from the following equation:

$$L_e = \left(2 \int_{l_{\text{piston}}} \bar{\varphi} dx \right) / l_{\text{piston}} \quad (4.8)$$

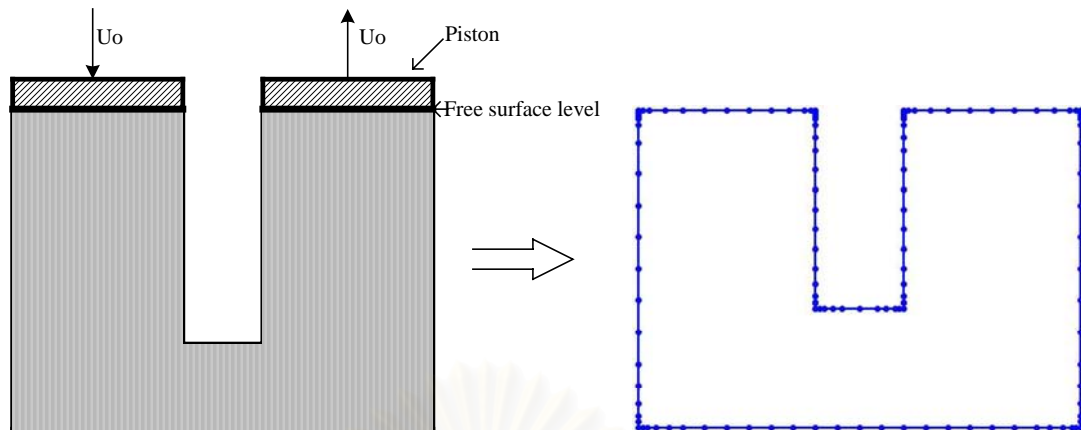


Fig. 4.3 Panel method modeling for TLCDs and LCVAs

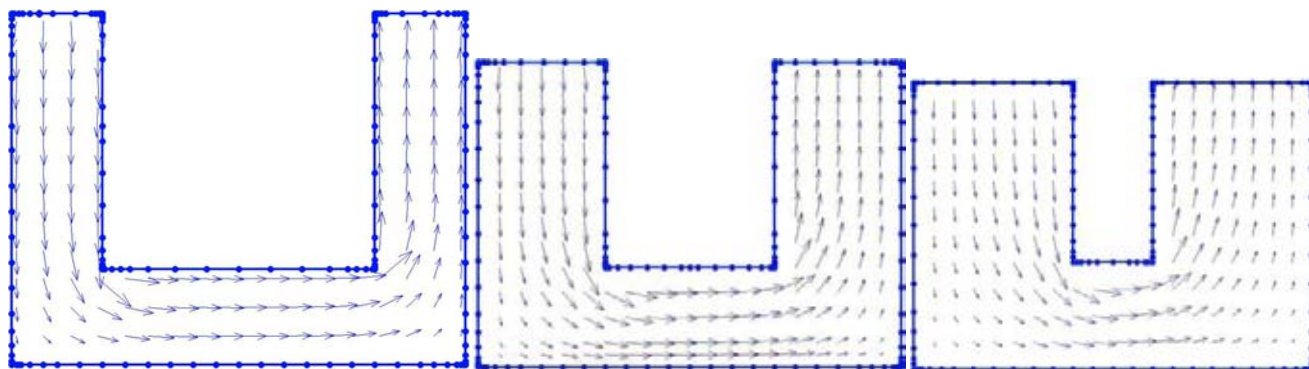
In the numerical computation, the damper model is simulated by a number of panels. After source panels are defined by the line segments, the velocity potential for the flow consisting of the uniform stream and source panels can be obtained from Eq. (4.3), together with induced velocities from source panel obtained from Eq. (4.4). Then applying the kinematic conditions of all boundary points, all panel strengths can be determined. The velocity and pressure at any point in the flow can be computed by taking derivatives of ϕ expressed in Eq. (4.4) and Eq. (4.6), respectively. The effective length of the TLCD can then be computed from Eq. (4.8).

4.2 Verification of Results from Numerical Panel Method

4.2.1 Effective lengths and natural frequencies

The accuracy of the analytical prediction of the damper characteristics hinges on the precision in estimating the natural frequency of the system. The effectiveness of the numerical panel method in predicting the natural frequencies is first verified with the experimental results obtained in this study and those in Hitchcock's tests (1997).

TLCD with insert type I and LCVA models with inserts types II and III are numerically simulated by 130 panels as shown in Fig. 4.4. It is to be noted that small source panels are chosen at each corner in all simulations to minimize the numerical error on calculation.



(a) TLCD with insert type I (b) LCVA with insert type II (c) LCVA with insert type III
 Fig. 4.4 Induced velocity distribution in liquid column vibration absorber model

Fig. 4.5 shows 5 LCVA configurations, which are part of the first series of the Hitchcock's experiments (1997). These dampers have the same horizontal fluid column length of 820 mm and vertical fluid column height of 180 mm, but different area ratios, which are 0.82, 1.39, 2.14, 3.14 and 4.11, respectively. The corner-to-corner width to horizontal length ratios range from 0.04 to 0.13. One hundred and twenty panels are used to model these LCVA dampers.

Fig. 4.4 shows the induced velocities from source panels for TLCD with insert type I and LCVA models with inserts types II and III, respectively. The resulting flow for the other LCVAs are shown in Fig 4.5. As depicted in Fig. 4.4, the flow in the transition region of LCVA model with insert type III is highly non-uniform, and the transition region constitutes a significant portion of the damper.

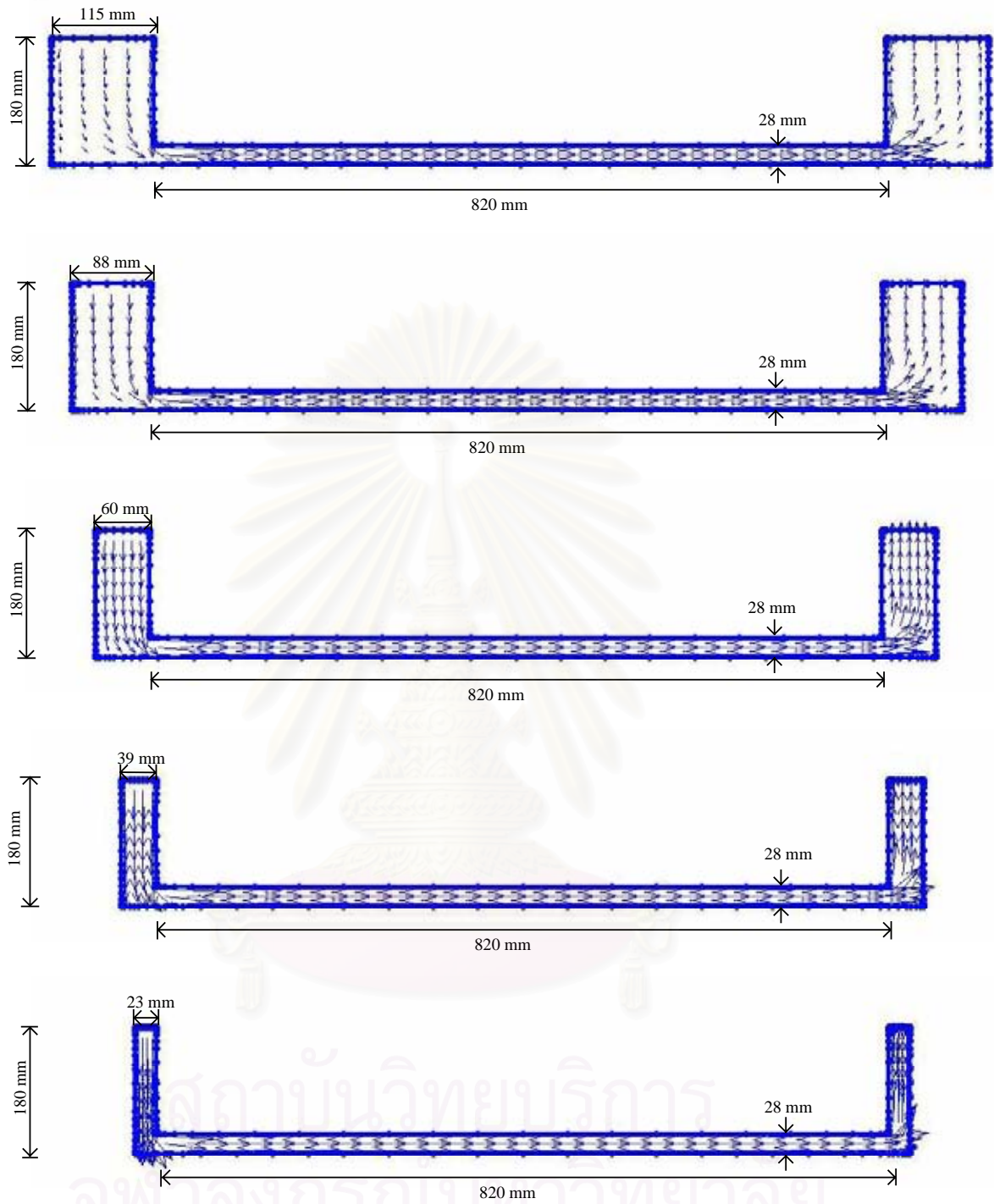


Fig. 4.5 Induced velocity distribution of 5 LCVA configurations investigated by Hitchcock (1997)

TABLE 4.1 The damper effective lengths and natural frequencies from various

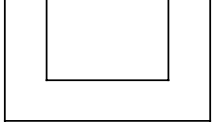
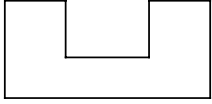
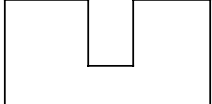
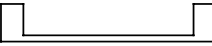
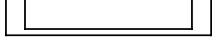
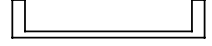
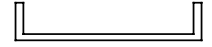

Damper Configuration	Corner-to-corner width to horizontal length ratio	Experiment		Gao and Kwok (1997) or Chang and Hsu (1998)		Hitchcock (1997)		Panel Method	
		L_e (m)	f_n (Hz)	L_e (m)	f_n (Hz)	L_e (m)	f_n (Hz)	L_e (m)	f_n (Hz)
	0.35	2.07	0.490	2.07 (0.0%)	0.490 (0.0%)	2.07 (0.0%)	0.490 (0.0%)	2.07 (0.0%)	0.490 (0.0%)
	0.52	1.91	0.510	2.07 (8.4%)	0.490 (3.9%)	1.82 (4.7%)	0.523 (2.5%)	1.91 (0.0%)	0.511 (0.2%)
	0.75	1.77	0.530	2.07 (16.9%)	0.490 (7.5%)	1.47 (16.9%)	0.580 (9.4%)	1.65 (6.8%)	0.548 (3.4%)
	0.13	4.27	0.341	4.17 (2.3%)	0.345 (1.2%)	3.73 (12.6%)	0.365 (7.0%)	4.17 (2.3%)	0.345 (1.2%)
	0.10	3.30	0.388	3.19 (3.3%)	0.395 (1.8%)	2.94 (10.9%)	0.411 (5.9%)	3.27 (0.9%)	0.390 (0.5%)
	0.08	2.42	0.453	2.22 (8.3%)	0.473 (4.4%)	2.12 (12.4%)	0.485 (7.1%)	2.35 (2.9%)	0.460 (1.5%)
	0.06	1.50	0.575	1.53 (2.0%)	0.570 (0.9%)	1.50 (0.0%)	0.575 (0.0%)	1.51 (0.7%)	0.574 (0.2%)
	0.04	1.15	0.656	1.02 (11.3%)	0.697 (6.3%)	1.03 (10.4%)	0.693 (5.6%)	1.10 (4.3%)	0.672 (2.4%)

Table 4.1 lists the effective lengths and the natural frequencies computed from 3 analytical methods, based on simplified effective length (Gao and Kwok (1997) or Chang and Hsu (1998), Hitchcock (1997)) and the panel method. The experimental results are also included for comparison. Except for LCVA with insert type III, the effective lengths computed from the existing analytical methods agree with less than 12.6% discrepancy compared with those based on the experimental results. However, a significant discrepancy of 16.9% is observed for LCVA with insert type III. The analytical model proposed by Gao and Kwok (1997) or Chang and Hsu (1998) results in error of about 7.5% in the natural frequency for LCVA with insert type III, while that proposed by Hitchcock (1997) gives rise to an error of 9.4%. The natural frequencies calculated based on the effective lengths obtained from the panel method, on the other hand, differ from the experimental values by not more than 3.4%. This reveals that the simplified effective length approximations in previous studies cannot represent the actual flow in the dampers with a relatively large size of the transition boundaries, while the panel method yields a more realistic approximation.

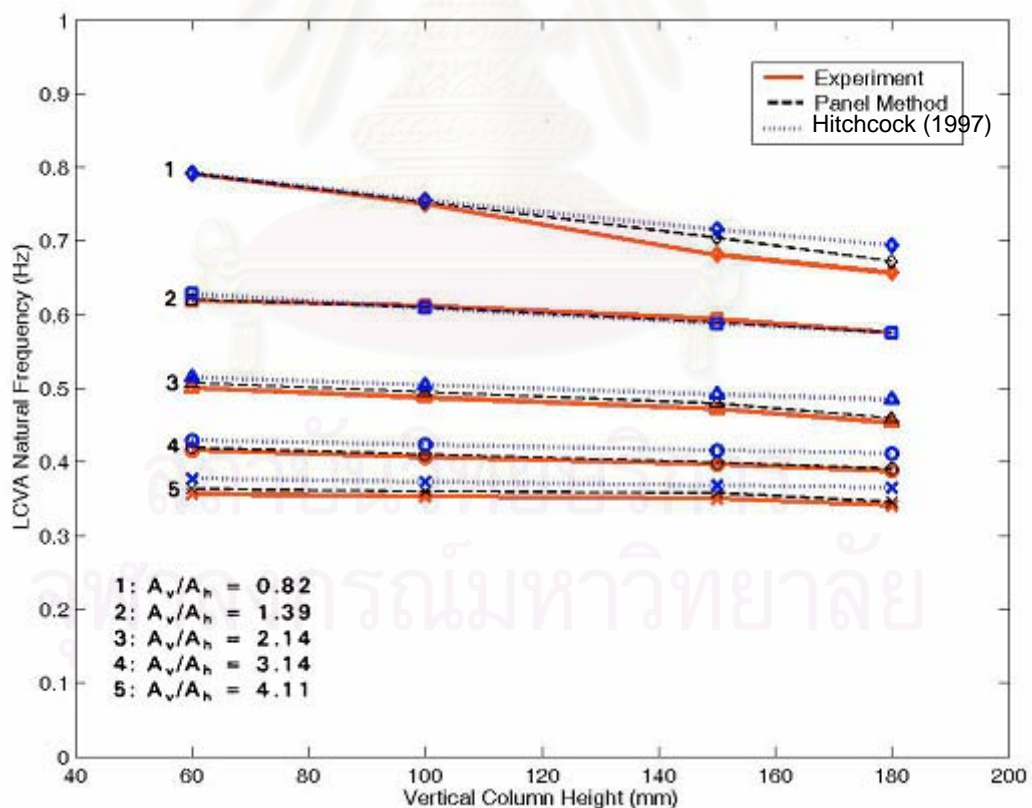
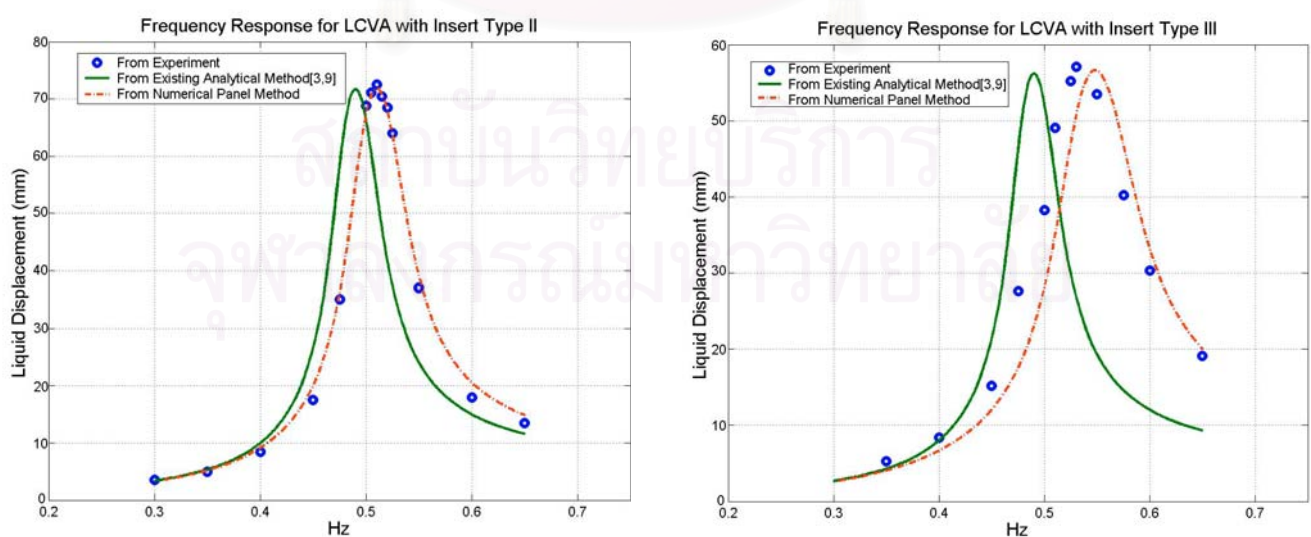


Fig. 4.6 Variation of LCVA natural frequency with area ratio and vertical column height

In Fig. 4.6, the test results of 20 LCVA dampers obtained by Hitchcock (1997) are compared with those computed based on the numerical panel method. It may be seen from the figure that the discrepancy between the measured and the calculated natural frequencies as proposed by Hitchcock (1997) varies from about 1% to approximately 5%, while the discrepancy between the measured and the calculated natural frequencies based on the numerical panel method varies from less than 0.5% to 3%. The numerical panel method clearly provides a better prediction of the natural frequencies of liquid motions for various LCVA configurations. It should be noted, however, that the panel method is much more complicated than the other methods. Improvement based on the latter can be made if some fine tuning is allowed for by providing a means to adjust the amount of water inside the LCVAs. Such a practical aspect, as well as fine tuning to account for building frequency changes stemming from age or damage over time need further extensive investigation.

4.2.2 Frequency response curves

With the better estimates of the natural frequencies, the frequency response curves for LCVAs with inserts types II and III are again determined using the effective lengths obtained from the numerical panel method. Fig. 4.7 shows the resulting frequency response curves together with those obtained earlier and test results.



(a) LCVA with insert type II

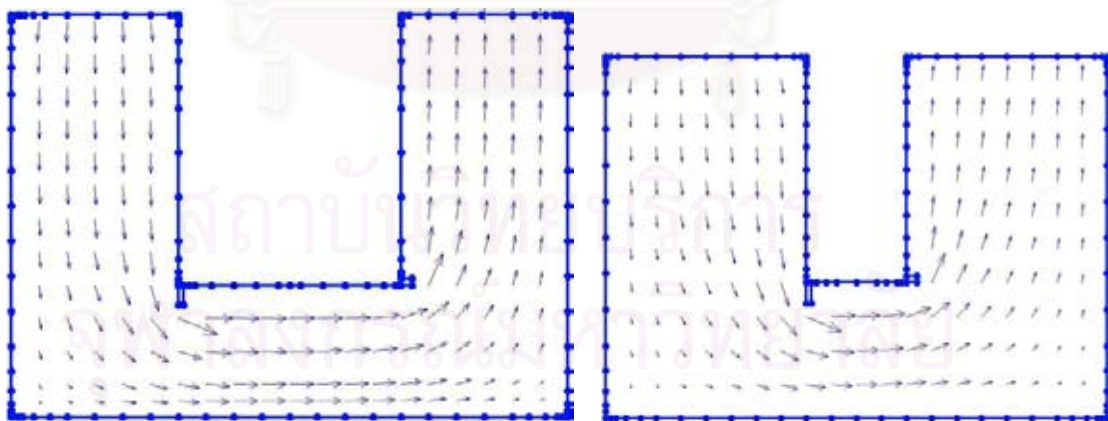
(b) LCVA with insert type III

Fig. 4.7 Frequency response curves from experiment, existing analytical method and panel method.

As evident from Fig. 4.7, the frequency response curves based on the numerical panel method match the experimental results much better than the ones obtained from the existing analytical method based on the simplified effective length. The agreement is almost perfect for LCVA with insert type II, and acceptable for LCVA with insert type III. In the latter, at the resonance frequency, for instance, the analytical solution based on the panel method underestimates the displacement response by about 10.5% compared with an excessive error of about 52.6% for the existing method.

4.2.3 Improvement of the panel method modeling

The difference between the natural frequency obtained from the experiment and that obtained from the numerical panel method is believed to result from the effect of the liquid viscosity. The numerical panel method in this study cannot model the effect of liquid viscosity, which can cause the vortices and separation in the flow. Because vortices are detected during the experiment at the corner of the transition boundaries between the vertical and horizontal portions, the “bump” source panels are introduced to simulate the effect of these vortices as seen in Fig. 4.8.



(a) LCVA with insert type II

(b) LCVA with insert type III

Fig. 4.8 Induced velocity distribution in liquid column vibration absorber models with estimate of the effect of vortices

After the bump source panels are input in the model to estimate the effect of vortices, the effective lengths for both models can be recalculated, which can be converted to 0.511 Hz and 0.548 Hz for LCVA models with inserts types II and III, respectively. These two natural frequencies are even closer to the experiment results than those values without considering the effect of vortices. For both models, the effect of input bump source panel on the left corner is larger than the effect of input bump source panel on the right corner, because the vortex at the left corner is more influential. This can be observed in experiments, and also determined from the numerical panel method results in both models. However, the use of two bump source panels in the model to estimate the effect of vortices is only a rough approximation, because it is difficult to define the dimension of the bump source panel to be consistent with the real characteristic of the vortices.

The numerical panel method is demonstrated to be a good theory for better prediction of liquid column mass damper's characteristics for many different configurations. It has been proven by the simulation results of various LCVA configurations compared to the experimental results, which can give the best correlation when compared to the existing analytical methods (Gao and Kwok (1997), Chang and Hsu (1998) and Hitchcock (1997)).

4.3 Conclusions

The numerical panel method, which is well known and widely accepted in the naval industry and in aerospace for calculating potential flows, is applied to simulate flows in the TLCs and LCVAs. The prediction of the characteristics of TLC and LCVA based on the panel method is found to be accurate over a wide range of damper configurations, which is crucial in control problems.

Significant improvement is achieved by using the numerical panel method with a discrepancy of not greater than 3.4% between the predicted natural frequencies and the experimental results, compared with about 7.5% discrepancy or more in the conventional analysis.

In view of damper applications, this observed order of improvement is significant since a slight mistuning of the damper frequency can substantially deteriorate the effectiveness of the designed damper. In addition, the panel method is

applicable to any configuration of the LCVA and TLCD. This method also provides the induced velocity distribution of the liquid motion inside the damper, which is useful in application with flow dampening devices, including orifices. Therefore the numerical panel method is a versatile and powerful tool for analysis and design of liquid column dampers.



สถาบันวิทยบริการ
จุฬาลงกรณ์มหาวิทยาลัย

CHAPTER V

EXPERIMENTS AND SIMULATIONS OF TLCDS EQUIPPED WITH A FLOW-TRIGGERING DEVICE

5.1 Introduction

Experimental studies using tuned liquid column dampers (TLCDS) for evaluating their control performance have been limited to passive systems. Sakai *et al.* (1991) verified the performance of a TLCDS installed on a scaled-down model of an actual cable stayed bridge tower. Balendra *et al.* (1995) conducted shaking table tests using TLCDS and studied the effect of different orifice opening ratios on the liquid motion. Experimental studies have also been reported by Hitchcock *et al.* (1997) using passive TLCDS with no orifice, termed as liquid column vibration absorbers (LCVAs). Recently Xue *et al.* (2000) presented experimental studies on the application of a passive TLCDS in suppressing the pitching motion of structures and conducted experiments to delineate the influence of different damper parameters on the TLCDS performance.

A full scale installation of a bi-directional passive liquid column vibration absorber (LCVA) on a 67m steel frame communications tower has been reported by Hitchcock *et al.* (1999). This device does not have an orifice/valve in the U-tube and hence, it is not possible to control the damping in the LCVA. They acknowledged that due to the lack of orifice, the damping ratio of the LCVA was not expected to be optimum. They also observed that the LCVA did not perform optimally at all wind speeds. Response reduction of almost 50% was noted, however, non-optimal performance of the damper was noted above and below the design wind speed. This observation re-affirms the fact that passive liquid damper systems are inadequate in performing optimally at all levels of excitation (Kareem, 1994).

This chapter discusses experiments of a semi-active LCVAs which have the initial liquid displacements set to non-zero values. In this chapter, the experimental study on a prototype LCVAs equipped with a flow-triggering device are presented. A flow-

triggering device, which can keep the initial liquid displacement of the LCVA, consists of 4 large size 3 port solenoid valves and the acrylic cover plate as shown in Fig. 5.1. LCVAs equipped with a flow-triggering device are newly proposed to be an effective liquid damper for mitigation of structural response subjected to highly transient earthquake excitation. First, the dynamic characteristics of the LCVAs equipped with a flow-triggering device are investigated and compared with previously obtained free-vibration test results reported in Chapter 3. The LCVAs with inserts types II and III equipped with a flow-triggering device are tested by releasing the flow from a number of different initial liquid displacement. The obtained experimental results are used to compare with those obtained from analytical model. Then the numerical simulations of SDOF system installed with LCVA equipped with a flow-triggering device subjected to various cases of external loadings (such as impulse load, harmonic load and earthquake ground motions) are investigated and compared to SDOF system without LCVA and SDOF system with typical LCVA to study the efficiency of LCVA equipped with a flow-triggering device.

5.2 Experimental Set-Up



Fig. 5.1 Photograph of the experimental set-up

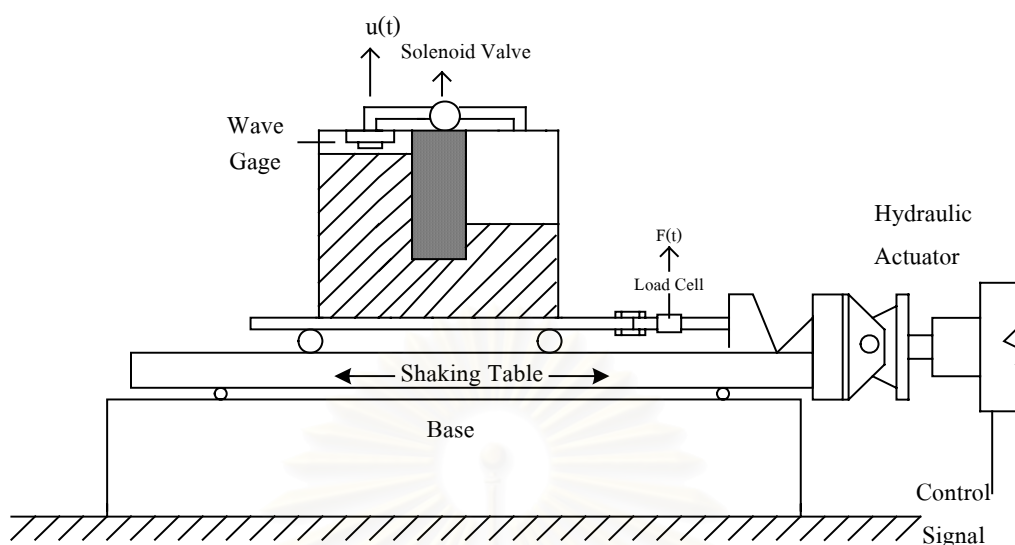


Fig. 5.2 Schematic diagram of the experimental set-up

The experimental set-up is shown in Figs. 5.1 and 5.2. In this chapter, the damper models tested in chapter III are equipped with a flow-triggering device and are experimentally investigated by varying a set of initial liquid displacements.

The flow-triggering device consists of 4 large size 3 port solenoid valves and the acrylic cover plate (as seen in Fig. 5.1). The specification of these solenoid valves is shown in Fig. 5.3. The maximum operating frequency is 8 Hz and the response time is 30 ms. Each side of the acrylic cover plate has 4 acrylic tubes, which have one and a half-inch inside diameter. Both sides of the acrylic tubes are connected through the solenoid valve by rubber tube. The air pressure pump is connected to the air chamber on one side of the tank. By applying the air pressure, the liquid level in that side will be decreased, while the liquid level in another side of the tank will be increased. The liquid level is measured by a Keyence laser displacement sensor (as shown in Fig.3.5). After the liquid level reach the desired level, the application of the air pressure will be stop. The solenoid valve is opened by applying voltage through the computer, then the liquid inside the tank is released and moved like a free-vibration testing. The interaction force and the liquid displacement are determined by a 2-kN Tokyo Sokki Kenkyujo load cell (as shown in Fig.3.6) and a Keyence laser displacement sensor, respectively.

Specifications

Fluid		Air					
Operation		N.C. or N.O. (Convertible)					
Pilot style		Internal pilot			External pilot		
		General			Vacuum/Low pressure	General	
Operating pressure range (MPa)	Main pressure	0.2 to 0.8			-101.2kPa to 0.2		0.2 to 0.8
	Pilot pressure				0.2 to 0.3		Refer to the graph on p.2.8-2
Ambient and fluid temperature (°C)		0 (No freezing) to 60					
Response time ⁽¹⁾ (ms)(at 0.5 MPa)		ON	AC	30 or less	OFF	AC	30 or less
			DC	40 or less		DC	30 or less
Max. operating frequency (Hz)		8					
Lubrication ⁽²⁾		Required (Equivalent to turbine oil class1 ISO VG32)					
Manual override		Non-locking					
Mounting		Free					
Shock/Vibration resistance ⁽³⁾ (m/s ²)		150/50					



Note 1) Based on dynamic performance test JIS B8374-1981. (Coil temperature 20°C, at rated voltage, without surge voltage suppressor)

Note 2) Shock resistance: No malfunction resulted from the impact test using a drop impact tester. The test was performed on the axis and right angle directions of the main valve and armature, for both energized and de-energized states.

Note 3) Vibration resistance: No malfunction occurred in a one-sweep test between 45 and 1000Hz. Test was performed at both energized and de-energized states to the axis and right angle directions of the main valve and armature. (Value in the initial stage.)

Fig. 5.3 Solenoid valve specification

5.3 Experiment Investigations

The LCVAs equipped with a flow-triggering device are firmly fixed on top of the shake table as shown in Figs. 5.1 and 5.2. Those LCVAs with inserts types II and III are experimentally investigated under 5 initial liquid displacements of about 5, 7.5, 10, 12.5, 15 cm. For each initial liquid displacement, the experiment is repeated for 4 times. In all tests, the interaction force of LCVA and the phase and the displacement of the liquid motion are measured.

5.3.1 Damping for LCVAs equipped with a flow-triggering device

Figs. 5.4 and 5.5 show the liquid amplitude histories of LCVA without cover plate and LCVA with cover plate for inserts types II and III, respectively.

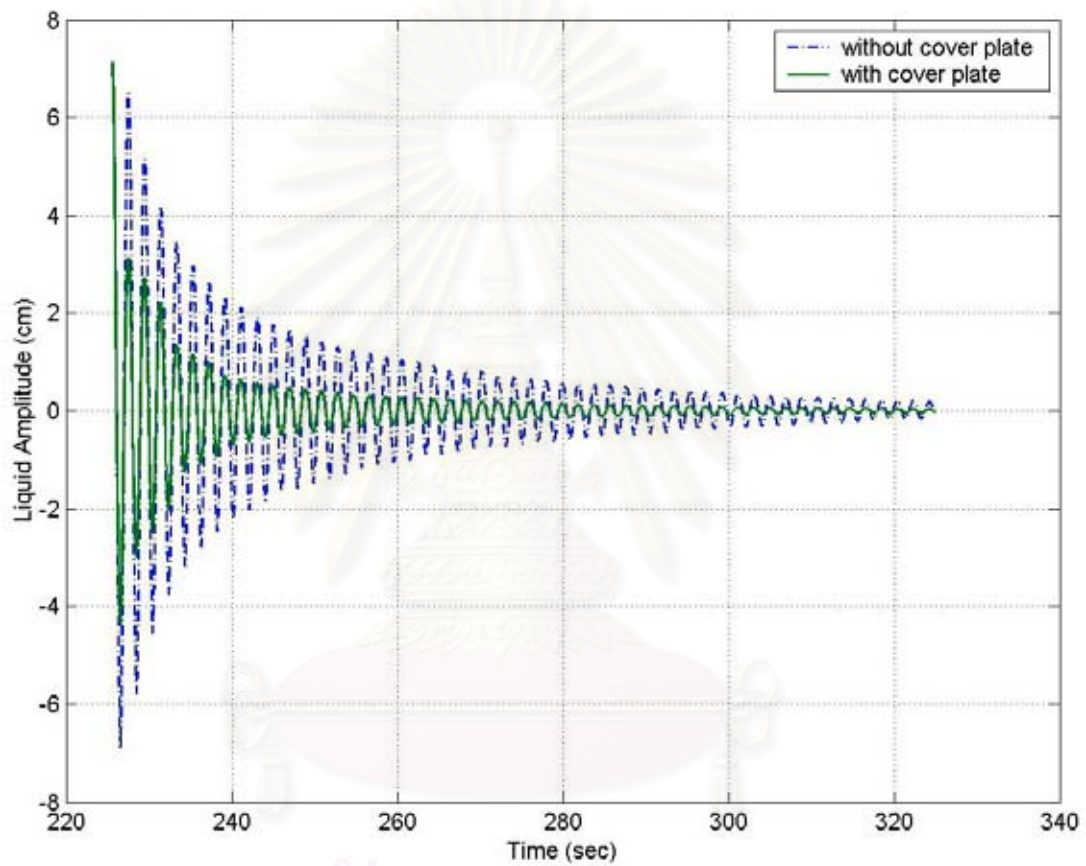


Fig. 5.4 The liquid amplitude histories of LCVA without cover plate and LCVA with cover plate for insert type II

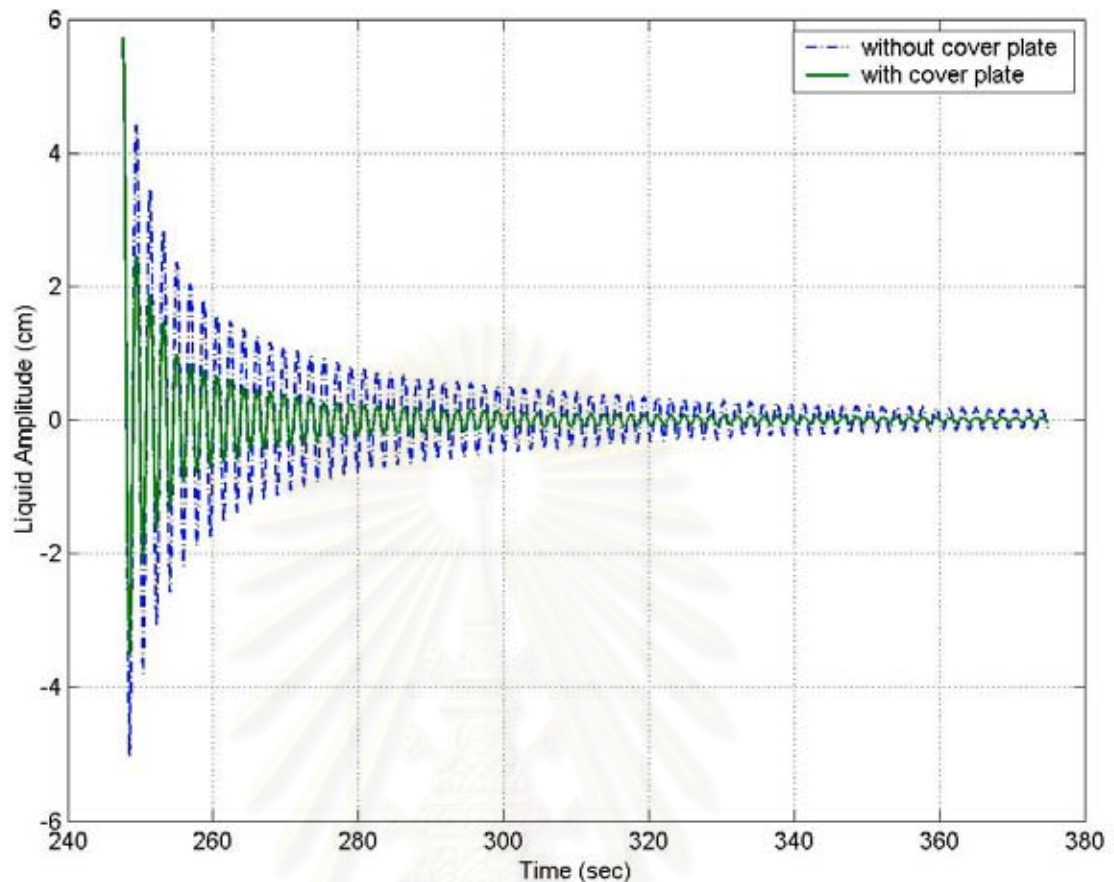


Fig. 5.5 The liquid amplitude histories of LCVA without cover plate and LCVA with cover plate for insert type III

The decay rate of liquid displacement without cover plate is obtained from the free-vibration tests in chapter 3, while the decay rate of liquid displacement with cover plate is obtained from the initial condition tests of the LCVAs equipped with a flow-triggering device. Approximately 3-4 times greater for damping ratio can be observed after the LCVAs with inserts types II and III are equipped with a flow-triggering device. This is due to the very high energy loss of airflow from one side of the tank through the rubber tubes and solenoid valves to another side of the tank.

The damping in the system of LCVAs equipped with a flow-triggering device is found to be quite highly nonlinear. The linear damping and quadratic damping are supposed to be obtained from the initial condition tests of the LCVA models equipped

with a flow-triggering device. As described in Chapter 3, the damping ratio ζ can be obtained from Eq. (3.1):

$$\zeta = \frac{1}{2\pi} \ln \left(\frac{u_i}{u_{i+1}} \right) = \frac{1}{2\pi} \ln \left(\frac{\dot{u}_i}{\dot{u}_{i+1}} \right) = \frac{1}{2\pi} \ln \left(\frac{\ddot{u}_i}{\ddot{u}_{i+1}} \right)$$

Figs. 5.6 and 5.7 show the relationship between the damping ratio and liquid velocity for the LCVAs with inserts types II and III equipped with a flow-triggering device together with those obtained from the free-vibration test in Chapter 3.

As seen in Figs. 5.6 and 5.7, the quadratic damping of LCVAs equipped with a flow-triggering device is obviously greater than that of typical LCVAs experimentally investigated in Chapter 3 for both inserts types II and III. This is due to the effect of a flow-triggering device. The damping ratio varies with the amplitude of the liquid velocity. This is coincident to the nonlinear damping characteristic of LCVAs. The damping ratio of LCVAs equipped with a flow-triggering device is higher than typical LCVAs about 4-5 times. Then, it might be the problem to apply LCVAs equipped with a flow-triggering device in actual applications because the damping ratio of them might exceed the designed optimum damping ratio.

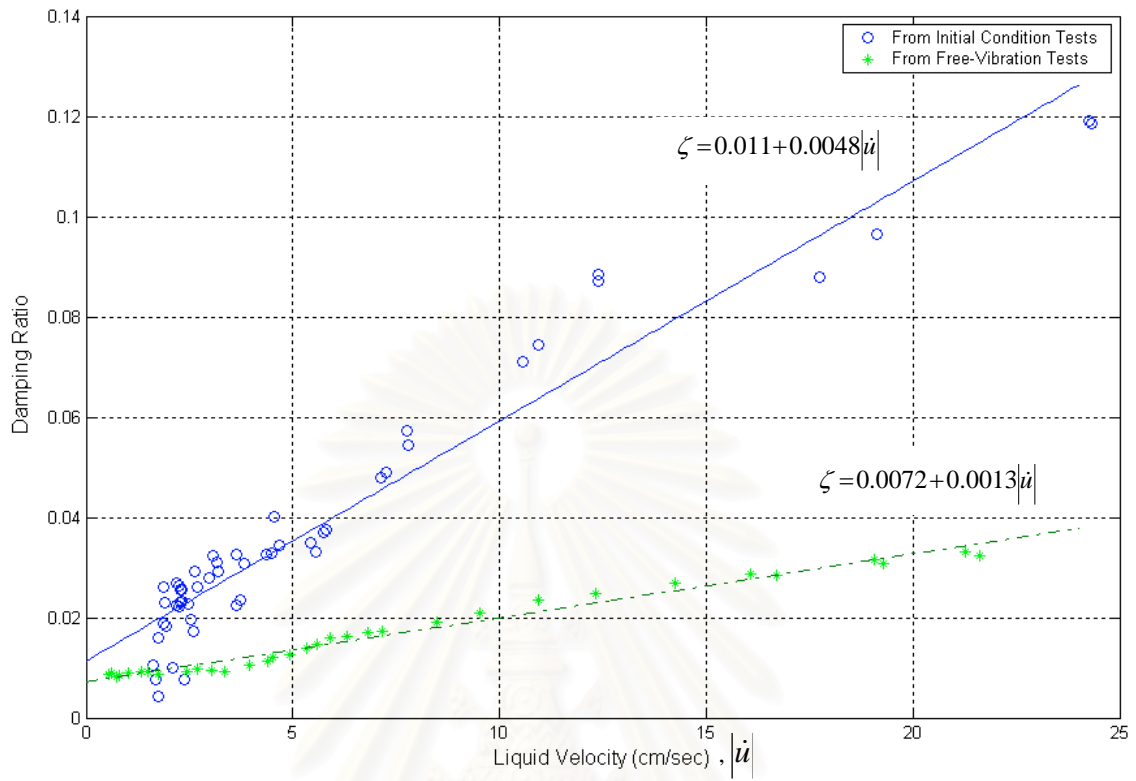


Fig. 5.6 The Relationship between the damping ratio and liquid velocity for LCVA with insert type II

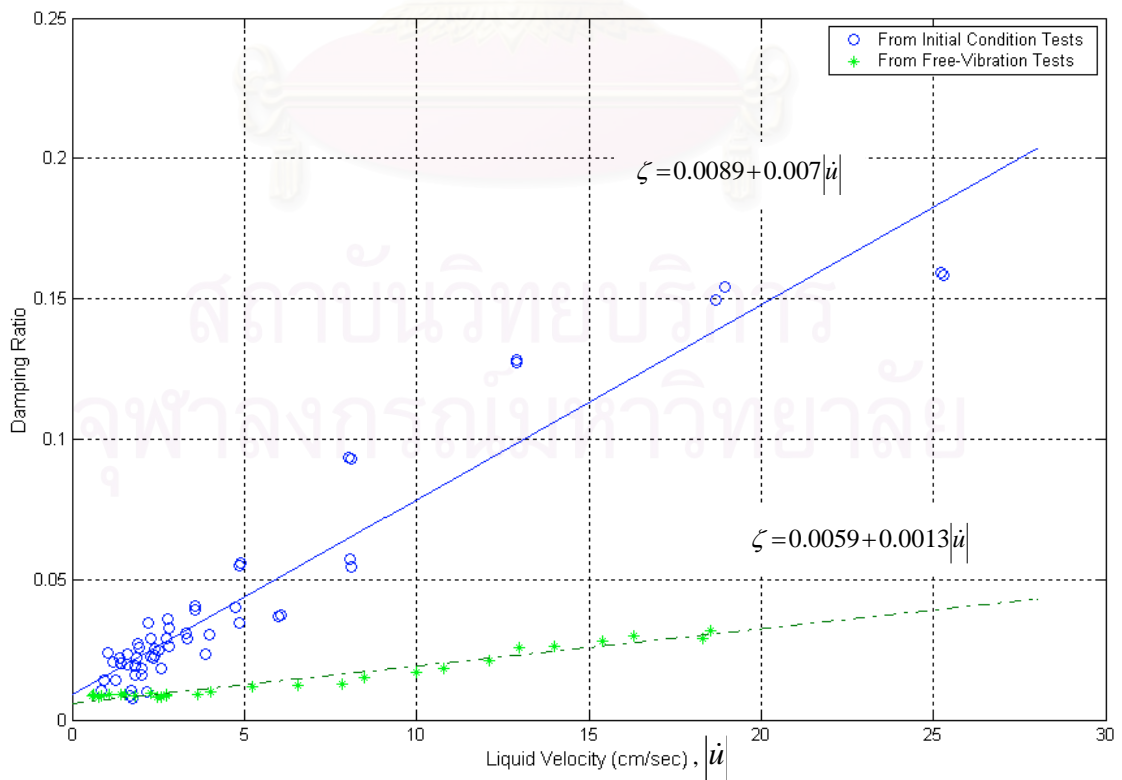


Fig. 5.7 The Relationship between the damping ratio and liquid velocity for LCVA with insert type III

5.3.2 Verification of initial condition test results from numerical panel method

To verify the equation of motion for simulation the characteristics of LCVAs equipped with a flow-triggering device, the numerical panel method is used. The natural frequency of the LCVAs equipped with a flow-triggering device is obtained by using the numerical panel method. By using the damping ratio obtained from the experiment in previous section (Figs. 5.6 and 5.7), the responses of the LCVAs equipped with a flow-triggering device can be analytically obtained by solving Eq. (2.5) as described in Chapter 3 and the results are compared with the initial condition test data for both inserts types II and III.

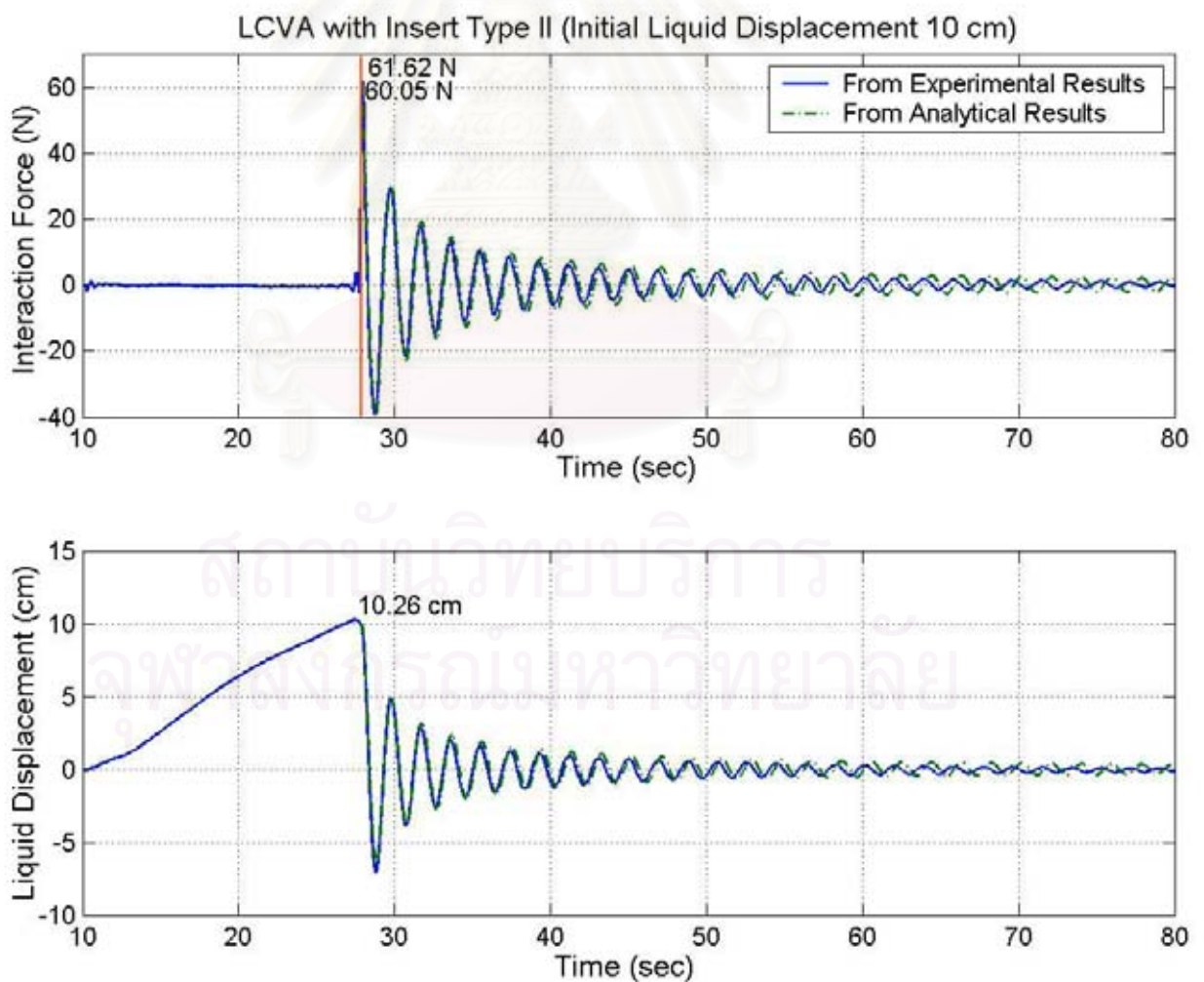


Fig. 5.8 Initial liquid displacement of 10 cm for LCVA with insert type II

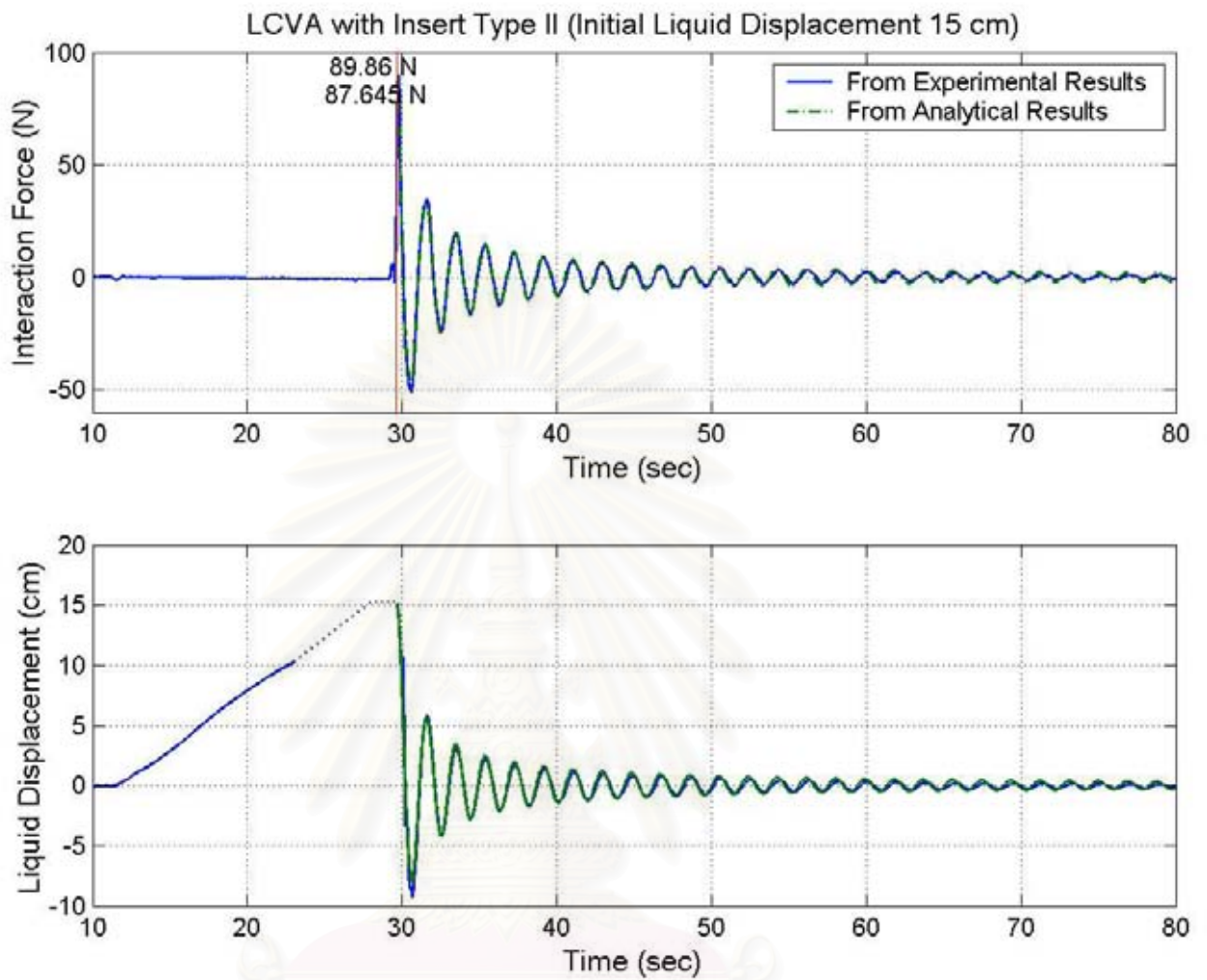


Fig. 5.9 Initial liquid displacement of 15 cm for LCVA with insert type II

สถาบันวิทยบริการ
จุฬาลงกรณ์มหาวิทยาลัย

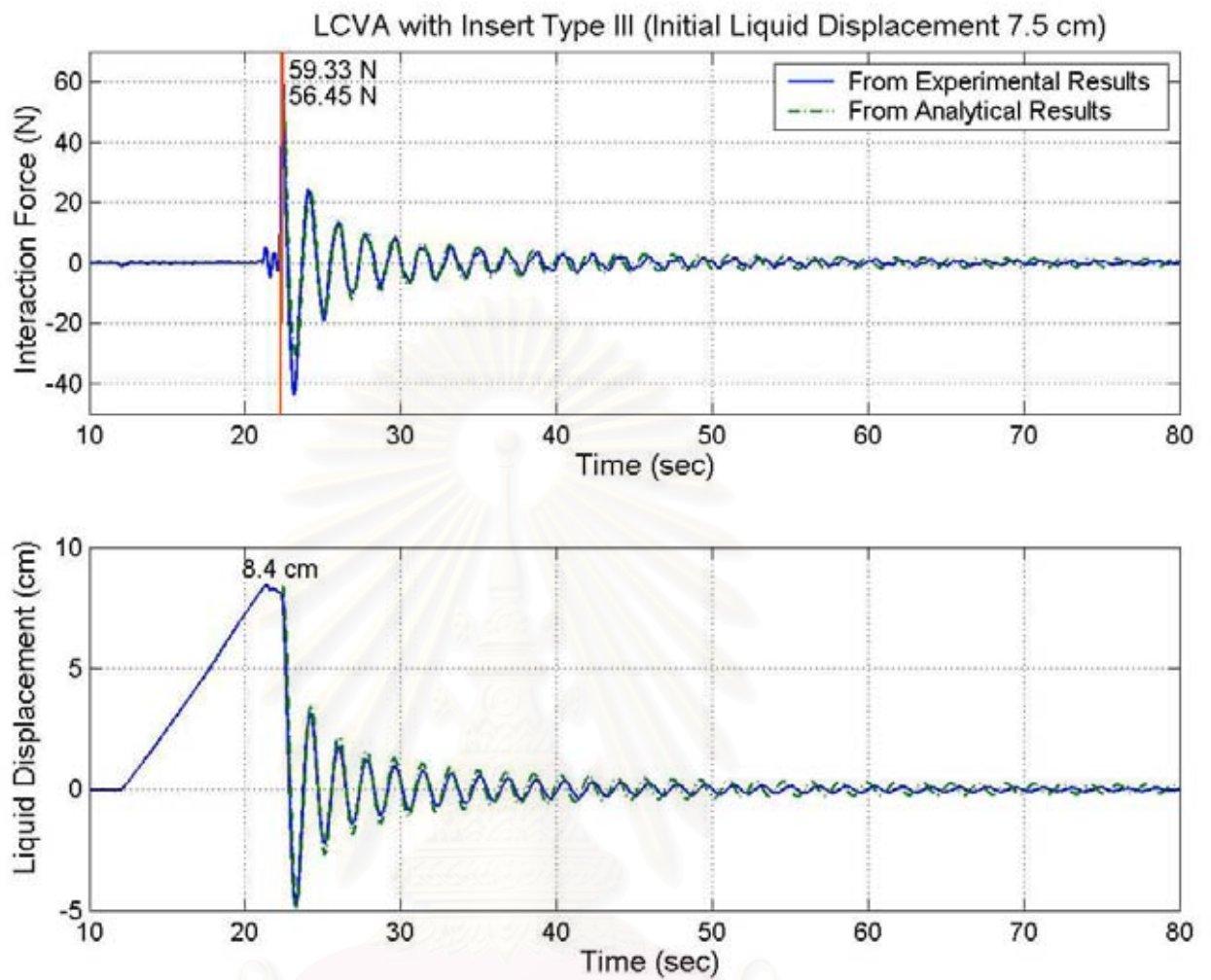


Fig. 5.10 Initial liquid displacement of 7.5 cm for LCVA with insert type III

สถาบันวิทยบริการ
จุฬาลงกรณ์มหาวิทยาลัย

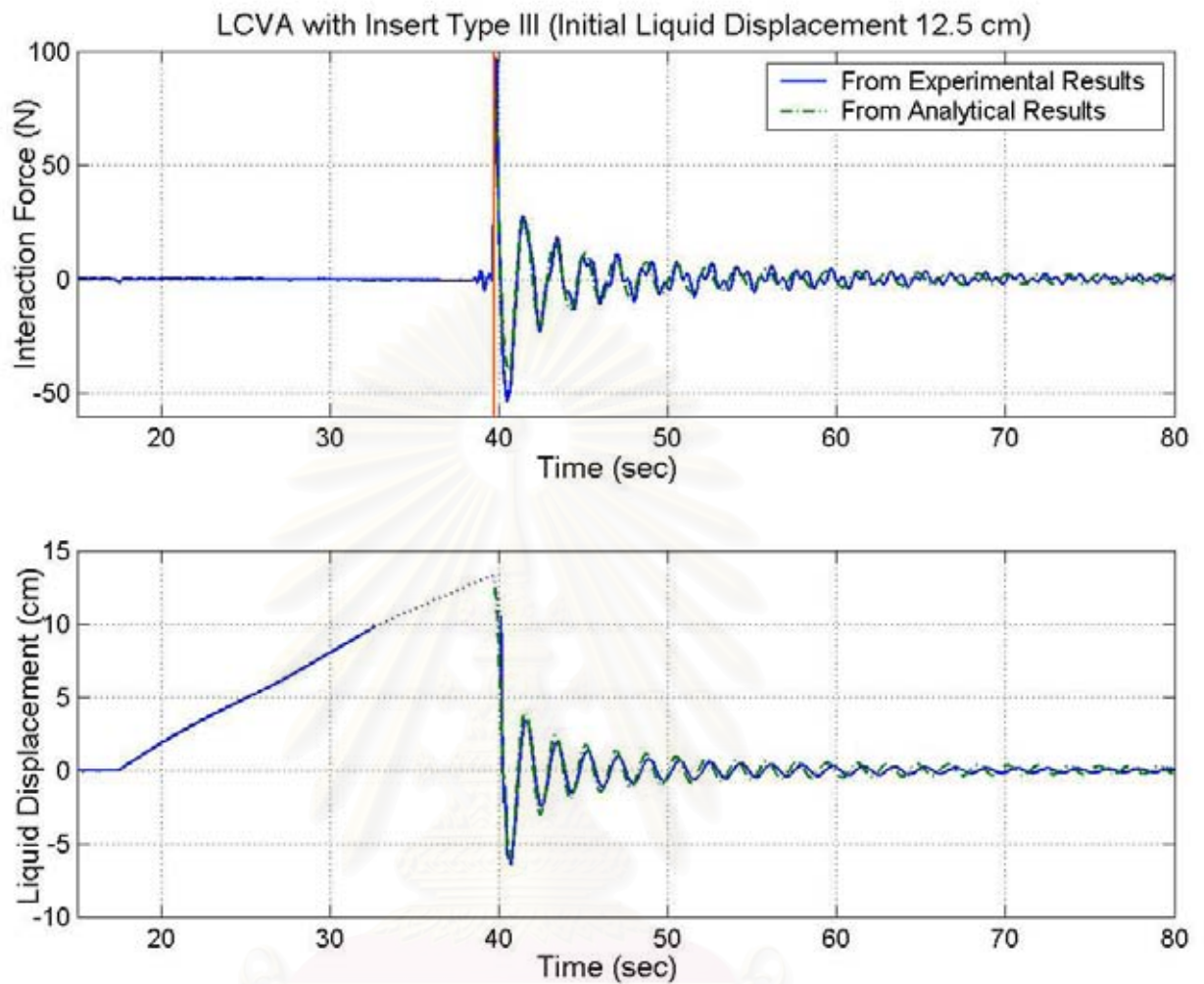


Fig. 5.11 Initial liquid displacement of 12.5 cm for LCVA with insert type III

Figs. 5.8 –5.11 show the analytical results compared with the initial condition test data. The vertical line on Figs. 5.8 – 5.11 is the signal of the applied voltage to the solenoid valves, which gives rise to 5 volts to open the valves. Before the solenoid valves are opened, the interaction force due to the liquid motion measured by a 2-kN Tokyo Sokki Kenkyujo load cell is almost zero for all tests due to the static equilibrium, while the liquid displacement measured by a Keyence laser displacement sensor is lifted up to the desire level. After the solenoid valves are suddenly opened, the liquid will move like a free vibration. Since the measurable range of the Keyence laser displacement sensor is limited to about ± 10 cm, the signal of the liquid displacement in Figs. 5.9 and

5.11 beyond this range are approximately replaced by the dotted line. So it should be noted that for those cases when the initial liquid displacement is higher than 10 cm, i.e. 12.5 cm and 15 cm, the exact liquid level after the solenoid valves are opened cannot be obtained (as seen in Figs 5.9 and 5.11). With the initial liquid displacement measured by the Keyence laser displacement sensor, the analytical solutions based on the numerical panel method can be obtained by solving Eq. (2.5). It is found from Figs 5.8 – 5.11, that the analytical solutions based on the numerical panel method agree very well with the experimental results for both amplitude and phase of the interaction force and liquid displacement. From these figures, the analytical solutions based on the numerical panel method can predict the characteristic of LCVA equipped with a flow-triggering device very well. In particular, the agreement is very good for LCVA with insert type II, and acceptable for LCVA with insert type III.

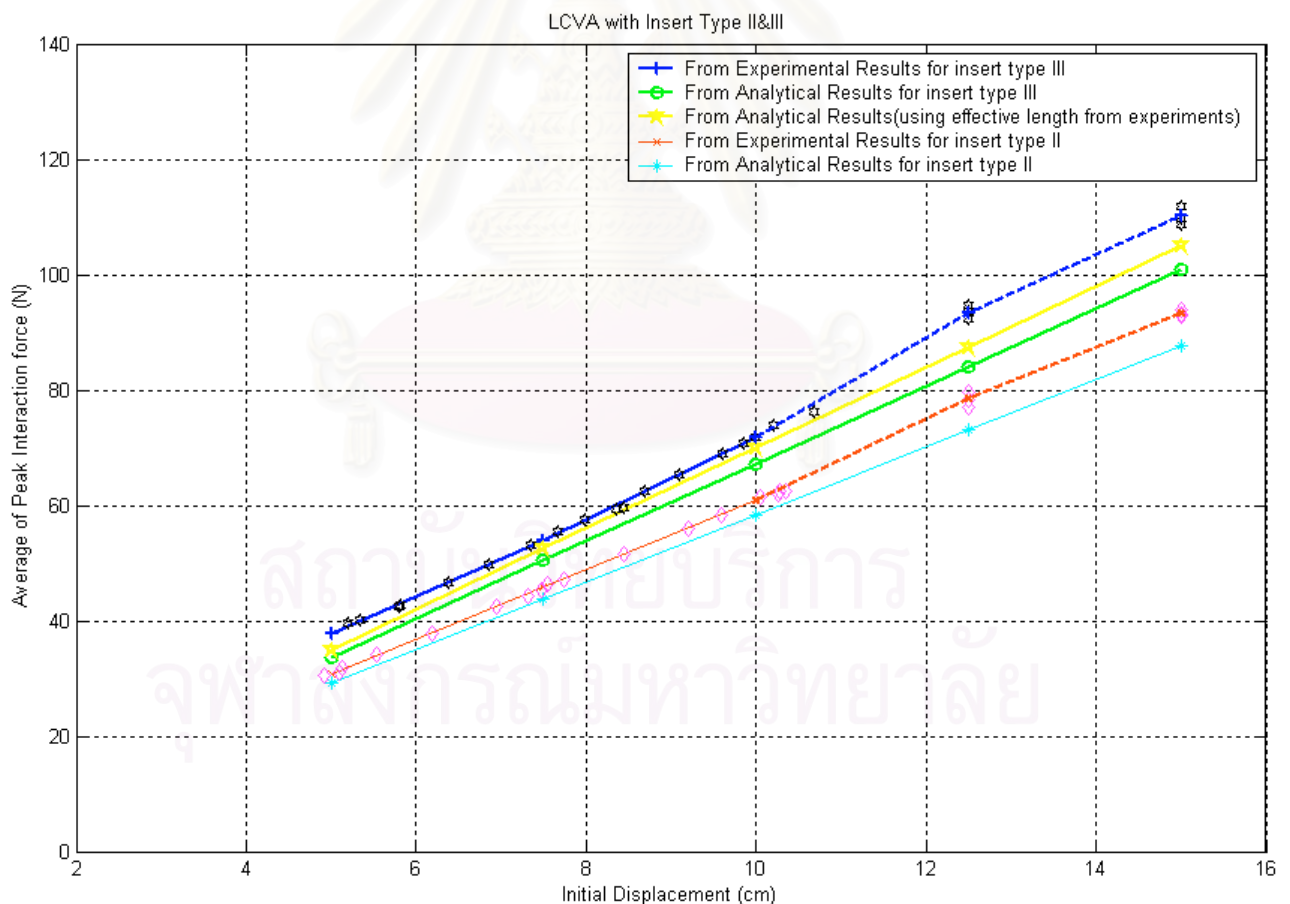


Fig. 5.12 The Relationship between the peak interaction force and initial displacement of 5-15 cm for LCVAs with inserts types II and III

Fig. 5.12 shows the peak interaction force of each initial liquid displacement for all tests compared to the analytical solutions based on the numerical panel method. While, the yellow line shows the analytical solutions using the effective length from the experiments. The analytical solutions based on the numerical panel method agree very well with the experimental results of LCVA with insert type II. This is due to the precise prediction of the natural frequency of the LCVA with insert type II (as seen in Table 4.1). The agreement between the analytical solutions based on the numerical panel method and the experimental results is acceptable. This is due to the slightly error of the prediction of the natural frequency of LCVA with insert type III.

The discrepancy between the measured and the calculated interaction force based on the numerical panel method varies from about 4% to 7% for LCVA with insert type II, while the discrepancy between the measured and the calculated interaction force based on the numerical panel method varies from about 12% to 15% for LCVA with insert type III. This is considered only in the range about 5 – 10 cm of initial liquid displacement.

Instead of using natural frequency of the LCVA with insert type III obtained from the numerical panel method, the natural frequency from the experimental results are used to compute the peak interaction force. After adjusting the natural frequency from the experiment, the yellow line is obtained by using Eq. (2.5), then the agreement becomes very good similar to the case of LCVA with insert type II. The discrepancy between the measured and the calculated interaction force based on the numerical panel method is reduced to about 4% to 7% for LCVA with insert type III (same to LCVA with insert type II). This implies the trustworthiness of the experiment. For the cases of the initial liquid displacement of 12.5 and 15 cm, since the initial liquid displacement cannot be measured due to the limitation of a Keyence laser displacement sensor, the data for those cases is manually approximated from meter shown by the dotted red line and blue line for LCVA inserts types II and III, respectively.

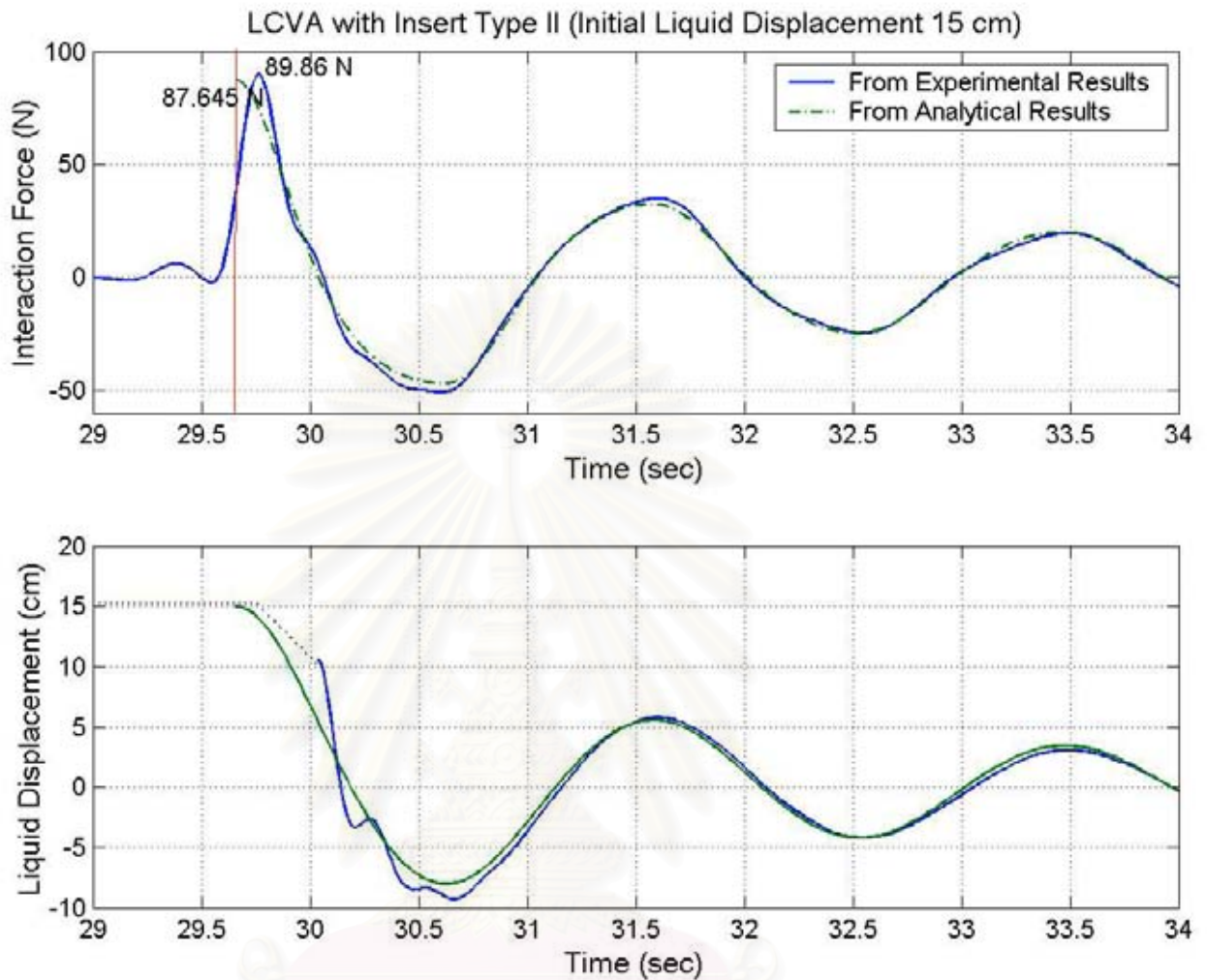


Fig. 5.13 Initial liquid displacement 15 cm for LCVA with insert type II (extended in axis of time)

Fig. 5.13 is the same plot of Fig. 5.9 but the time axis is zoomed in for the first few cycle of fluid flow after opening the solenoid valves. As obviously observed from Eq. (2.5), the liquid acceleration is at the maximum immediately after the liquid is released since the initial velocity of the liquid and the external base excitation acceleration is at zero. Thus, from analytical model the interaction force which is coincident to the liquid acceleration will be at the maximum value at the time when the liquid inside LCVA is released. However, it can be observed from Fig. 5.13 that there is the delay between the peak interaction force from analytical result and the peak interaction force from experimental result in which the peak interaction force from

experimental result becomes slower. The delay is observed to be about 0.12 sec for the case shown in Fig. 5.12 while the delay for other initial condition tests varies from about 0.1 – 0.15 second. This delay is from the effect of the analog low pass filter used during experiment which imposes the delay to the acquired signals about 0.1 sec and the delay of the response time of the solenoid valves (see Fig. 5.3), which are about 0.03 sec. This delay is believed to be vanished, if the digital filter is used instead of the analog low pass filter and the solenoid valves with higher speed are replaced.

5.4 Numerical Examples of LCVA with the Initial Liquid Displacement

Numerical examples are given to illustrate applications of the LCVA equipped with a flow-triggering device. The first set of examples is a numerical simulation that evaluates the performance of the LCVA equipped with a flow-triggering device installed on the top of the structure subjected to impulse load and harmonic load. The second set of examples is for the structure subjected to seismic ground motions, where ground motion records from historical earthquakes have been used to obtain statistical descriptions of the system performance. Fig. 5.14 shows the properties of the structure and LCVA. For convenience, the structure is modeled using SDOF system. The SDOF system with the LCVA equipped with a flow-triggering device is numerically simulated. The equation of motion governing the vibration of the SDOF-LCVA system is solved by the sub-system concept as described in Chapter 2.

A SDOF system has natural period $T = 2$ s, and damping ratio $\zeta_s = 0.02$. LCVA is attached on the top of the SDOF system. The mass ratio μ is assumed to be 0.04. The tuning ratio γ and the damping ratio of LCVA ζ_f are obtained from Table 2.1 as $\gamma = 0.976$ and $\zeta_f = 0.032$, respectively. As observed from Fig. 5.6, this optimum damping ratio is much lower than the damping ratio obtained from the experiment. The tuning ratio is used to compute the effective length $L_e = 2.086$ m. To get this effective length,

the horizontal width B and vertical column height H of the LCVA is determined from the numerical panel method as $B = 0.70$ m and $H = 0.607$ m.

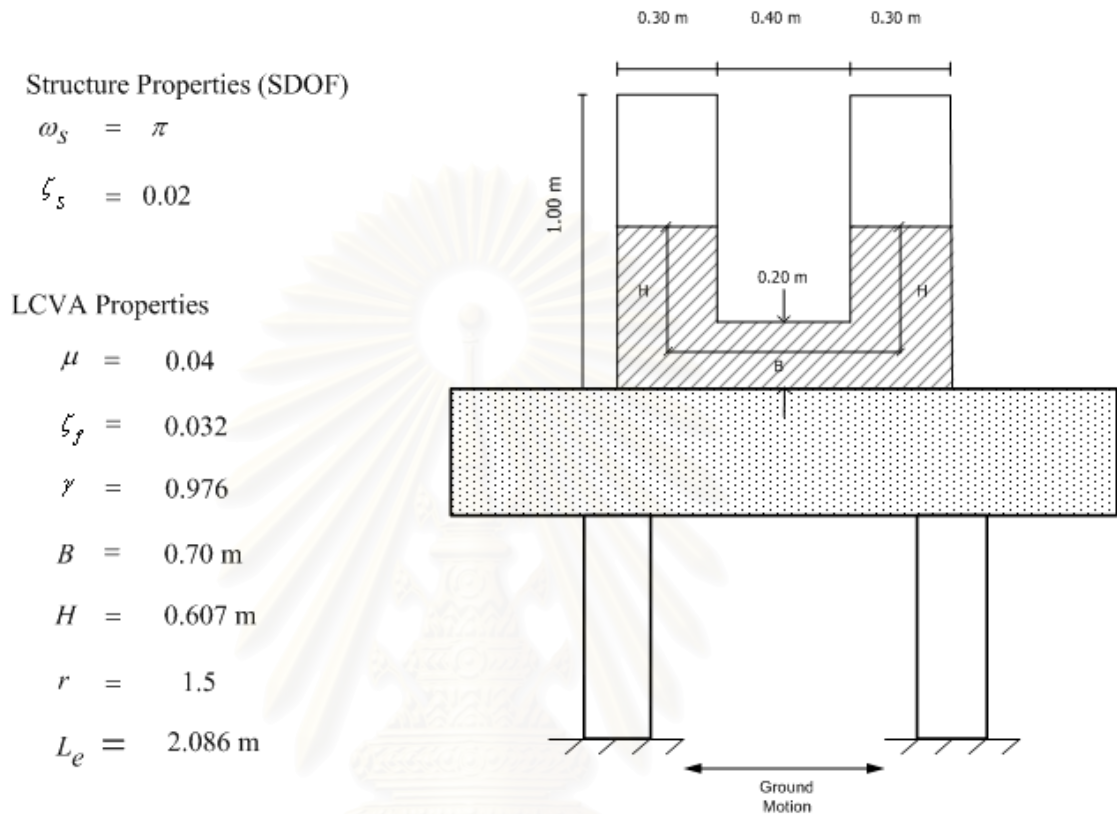


Fig. 5.14 SDOF system with LCVA

5.4.1 Impulse load and harmonic load

In this section, the performances of typical LCVA and LCVA equipped with a flow-triggering device have been reported. For this simulation, the performance of SDOF system installed a typical LCVA or LCVA equipped with a flow-triggering device (as shown in Fig. 5.14) are compared under impulse load for initial velocity = 0.2 m/s and harmonic load for peak ground acceleration (PGA) = 0.02g. The initial liquid displacement of 0.50 m, which is the possible maximum value for the LCVA equipped with a flow-triggering device, is considered.

For the impulse load case, the structural impulse conditions are specified by zero initial displacement and initial velocity of 0.2 m/s. Immediately after the impulse, the liquid inside LCVA is released. Thus the initial conditions for the LCVA are initial liquid displacement of 0.5 m and initial liquid velocity of 0 m/s.

For the harmonic load case, the SDOF system shown in Fig. 5.14 is subjected to the 0.5 Hz harmonic base excitation with $PGA = 0.02g$. This excitation has the same exciting frequency to the natural frequency of the structure. The iteration to release the initial liquid displacement for every time steps is used to observe the structure response.

Fig. 5.15 shows the displacement history of the SDOF structure subjected to impulse load for uncontrolled SDOF system, SDOF system with typical LCVA, SDOF system with LCVA equipped with a flow-triggering device and SDOF system with LCVA equipped with a flow-triggering device using damping ratio from the experiment (Fig. 5.6). The case using damping ratio from the experiment is investigated to show the consequences of excessive damping ratio as observed from test set up. The damping ratio from experiment, which is much higher than the optimum value, causes to deteriorate the performance of LCVA equipped with a flow-triggering device as observed from the dotted in Fig 5.15. The peak displacement response is a little bit higher than the case of SDOF system with LCVA equipped with a flow-triggering device using optimum damping ratio, while the root mean square (rms, which is considered for 20 cycles since the start of event) is much higher. The test set up that can keep the initial liquid displacement without generated excessive damping ratio is the interesting topic in the future study.

Table 5.1 summarizes the simulation results, where X and A are the values of the relative displacements and absolute accelerations of the structure, respectively. As shown in Table 5.1 the response of the SDOF system equipped with the typical LCVA is worse than the case of uncontrolled SDOF system for the peak displacement, while the improvement of 5.19% reduction in the peak displacement and 35.98% reduction in the rms of the displacement is obtained for the SDOF system with LCVA equipped with a flow-triggering device in case of impulse load. However, no improvement can be obtained in case of harmonic load when compared to the typical LCVA, because the steady state response is the same as the case of the typical LCVA. After releasing the

initial liquid displacement in case of harmonic load in every time steps, the structure response takes time about 1-2 cycle to go to the same displacement level as in the typical LCVA case. The improvement for harmonic load case can be effectively obtained by using the semi-active LCVA with damping adjustable in real time (Yalla *et al.* 2001).

TABLE 5.1 Summary of simulation results in case of impulse load and harmonic load

Excitation Type of control	Impact-induced transient vibration				Harmonic (PGA=0.02g)			
	Xmax	Amax	Xrms	Arms	Xmax	Amax	Xrms	Arms
Uncontrolled	0.0617	0.6097	0.0164	0.1619	0.4961	4.8962	0.3068	3.0276
LCVA	0.0631	0.5987	0.0136	0.129	0.3015	3.1597	0.2101	2.0652
% of reduction	-2.27	1.80	17.07	20.32	39.23	35.47	31.52	31.79
LCVA (with ini cond)	0.0585	0.5481	0.0105	0.0996	0.3015	3.1597	0.2101	2.0652
% of reduction	5.19	10.10	35.98	38.48	39.23	35.47	31.52	31.79

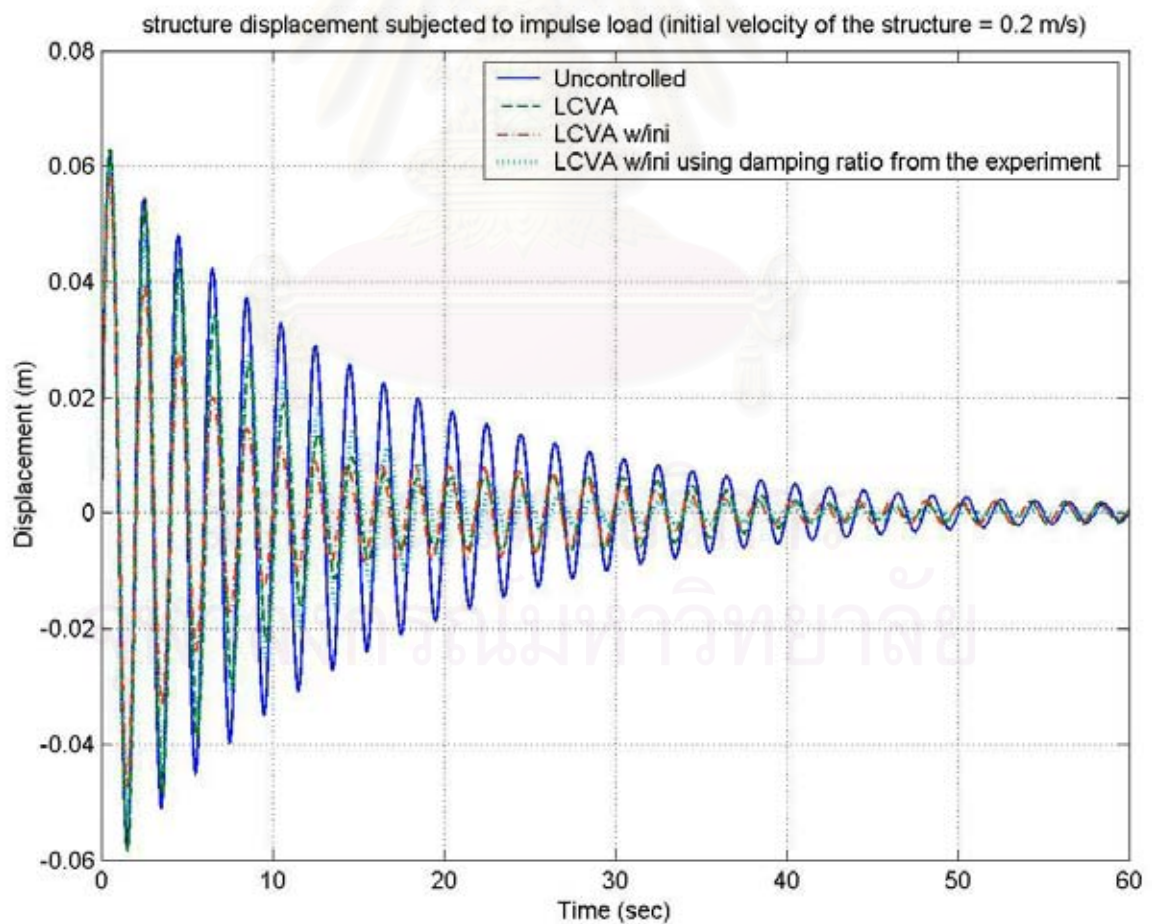


Fig. 5.15 Displacement response under impulse load type (initial velocity = 0.2 m/s)

5.4.2 Earthquake ground motions

This section, the numerical simulations are repeated for several earthquake ground motion records. Fig. 5.16 shows 4 earthquake ground motion records, which are used for response simulate in this section. The near field ground motions (1952 Taft Kern County ground motion and 1989 Loma Prieta ground motion) are scaled to the value of 0.50 times the acceleration due to gravity ($PGA = 0.5g$). The far field ground motions (1985 Mexico ground motion and 1995 Bangkok ground motion) are scaled to the value of 0.10 times the acceleration due to gravity ($PGA = 0.1g$).

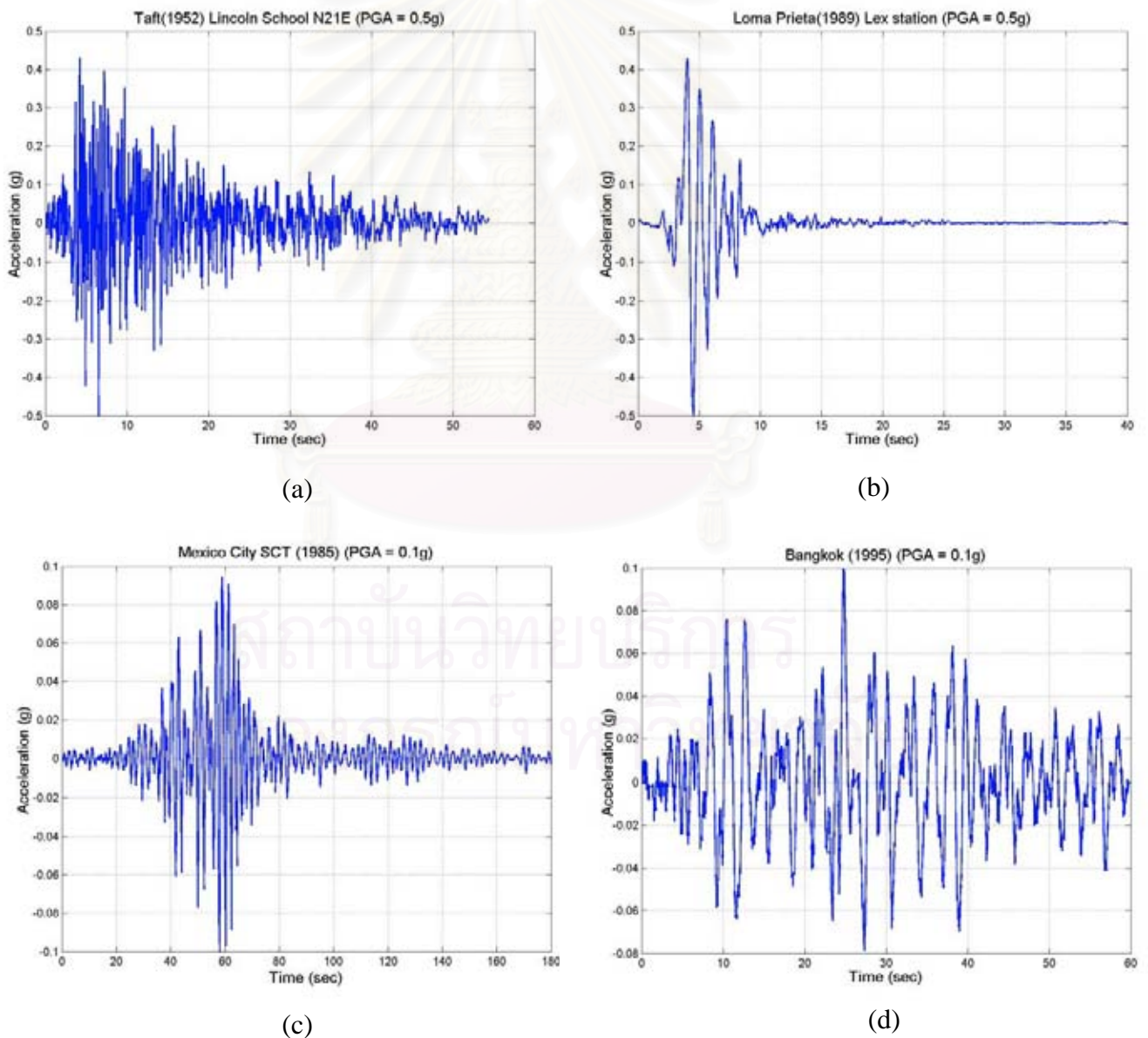
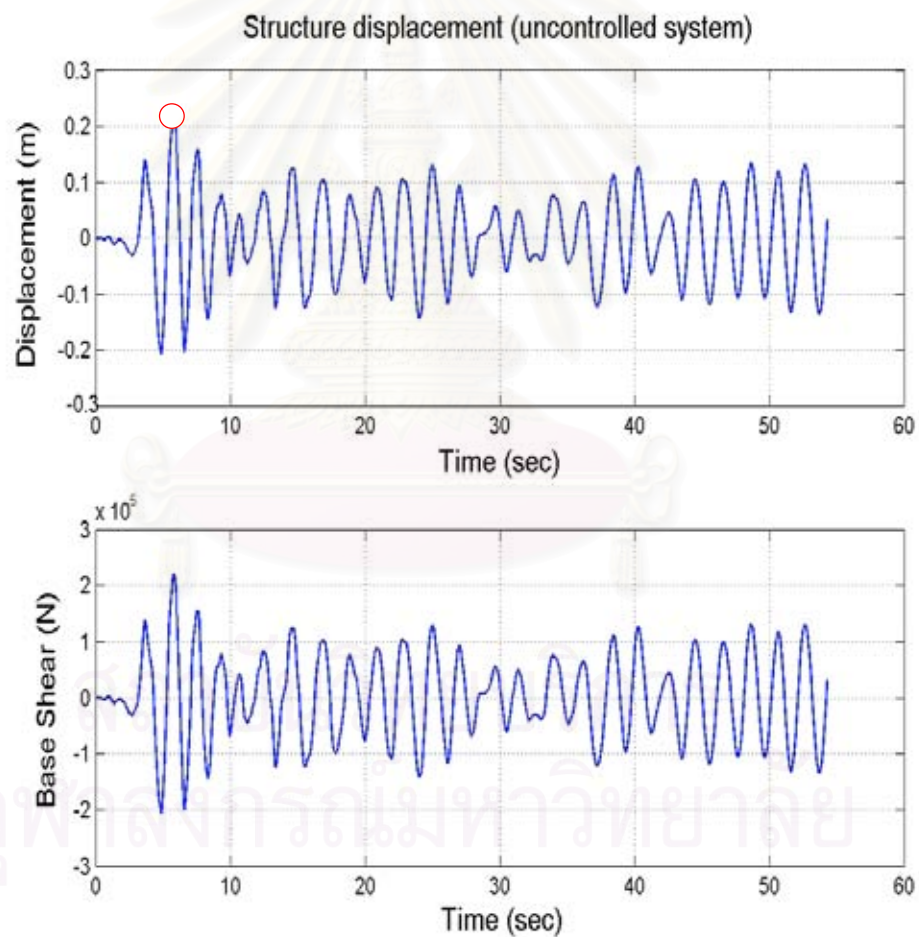


Fig. 5.16 Scale ground motion records: (a) 1952 Taft; (b) 1989 Loma Prieta; (c) 1985 Mexico city (SCT); (d) 1995 Bangkok

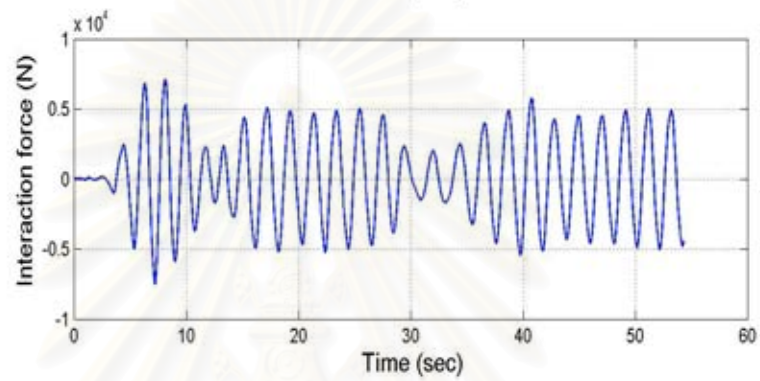
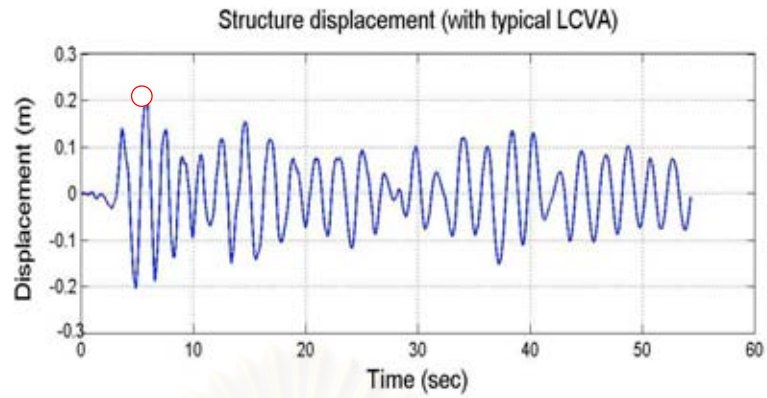
The SDOF system as shown in Fig. 5.14 is simulated by using 4 earthquake ground motion records as shown in Fig. 5.16 for 3 cases of uncontrolled SDOF system, SDOF system with typical LCVA and SDOF system with LCVA equipped with a flow-triggering device. In case of the LCVA equipped with a flow-triggering device, the computation process is repeated to release 2 initial liquid displacements (+0.5 m and -0.5 m) for every time step to find the maximum reduction of the structure displacement.

Fig. 5.17 shows the response of SDOF system subjected to 1952 Taft ground motion for 3 cases of uncontrolled SDOF system, SDOF system with typical LCVA and SDOF system with LCVA equipped with a flow-triggering device, respectively.

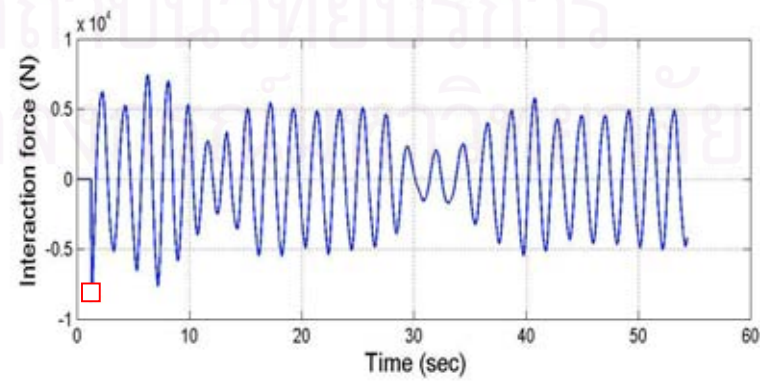
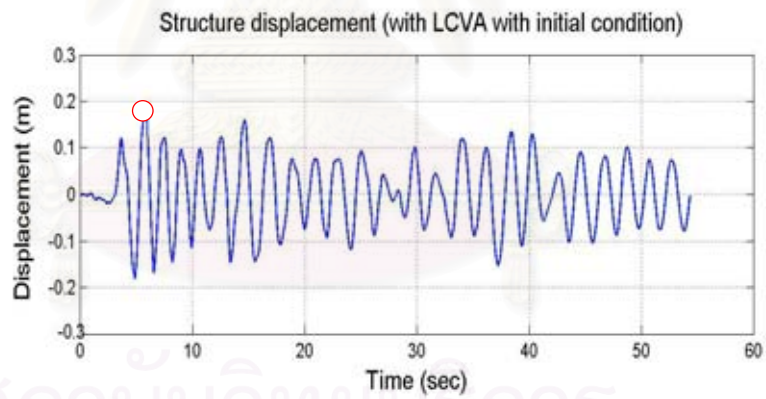


(a)

Fig. 5.17 SDOF system response under 1952 Taft; (a) uncontrolled SDOF system; (b) typical LCVA; (c) LCVA equipped with a flow-triggering device



(b)



(c)

Fig. 5.17 (continued)

As shown in Fig. 5.17, the peak displacement response cannot be reduced much by using typical LCVA. The improvement of only about 3.39% reduction in the peak displacement is obtained for the SDOF system with typical LCVA, while the best improvement of about 14.51% reduction in the peak displacement is obtained for the SDOF system with LCVA equipped with a flow-triggering device. The peak displacement of the uncontrolled SDOF system and SDOF system with LCVA is at about 5.8 sec as shown in the circle in Fig. 5.17. To reduce this peak displacement by LCVA equipped with a flow-triggering device, 2 initial liquid displacements of +0.5m and -0.5m are considered. The simulation by releasing those initial liquid displacements of the LCVA in every time step before 5.8 sec is investigated. Fig. 5.18 shows the plot of peak displacement from releasing initial liquid displacement of -0.5 m for each time step from start of event. The minimum peak displacement of 0.1868 m is found at the releasing initial liquid displacement of -0.5 m at the time 1.28 sec as shown in Fig. 5.18 (square mark). After the time of 5.8 sec from start of event, the peak displacement is constantly at about 0.2226 m because the peak displacement for this SDOF system subjected to 1952 Taft ground motion is occurred at the time of 5.8 sec. As observed from Fig. 5.18, releasing initial liquid displacement at improper time can give the worse peak displacement response when compared to both uncontrolled SDOF system and SDOF system with typical LCVA. The peak displacement is given rise to about 0.24 m, if the liquid inside LCVA is released to suppress the motion of SDOF system at the time 0.34 sec. So the time to release this initial liquid displacement is very important. The oscillation frequency of the plot in Fig. 5.18 (before the time of 5.8 sec from start of event) can be observed to be the natural frequency of the SDOF system (0.5 Hz).

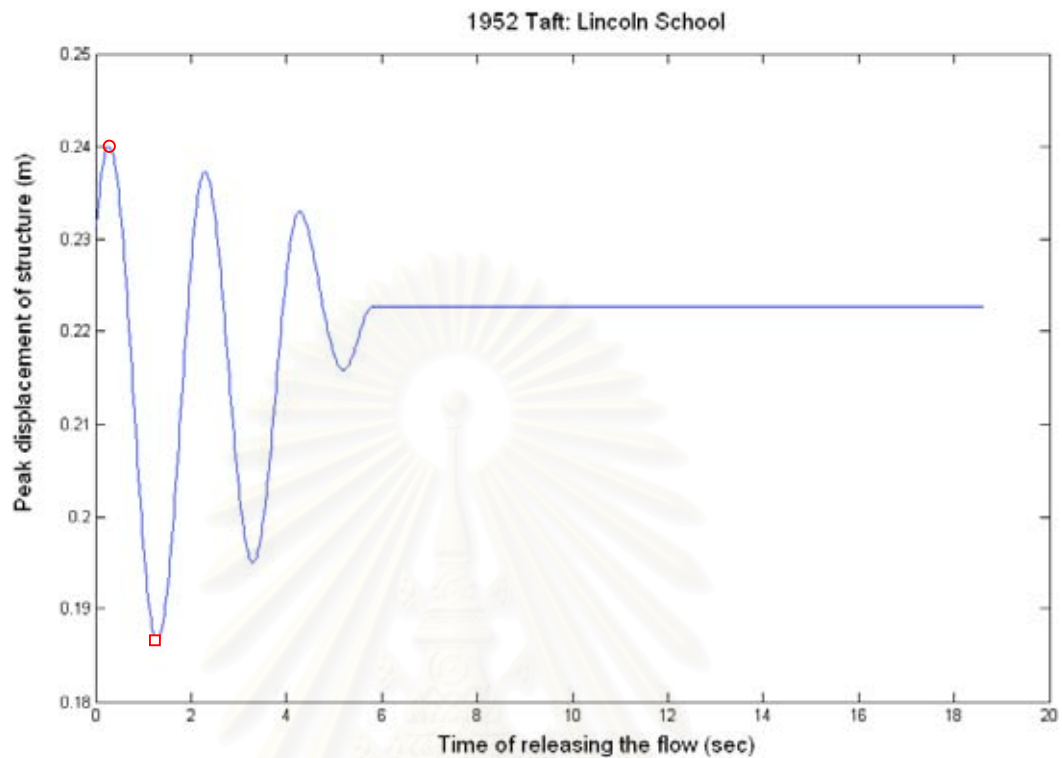
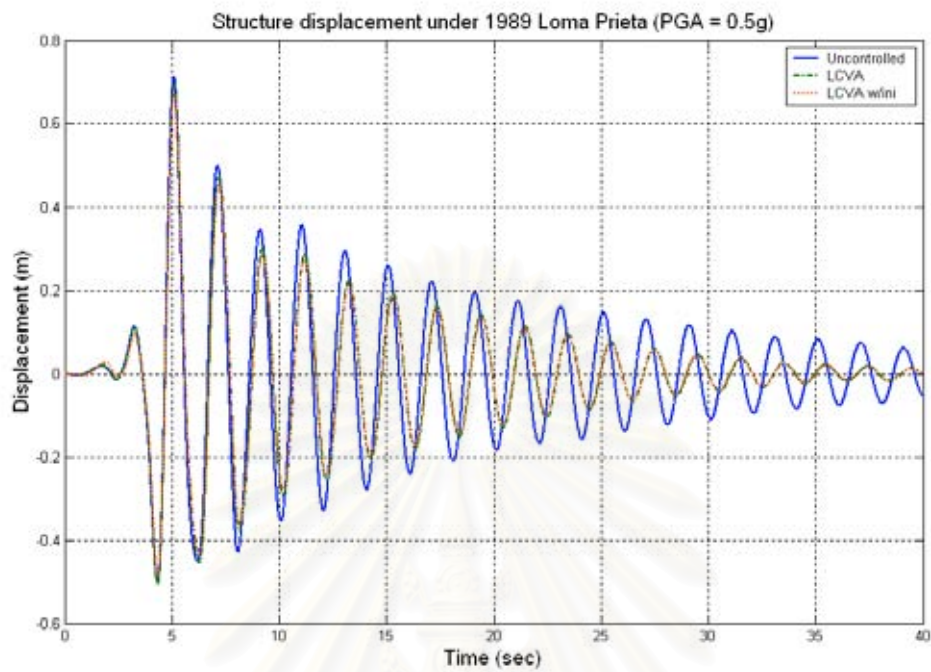


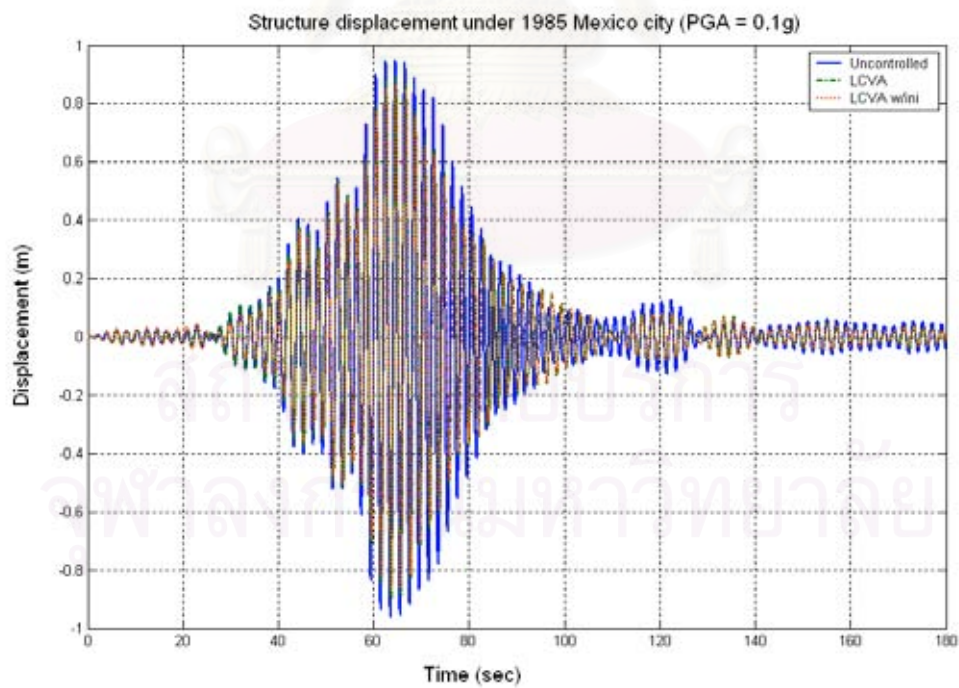
Fig. 5.18 Find minimum peak displacement by releasing the flow in every time step from start of event of 1952 Taft ground motion (Initial liquid displacement = -0.5 m)

Fig. 5.19 shows the responses of SDOF system subjected to 1989 Loma Prieta ground motion and 1985 Mexico city ground motion, respectively. In these figures, the cases of uncontrolled SDOF system, SDOF system with typical LCVA and SDOF system with LCVA equipped with a flow-triggering device are considered.

สถาบันวิทยบริการ
จุฬาลงกรณ์มหาวิทยาลัย



(a)



(b)

Fig. 5.19 SDOF system response; (a) 1989 Loma Prieta; (b) 1985 Mexico city

Shown in Table 5.2, are the peak displacement, peak acceleration, rms displacement and rms acceleration of the SDOF system subjected to 4 different earthquake ground motions. In case of peak response, the improvement of the control performance about 3 - 8% is obtained from typical LCVA, while the improvement of the control performance about 6 - 15% is obtained from LCVA equipped with a flow-triggering device. For rms response, not much of the improvement of the control performance is obtained from both types of LCVAs. The improvement for rms response can be obtained by using the semi-active LCVA with damping adjustable in real time. As seen in Table 5.2 for 4 cases of simulation, the performance of LCVA equipped with a flow-triggering device is always better than the performance of typical LCVA. It should be noted that the control performance of LCVA equipped with a flow-triggering device shown in this table is the best possible cases because the values are the minimum of peak response after trying to release the initial liquid displacement in every possible time step. The practical algorithm for releasing the initial liquid displacement of LCVA is given in the next section.

TABLE 5.2 Summary of simulation results in case of earthquake ground motion records

Excitation Type of control		Near field earthquake record							
		Taft Kerncounty(PGA=0.5g)				Loma Prieta(PGA=0.5g)			
		Xmax	Amax	Xrms	Arms	Xmax	Amax	Xrms	Arms
Uncontrolled		0.2185	7.0173	0.0761	1.1602	0.7121	10.3607	0.1775	1.9993
LCVA		0.2111	6.7247	0.0736	1.1184	0.6953	9.8937	0.1546	1.746
% of reduction		3.39	4.17	3.29	3.60	2.36	4.51	12.90	12.67
LCVA (with ini cond)		0.1868	6.5758	0.0708	1.1054	0.665	9.6576	0.1481	1.692
% of reduction		14.51	6.29	6.96	4.72	6.61	6.79	16.56	15.37

Excitation Type of control		Far field earthquake record							
		SCT-85 (PGA=0.1g)				Bangkok (PGA=0.1g)			
		Xmax	Amax	Xrms	Arms	Xmax	Amax	Xrms	Arms
Uncontrolled		0.9593	9.3211	0.2358	2.2899	0.4126	4.0835	0.1516	1.5141
LCVA		0.8961	8.584	0.209	1.9706	0.4115	3.876	0.1332	1.2709
% of reduction		6.59	7.91	11.37	13.94	0.27	5.08	12.14	16.06
LCVA (with ini cond)		0.8734	8.367	0.201	1.9098	0.3991	3.7568	0.1301	1.2417
% of reduction		8.95	10.24	14.76	16.60	3.27	8.00	14.18	17.99

5.4.3 Algorithm for releasing the initial liquid displacement

The control performance of LCVA equipped with a flow-triggering device greatly depends on the time for releasing the initial liquid displacement. Since, in practice, the excitations such as wind and earthquake ground motion cannot be known a priori, the criteria to determine the suitable time to release the initial liquid displacement need to be established.

For impulse load case, Abe and Igusa (1996) proposed the algorithms to control the impact-induced transient vibrations for tuned mass damper with initial displacement. Closed form analytical results are derived to provide insight into the complex interaction between the structure and damper. The structural impulse conditions are specified by initial structure displacement = 0 and initial structure velocity $\neq 0$. Based on his study, the liquid inside LCVA should be released immediately after the impulse. The closed form of the optimal initial absorber displacement can be also determined in terms of the initial structure velocity, absorber damping, mass ratio and natural frequency of the structure.

For earthquake ground motion, releasing the initial liquid displacement at the time when the structure displacement is 0 and the structure velocity is maximum is preferable if the interaction force from LCVA has the opposite direction to the motion of the structure. Together with the consideration of the term of total energy input to the structure from the earthquake, the suitable time of releasing the initial liquid displacement should be done also when the total energy input to the structure becomes maximum. Therefore, the guideline criteria for releasing the initial liquid displacement can be outlined as follows:

1. The structure displacement is approximately to be zero.
2. The structure velocity approaches to maximum for that cycle of motion.
3. The trend of the total energy input to the structure from earthquake starts to decrease.

The various energy terms can be defined by integrating the equation of motion of the primary structure, Eq. (2.6b), as follows:

$$\int_0^{X_S} (M_S + \rho A_V (\frac{b}{r} + 2h)) \ddot{X}_S(t) dX_S + \int_0^{X_S} C_S \dot{X}_S(t) dX_S + \int_0^{X_S} K_S X_S(t) dX_S =$$

$$- \int_0^{X_S} (M_S + \rho A_V (\frac{b}{r} + 2h)) \ddot{u}_g(t) dX_S - \int_0^{X_S} \rho A_V b \ddot{x}_f(t) dX_S \quad (5.1)$$

The total energy input to the structure since the earthquake excitation began is

$$E_I(t) = \int_0^{X_S} (M_S + \rho A_V (\frac{b}{r} + 2h)) \ddot{u}_g(t) dX_S \quad (5.2)$$

The energy dissipated by LCVA is

$$E_{LCVA}(t) = \int_0^{X_S} \rho A_V b \ddot{x}_f(t) dX_S \quad (5.3)$$

The first term on the left hand side of Eq. (5.1) is the kinetic energy of the system, while the second term and the third term on the left hand side are the energy dissipated by viscous damping and the recoverable strain energy of the structure, respectively.

Fig. 5.20 shows the displacement, velocity and the input energy from earthquake excitation of the SDOF system with LCVA when the liquid in LCVA is kept unreleasing for all the time of excitation. The peak displacement from Fig. 5.20 is 0.70 m which is different from uncontrolled SDOF system due to the change of the SDOF system's natural frequency from adding LCVA mass. As observed from Fig. 5.20, at the time of about 4.8 sec since the earthquake excitation began, the trend of the input energy from earthquake excitation starts to decrease. At this instance, the SDOF system velocity also reaches to maximum, and the SDOF system displacement is closed to zero. This is more practical to apply to real structure by using this guideline criteria because the input energy from earthquake excitation, the primary structure velocity and displacement can

be either calculated or measured in real time during the earthquake excitation. In this particular case, thus, the initial liquid displacement is released at the time of 4.8 sec after the earthquake began.

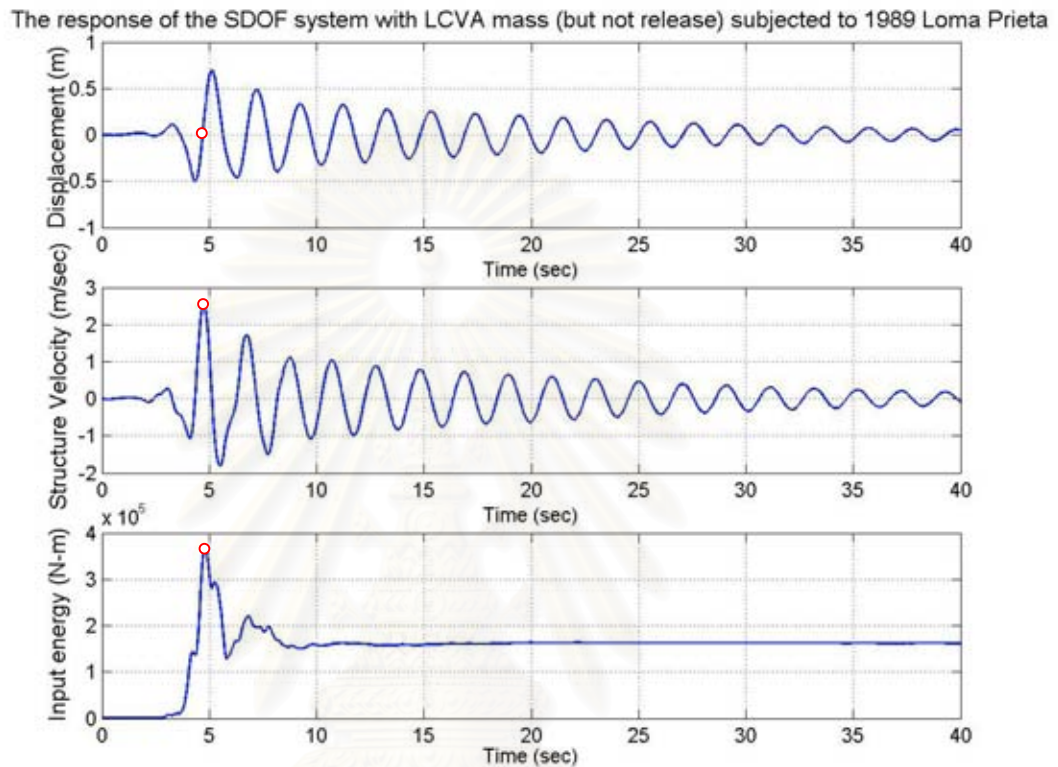


Fig. 5.20 SDOF system with LCVA mass response (but not released) subjected to 1989 Loma Prieta

Fig. 5.21 shows the response of the SDOF system subjected to 1989 Loma Prieta ground motion for SDOF system with LCVA equipped with a flow-triggering device by releasing at the time of 4.8 sec since the earthquake began. The maximum interaction force is obtained immediately at the time when the initial liquid displacement is released. The dissipated energy due to LCVA also starts to dissipate from the SDOF system immediately after the initial liquid displacement is released. The peak displacement of the SDOF system is 0.6875 m, which is lower than the case of typical LCVA as seen in Table 5.2. This can be implied that by using these guideline criteria, the suitable time to release the initial liquid displacement can be determined. However, it should be noted that more suitable criteria for releasing initial liquid displacement might be obtained in the future study so that the structure response can be better controlled.

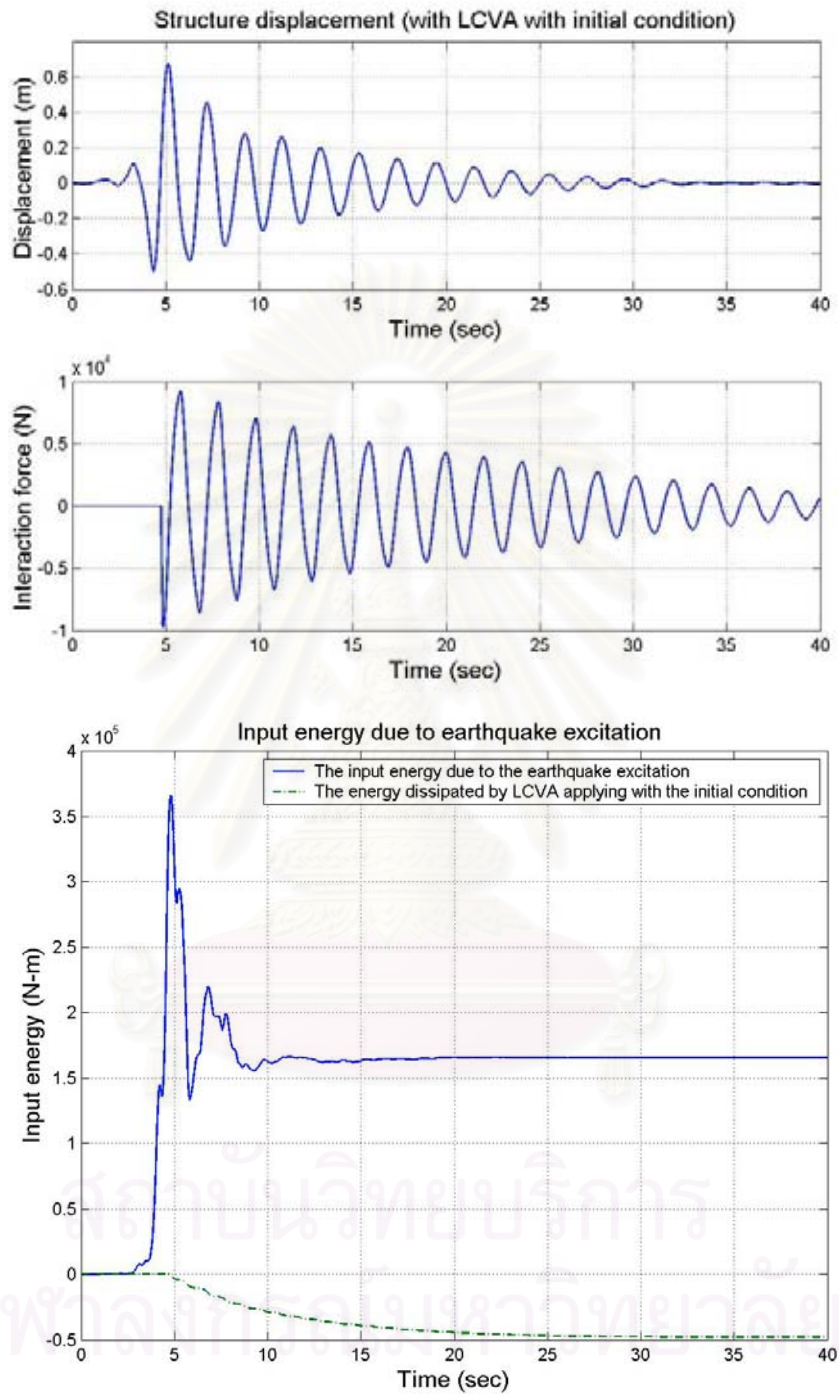


Fig. 5.17 SDOF system with LCVA equipped with a flow-triggering device response (releasing time = 4.8 sec since the earthquake began) subjected to 1989 Loma Prieta

5.5 Conclusions

The experimental and numerical results of LCVAs equipped with a flow-triggering device under impulse and harmonic excitations are studied and compared. It is found from Figs 5.8 – 5.11, that the analytical solutions based on the numerical panel method agree very well with the experimental results for both amplitude and phase of the interaction force and liquid displacement. The agreements are almost perfect for LCVA with insert type II, and acceptable for LCVA with insert type III. The discrepancy between the measured and the calculated interaction force based on the numerical panel method varies from about 4% to 7% for LCVA with insert type II, while the discrepancy between the measured and the calculated interaction force based on the numerical panel method varies from about 12% to 15% for LCVA with insert type III.

For numerical investigations, the optimum damping ratio obtained from Table 2.1 is used. This is due to the excessive damping ratio as observed from test set up that can cause to deteriorate the performance of LCVA equipped with a flow-triggering device. The improvement of 5.19% reduction in the peak displacement and 35.98% reduction in the root mean square of the displacement is obtained for the SDOF system with LCVA equipped with a flow-triggering device in case of impulse load. For numerical investigation by using 4 different records of earthquake ground motions, in case of peak response, the improvement of the control performance about 3 - 8% is obtained in case of typical LCVA, while the improvement of the control performance about 6 - 15% is obtained in case of LCVA equipped with a flow-triggering device. For rms response, the obtained improvement of the control performance is insignificant in case of LCVA equipped with a flow-triggering device compared to typical LCVA. The improvement for rms response can be obtained by using the semi-active LCVA with damping adjustable in real time. As seen in Table 5.2 for 4 cases of simulation, the performance of LCVA equipped with a flow-triggering device is always better than that of typical LCVA. The guideline criteria to determine the suitable time to release the initial liquid displacement of LCVA are also given. It should be noted that more suitable criteria for releasing initial liquid displacement might be obtained in the future study for better control of the structure response.

CHAPTER VI

SUMMARY AND CONCLUSION

This research focuses on the development of liquid dampers to mitigate adverse effects of building vibration due to earthquake excitations. The control characteristics of TLCDs with various configurations and TLCDs equipped with a flow-triggering device are studied numerically and experimentally. The control performances of a SDOF system installed with TLCD and TLCD equipped with a flow-triggering device subjected to various cases of external loadings are numerically investigated.

The test results of the tuned liquid column dampers (TLCDs) on the shake table are reported. Three TLCD models having the same natural period (based on the existing analytical model) are investigated under free-vibration tests, spectral tests and time history tests. From these test results, it is evident that the simplified effective length approach in existing literature is not able to give an accurate estimation of the responses of LCVA dampers with relatively large transition boundaries. Poor agreements on frequency responses of the liquid motion are observed between the existing analytical results based on the simplified effective length approach and the experimental values in the case of LCVAs with large transition zones.

The numerical potential-flow method, known as the numerical panel method developed to determine the hydrodynamic forces on rigid sections is used to simulate the characteristics of various TLCD and LCVA configurations. The numerical results are verified with those obtained from experimental results. Significant improvement is achieved by using the numerical panel method with less than 3.4% of discrepancy between the predicted natural frequencies and the experimental results, as compared to about 7.5% discrepancy or more in the conventional analysis.

The LCVAs equipped with a flow-triggering device which have the initial liquid displacements set to non-zero values and subsequently released under free-vibration are investigated experimentally and numerically. It is found that the analytical solutions based on the numerical panel method agree well with the experimental results in both amplitude and phase of both the interaction force and liquid motion. The agreement is almost perfect for LCVA with insert type II, and acceptable for LCVA with insert type III. The discrepancy between the measured and

the calculated interaction force based on the numerical panel method varies from about 4% to 7% for LCVA with insert type II, while the discrepancy between the measured and the calculated interaction force based on the numerical panel method varies from about 12% to 15% for LCVA with insert type III.

The potential of TLCDs and LCVAs as a vibration suppression device for earthquake excitations has been examined by numerical investigations. The numerical simulations are used to evaluate the control performance of the LCVA equipped with the flow-triggering device under impulse load, harmonic load and earthquake load. Based on numerical results, the improvement of 5.19% reduction in the peak displacement and 35.98% reduction in the root mean square (rms) of the displacement are obtained for the SDOF system with LCVA equipped with the flow-triggering device for impulse load case. For the cases of earthquake loads, the improvement of the control performance of approximately 3 to 8% is obtained for peak response in case of typical LCVA, while the improvement of the control performance of approximately 6 to 15% is obtained in case of LCVA equipped with a flow-triggering device. For rms response, the control performance is not considerably improved in case of LCVA equipped with a flow-triggering device compared to typical LCVA. It should be noted that these performances of LCVA equipped with a flow-triggering device are, however, obtained assuming the damping can be set to optimum value. Since the damping ratio of the LCVA equipped with a flow-triggering device is much higher as proposed in Chapter 5. This excessive damping ratio can deteriorate the control performance of the damper. Then, the modification of LCVA configuration that can keep the initial liquid displacement with lower damping ratio is required for real application.

The following future studies in this area are recommended as follows:

1. Experiments concerning semi-active TLCDs are done in case of TLCDs which have the initial liquid displacements set to non-zero values. Further experimental studies in case of semi-active TLCDs which have both following capabilities: (a) initial liquid displacements set to non-zero values and (b) damping adjustable in real time are the recommended topics. Furthermore, a more elaborate experiment of the shake table using a structure model attached with a semi-active TLCD

which have those capabilities is needed before the application of these dampers on actual structural systems.

2. Numerical studies for structure installed with TLCD with two aforementioned capabilities under various earthquake ground motion records are the interesting topics for future studies for both the performances and design guideline criteria.



สถาบันวิทยบริการ
จุฬาลงกรณ์มหาวิทยาลัย

REFERENCES

- Abe, M., Kimura, S. and Fujino, Y. (1996). Control laws for semi-active tuned liquid column damper with variable orifice opening. 2nd International Workshop on Structural Control, Hong Kong.
- Abe, M. and Igusa, T. (1996). Semi-active dynamic vibration absorbers for controlling transient response. Journal of Sound and Vibration 198(5): 547-569.
- Aparna, G. and Biswajit, B. (2004). Seismic vibration control of short period structures using the liquid column damper. Engineering Structures 26(13): 1905-13.
- ATC (1996). Seismic Evaluation and Retrofit of Concrete Buildings. ATC-40 Report, Applied Technology Council, Redwood City, California.
- Balendra, T., Wang, C.M. and Cheong, H.F. (1995). Effectiveness of tuned liquid column dampers for vibration control of towers. Engineering Structures 17 (9): 668-675.
- Balendra, T., Wang, C.M. and Rakesh, G. (1998). Vibration control of tapered buildings using TLCD. Journal of Wind Engineering and Industrial Aerodynamics 77and78: 245-257.
- Balendra, T., Wang, C.M. and Rakesh, G. (1999). Vibration control of various type buildings using TLCD. Journal of Wind Engineering and Industrial Aerodynamics 83: 197-208.
- Balendra, T., Wang, C.M. and Rakesh, G. (1999). Effectiveness of TLCD on various structural systems. Engineering Structures 21: 291-305.
- Balendra, T., Wang, C.M. and Yan N. (2001). Control of wind-excited towers by active tuned liquid column damper. Engineering Structures 23: 1054-1067.
- Banerji, P., Murudi, M., Shah, A. H., and Popplewell, N. (2000). Tuned liquid dampers for controlling earthquake response of structures. Earthquake Engineering and Structural Dynamics 29: 587-602.
- Bergman, L.A., Mc Farland, D.M., Hall, J.K., Johnson, E.A. and Kareem, A. (1989). Optimal distribution of tuned mass dampers in wind sensitive structures. Proceedings of 5th ICOSSAR. New York.
- Blevins, R.D. (1984). Applied Fluid Dynamics Handbook. Van Nostrand Reinhold.

- Chang, C.C. and Hsu, C.T. (1998). Control performance of liquid column vibration absorbers. Engineering Structures 20(7): 580-586.
- Chang, C.C., Hsu, C.T. and Swei, S.M. (1998). Control of buildings using single and multiple tuned liquid column dampers. Structural Engineering and Mechanics 6(1): 77-93.
- Chang, C.C. and Qu, W.L. (1998). Unified dynamic absorber design formulas for wind-induced vibration control of tall buildings. Structural Design of Tall Buildings 7: 147-166
- Chang, C.C. and Hsu, C.T. (1999). Control performance of Liquid column vibration absorber. Engineering Structures 20(7): 580-586.
- Chang, C.C. (1999). Mass dampers and their optimal designs for building vibration control. Engineering Structures 21: 454-463.
- Chopra, A.K. (1995). Dynamics of Structures. Prentice Hall New Jersey.
- Chow, C.Y. (1979). Computational fluid mechanics. John Wiley New York.
- Delrieu, J.L. (1994). Cost effect deepwater platform dedicated to West Africa and Brazil. Proceedings 7th International Conference on the behavior of Offshore Structures. 2:805-812.
- Den Hartog, J.P. (1956). Mechanical Vibrations, 4th Ed, McGraw-Hill.
- Ehlers, J. (1987). Active and Semi-Active Control Methods in Wave-Structure Interaction.
- ENR. (1971). Tower cables handle wind, water tank dampens it. Engineering News-Record Dec.9, 23.
- Frank, W. (1967). Oscillation of cylinders in or below the free surface of deep fluids. Naval Ship Research and Development Center Report 2375
- Fujino, Y., and Sun, L. M. (1993). Vibration control by multiple tuned liquid dampers (MTLDs). Journal of Structural Engineering ASCE 119(12): 3482-3501.
- Gao, H., Kwok, K.C.S. and Samali, B. (1997). Optimization of Tuned Liquid Column Dampers. Engineering Structures 19: 476-486.
- Gao, H., Kwok, K.C.S. and Samali, B. (1999). Characteristics of multiple Tuned Liquid Column Dampers in suppressing Structural Vibration. Engineering Structures 21: 316-331.
- Haroun, M.A. and Pires J.A. (1994). Active orifice control in Hybrid liquid column dampers. Proceedings of the First World Conference on Wind Engineering. vol. I, Los Angeles.

- Hess, J.L. and Smith A.M. O. (1966). Calculation of potential flow about arbitrary bodies. Progress in Aeronautical Sciences 8:1-138.
- Hess, J.L. (1990). Panel methods in computational fluid dynamics. Annual Review Fluid Mechanics 22:255-74.
- Hitchcock, P.A., Kwok, K.C.S., Watkins, R.D. and Samali, B. (1997). Characteristics of Liquid column vibration absorbers (LCVA) -I and II. Engineering Structures 19(2).
- Hitchcock, P.A., Glanville, M.J., Kwok, K.C.S., Watkins, R.D. and Samali, B. (1999). Damping properties and wind-induced response of a steel frame tower fitted with liquid column vibration absorbers. Journal of Wind Engineering and Industrial Aerodynamics (83): 183-196.
- Honkanen, M.G. (1990). Heel and roll control by water tank. Naval Architect. 215-216
- Hrovat, D., Barak, P. and Rabins, M. (1983). Semi-active versus Passive or Active Tuned Mass Dampers for Structural Control. Journal of Engineering Mechanics ASCE 109(3): 691-705.
- Huse, E. (1987). Free surface damping tanks to reduce motions of offshore structures. Proceedings of 6th International Symposium on Offshore Mechanics and Arctic Engineering, 313-324.
- Izumi, M., Teramoto, T., Kitamura, H. and Sekkei, N. (1993). Buildings with response control systems in Japan. Proceedings of Structural Congress. Irvine, California, pp. 107-114.
- Jong-Cheng, W., Ming-Hsiang, S., Yuh-Yi, L. and Ying-Chang, S. (2005). Design guidelines for tuned liquid column damper for structures responding to wind. Engineering Structures 27(13): 1893-905.
- Kareem, A. and Kline, S. (1995). Performance of multiple mass dampers under random loading. Journal of Structural Engineering ASCE 121(2): 348-361.
- Katz, J. and Plotkin, A. (1991). Low-Speed Aerodynamics. McGraw-Hill New York.
- Kwok, K.C.S. and McDonald, P.A. (1987). Wind-induced response of Sydney tower. Proceedings of the First National Structural Engineering Conference. pp.19-24.
- Lukkunaprasit, P., and Wanitkorkul, A. (2001). Inelastic buildings with tuned mass dampers under moderate ground motions from distant earthquakes. Earthquake Engineering and Structural Dynamics Journal. 30: 537-551.

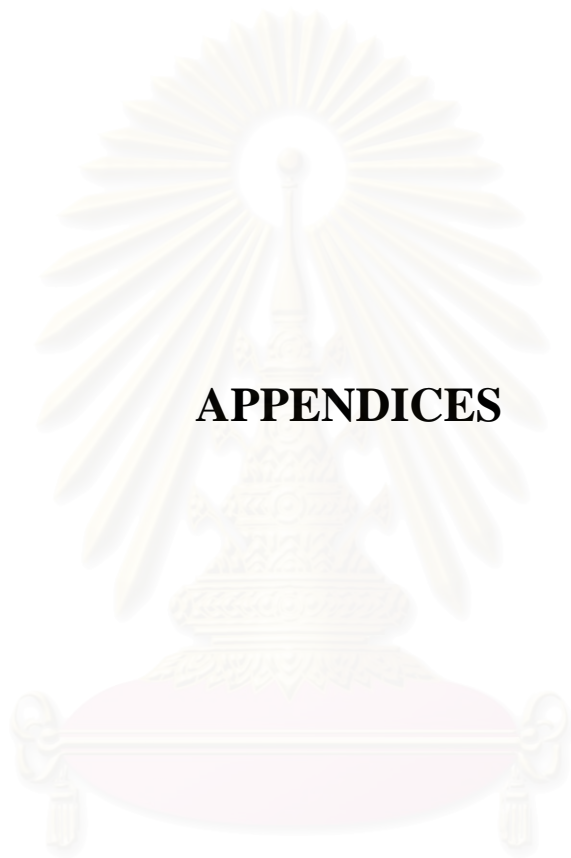
- Lou, Y.K., Lute, L.D. and Li., J.J. (1994). Active tuned liquid damper for structural control. Proceedings of the First World Conference on Wind Engineering. Vol. I, Los Angeles.
- Newmark, N.M. (1959). A method of computation for structural dynamics. Journal Engineering Mechanics Division. ASCE 85: 67-94.
- Patel, M.H. and Witz, J.A. (1985). On improvements to the design of tensioned buoyant platforms. Behavior of Offshore Structures. 563-573.
- Pinkaew, T., Lukkunaprasit, P., and Chatupote, P. (2001). Seismic effectiveness of tuned mass dampers for damage reduction of structures. Engineering Structures 25(1): 39-46.
- Roberts, J.B. and Spanos, P.D. (1990). Random Vibration and Statistical Linearization. Wiley, New York.
- Sadek, F., Mohraz, B. and Lew, H.S. (1998). Single- and multiple-tuned liquid column dampers for seismic applications. Earthquake Engineering and Structural Dynamics 27: 439-463.
- Sakai, F. *et al.* (1989). Tuned Liquid Column Damper - New Type Device for Suppression of Building Vibrations. Proceedings International Conference on High Rise Buildings. Nanjing, China, March 25-27.
- Sellars, F.H. and Martin, P.M. (1992). Selection and evaluation of ship roll stabilization systems. Marine Technology 29(2): 84-101.
- Soong, T.T. and Constantinou, M.C. (Editors). (1994). Passive and Active structural Vibration Control In Civil Engineering. Springer-Verlag, Wein-New York.
- Soong, T.T. and Dargush, G.F. (1997). Passive Energy Dissipation Systems in Structural Engineering. Wiley, New York.
- Shimizu, K. and Teramura, A. (1994). Development of vibration control system using U-shaped tank. Proceedings of the 1st International Workshop and Seminar on Behavior of Steel Structures in Seismic Areas. Timisoara, Romania, 7.25-7.34.
- Shum, K.M. and Xu, Y.L. (2002). Multiple-tuned liquid column dampers for torsional vibration control of structures: experimental investigation. Earthquake Engineering and Structural Dynamics 31(4): 977-991.
- Sudjic, D. (1993). Their love keeps lifting us higher. Telegraph Magazine. May, 17-25.

- Suhardjo, J. and Kareem, A. (1997). Structural control of offshore platforms. Proceedings of the 7th International Offshore and Polar Engineering Conference. IOSPE-97, Honolulu.
- Vandiver, J.K. and Mitome, S. (1978). Effect of liquid storage tanks on the dynamic response of offshore platforms. Dynamic Analysis of Offshore Structures.
- Warburton, G.B. and Ayorinde, E.O. (1980). Optimum absorber parameters for simple systems. Earthquake Engineers and Structural Dynamics 8: 197-217.
- Warburton, G.B. (1982). Optimal absorber parameters for various combination of response and excitation parameters. Earthquake Engineering and Structural Dynamics 10: 381-401.
- Watkins RD. (1991). Tests on a liquid column vibration absorber for tall structures. In: Proceedings of the international conference on steel and aluminium structures.
- Webster, W.C., Beck, R.F., Cummins, W.F., Dalzell, J.F. and Mandel, P. (1989). Motions in waves, a chapter in principles of naval architecture. Volume III, SNAME (Society of Naval Architects and Marine Engineers) New York: 1-188.
- Webster, W.C., Dalzell, J.F. and Barr, R.F. (1998). Prediction and measurement of the performance of free flooding ship antirolling tanks. SNAME Transactions New York: 96.
- Won, A.Y.J., Pires, J.A. and Haroun, M.A. (1996). Stochastic seismic performance evaluation of tuned liquid column dampers. Earthquake Engineering and Structural Dynamics 25: 1259-1274.
- Won, A.Y.J., Pires, J.A. and Haroun, M.A. (1997). Performance assessment of tuned liquid column dampers under random seismic loading. Int. Journal of Non-Linear Mechanics 32(4): 745-758.
- Xu, Y.L., Samali B. and Kwok, K.C.S. (1992). Control of along-wind response of structures by mass and liquid dampers. Journal of Wind Engineering and Industrial Aerodynamics 118(1): 20-39.
- Xue, S.D., Ko, J.M. and Xu, Y.L. (2000). Tuned liquid column damper for suppressing pitching motion of structures. Engineering Structures 23: 1538-1551.

- Xue, S.D., Ko, J.M. and Xu, Y.L. (2002). Optimal performance of the TLCD in structural pitching vibration control. Journal of Vibration and Control 8(5): 619-642.
- Yalla, S.K. and Kareem, A. (2000). Optimum absorber parameters for tuned liquid column dampers. Journal of Structural Engineering ASCE 125(8): 906-915.
- Yalla, S.K. and Kareem, A. (2001). Beat phenomenon in combined structure-liquid damper systems. Engineering Structures 23: 622-630.
- Yalla, S.K., Kareem, A. and Kantor, J.C. (2001). Semi-Active Tuned Liquid Column Dampers for vibration control of structures. Engineering Structures 23:1469-1479.
- Yamaguchi, H. and Harnpornchai, N. (1993). Fundamental characteristics of multiple tuned mass dampers for suppressing harmonically forced oscillation. Journal of Earthquake Engineering and Structural Dynamics. 22.



สถาบันวิทยบริการ
จุฬาลงกรณ์มหาวิทยาลัย



APPENDICES

สถาบันวิทยบริการ
จุฬาลงกรณ์มหาวิทยาลัย

APPENDIX A

Integral of Velocity Potential

From Eq. (4.3), the induced potential at the field point is

$$\begin{aligned} \phi &= \int_{-s}^s \frac{1}{2} \ln \left[\frac{1}{(x-x_a)^2 + y_a^2} \right] dx \\ &= \frac{1}{4} \left\{ \begin{aligned} &8s - \pi y_a - 2y_a \text{Arg}[s-x_a-iy_a] + 2y_a \text{Arg}[-is-ix_a+y_a] \\ &+ 2y_a \text{Arg}[-is+ix_a+y_a] - 2y_a \text{Arg}[is+ix_a+y_a] \\ &-s \ln \left[(s^2 - 2sx_a + x_a^2 + y_a^2)^2 \right] + x_a \ln \left[(s^2 - 2sx_a + x_a^2 + y_a^2)^2 \right] \\ &-s \ln \left[(s^2 + 2sx_a + x_a^2 + y_a^2)^2 \right] - x_a \ln \left[(s^2 + 2sx_a + x_a^2 + y_a^2)^2 \right] \end{aligned} \right\} \\ &= \frac{1}{4} \left\{ \begin{aligned} &8s - \pi y_a - 2y_a \left\{ \text{Arg}[s-x_a-iy_a] - \text{Arg}[-is-ix_a+y_a] \right. \\ &\left. - \text{Arg}[-is+ix_a+y_a] + \text{Arg}[is+ix_a+y_a] \right\} \\ &-s \ln \left[(s^2 - 2sx_a + x_a^2 + y_a^2)^2 \right] + x_a \ln \left[(s^2 - 2sx_a + x_a^2 + y_a^2)^2 \right] \\ &-s \ln \left[(s^2 + 2sx_a + x_a^2 + y_a^2)^2 \right] - x_a \ln \left[(s^2 + 2sx_a + x_a^2 + y_a^2)^2 \right] \end{aligned} \right\} \end{aligned}$$

Note that : $\text{Arg}[is+ix_a+y_a] = \frac{\pi}{2} - \text{Arg}[s+x_a+iy_a]$

$$\text{Arg}[s+x_a-iy_a] = -\text{Arg}[s+x_a+iy_a]$$

Therefore,

$$\phi = \frac{1}{4} \left\{ \begin{aligned} &8s - \pi y_a + y_a \left\{ -3\pi + 4\text{Arg}[s-x_a+iy_a] + 4\text{Arg}[s+x_a+iy_a] \right\} \\ &-s \ln \left[(s^2 - 2sx_a + x_a^2 + y_a^2)^2 \right] + x_a \ln \left[(s^2 - 2sx_a + x_a^2 + y_a^2)^2 \right] \\ &-s \ln \left[(s^2 + 2sx_a + x_a^2 + y_a^2)^2 \right] - x_a \ln \left[(s^2 + 2sx_a + x_a^2 + y_a^2)^2 \right] \end{aligned} \right\}$$

$$= \frac{1}{4} \left\{ \begin{aligned} &8s - \pi y_a + y_a \left\{ \pi - 4 \operatorname{Arc} \tan \left(\frac{x_a - s}{y_a} \right) + 4 \operatorname{Arc} \tan \left(\frac{x_a + s}{y_a} \right) \right\} \\ &-s \ln \left[\left(s^2 - 2sx_a + x_a^2 + y_a^2 \right)^2 \right] + x_a \ln \left[\left(s^2 - 2sx_a + x_a^2 + y_a^2 \right)^2 \right] \\ &-s \ln \left[\left(s^2 + 2sx_a + x_a^2 + y_a^2 \right)^2 \right] - x_a \ln \left[\left(s^2 + 2sx_a + x_a^2 + y_a^2 \right)^2 \right] \end{aligned} \right\}$$

Also noting that $\ln[a^2] = 2\ln[a]$, we can simplify this expression further. Thus,

$$\phi = \frac{1}{4} \left\{ \begin{aligned} &8s - 4y_a \operatorname{Arc} \tan \left(\frac{x_a - s}{y_a} \right) + 4y_a \operatorname{Arc} \tan \left(\frac{x_a + s}{y_a} \right) \\ &+ 4(x_a - s) \ln \sqrt{(s - x_a)^2 + y_a^2} - 4(x_a + s) \ln \sqrt{(s + x_a)^2 + y_a^2} \end{aligned} \right\}$$

which simplifies to

$$\begin{aligned} \phi &= 2s + y_a \left\{ -\operatorname{Arc} \tan \left(\frac{x_a - s}{y_a} \right) + \operatorname{Arc} \tan \left(\frac{x_a + s}{y_a} \right) \right\} \\ &+ (x_a - s) \ln \sqrt{(x_a - s)^2 + y_a^2} - (x_a + s) \ln \sqrt{(x_a + s)^2 + y_a^2} \end{aligned}$$

สถาบันวิทยบริการ
จุฬาลงกรณ์มหาวิทยาลัย

VITA

Passagorn Chaiviriyawong

I was born in Hatyai, the southernmost part of Thailand, on October 5, 1977. The elementary and secondary schools where I studied in Hatyai were Seangthongwittaya and Hatyai Witthayalai, respectively. Then, I moved to Bangkok to study Bachelor of Civil Engineering at Chulalongkorn University and graduated in 1999. After that, I got a Royal Golden Jubilee Ph.D program (RGJ) scholarship from Thailand Research Fund (TRF) to further a study in Ph.D. program, which this dissertation is in partial fulfillment of the requirements.



สถาบันวิทยบริการ
จุฬาลงกรณ์มหาวิทยาลัย